

**AN ONIOM-XS MD SIMULATION OF METHYLAMMONIUM
ION IN AQUEOUS SOLUTION**



**A Thesis Submitted in Partial Fulfillment of the Requirements for the
Degree of Doctor of Philosophy in Chemistry
Suranaree University of Technology
Academic Year 2017**

การจำลองพลวัตเชิงโมเลกุลโอเนียม-เอ็กซ์เอสของ
ไอออนเมทิลแอมโมเนียมในสารละลายน้ำ

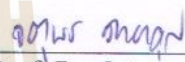


วิทยานิพนธ์นี้เป็นส่วนหนึ่งของการศึกษาตามหลักสูตรปริญญาวิทยาศาสตรดุษฎีบัณฑิต
สาขาวิชาเคมี
มหาวิทยาลัยเทคโนโลยีสุรนารี
ปีการศึกษา 2560

**AN ONIOM-XS MD SIMULATION OF METHYLAMMONIUM
ION IN AQUEOUS SOLUTION**

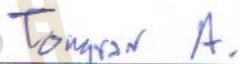
Suranaree University of Technology has approved this thesis submitted in partial fulfillment of the requirements for the Degree of Doctor of Philosophy.

Thesis Examining Committee



(Prof. Dr. Jatuporn Wittayakun)

Chairperson



(Assoc. Prof. Dr. Anan Tongraar)

Member (Thesis Advisor)



(Assoc. Prof. Dr. Viwat Vchirawongkwin)

Member



(Prof. Dr. Kritsana Sagarik)

Member



(Assoc. Prof. Dr. Rattikorn Yimnirun)

Member



(Prof. Dr. Santi Maensiri)
Acting Vice Rector for Academic
Affairs and Internationalisation



(Prof. Dr. Santi Maensiri)
Dean of Institute of Science

ปรารภชื่อ : ไชยสิทธิ์ : การจำลองพลวัตเชิงโมเลกุลไอออนัม-เอ็กซ์เอสของไอออนเมทิลแอมโมเนียมในสารละลายน้ำ (AN ONIOM-XS MD SIMULATION OF METHYLAMMONIUM ION IN AQUEOUS SOLUTION) อาจารย์ที่ปรึกษา : รองศาสตราจารย์ ดร.อนันต์ ทองระอา, 77 หน้า.

เทคนิคการจำลองพลวัตเชิงโมเลกุลที่ผสมผสานกลศาสตร์ควอนตัมและกลศาสตร์โมเลกุลบนพื้นฐานของวิธี ไอออนัม-เอ็กซ์เอส (ONIOM-XS MD) ถูกนำมาประยุกต์เพื่อศึกษาการเกิดพันธะไฮโดรเจนระหว่างไอออนเมทิลแอมโมเนียม (CH_3NH_3^+) กับตัวทำละลายที่เป็นน้ำ โดยเทคนิคการจำลองพลวัตเชิงโมเลกุลไอออนัม-เอ็กซ์เอสนี้ ระบบที่ศึกษาจะถูกแบ่งออกเป็นสองส่วน ได้แก่ ส่วนที่เป็นกลศาสตร์ควอนตัมซึ่งประกอบด้วยไอออน CH_3NH_3^+ และน้ำที่อยู่รอบ ๆ ไอออน และส่วนที่เหลือที่เป็นกลศาสตร์โมเลกุลซึ่งประกอบด้วยตัวทำละลายที่เป็นน้ำ ส่วนของระบบที่เป็นทรงกลมซึ่งประกอบด้วยไอออน CH_3NH_3^+ และน้ำที่อยู่รอบ ๆ ไอออนนั้น จะถูกอธิบายโดยใช้กลศาสตร์ควอนตัมในระดับฮาร์ตรี-ฟอก (HF) โดยใช้เบสิสเซตชนิด DZP ในขณะที่ส่วนที่เหลือของระบบจะถูกอธิบายโดยใช้ฟังก์ชันศักร์คู่ การเลือกใช้การคำนวณในระดับ HF และเบสิสเซตชนิด DZP พิสูจน์ว่าจะสามารถให้ผลการศึกษาที่น่าเชื่อถือและเหมาะสมกับเวลาที่ต้องใช้ในการจำลองพลวัตเชิงโมเลกุลดังกล่าว ผลลัพธ์ของการจำลองพลวัตเชิงโมเลกุลบนพื้นฐานของวิธี ไอออนัม-เอ็กซ์เอส แสดงให้เห็นความยืดหยุ่นของโครงสร้างไฮเดรชันของไอออน CH_3NH_3^+ ในสารละลายน้ำอย่างชัดเจน โดยมีจำนวนโมเลกุลน้ำที่หลากหลายแตกต่างกันตั้งแต่ 3 ถึง 8 โมเลกุล และตั้งแต่ 12 ถึง 19 โมเลกุลที่เข้ามาเกี่ยวข้องกับซอลเวชันชั้นแรกของหมู่แอมโมเนียม ($-\text{NH}_3^+$) และหมู่เมทิล ($-\text{CH}_3$) ตามลำดับ โดยหมู่ $-\text{NH}_3^+$ จะเกิดพันธะไฮโดรเจนกับน้ำที่อยู่ใกล้เคียงประมาณ 3.6 พันธะ และพบว่า พันธะไฮโดรเจนดังกล่าวจะมีความแข็งแรงน้อยกว่าพันธะไฮโดรเจนที่เกิดจากน้ำด้วยกันเอง นอกจากนี้ มีหลักฐานชัดเจนว่าผลของด้านที่ไม่ชอบน้ำของหมู่ $-\text{CH}_3$ มีผลให้พันธะไฮโดรเจนของโมเลกุลน้ำในบริเวณนี้มีความแข็งแรงมากขึ้น ลักษณะดังกล่าวสอดคล้องกับความสามารถในการสลายโครงสร้างของไอออน CH_3NH_3^+ ในสารละลายน้ำ

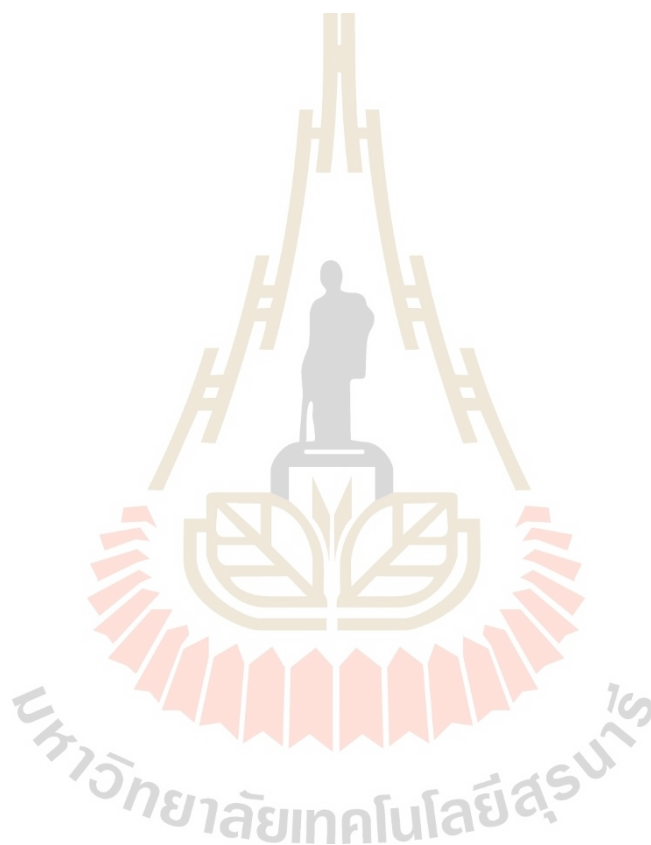
PRANGTHONG CHAIYASIT : AN ONIOM-XS MD SIMULATION OF
METHYLAMMONIUM ION IN AQUEOUS SOLUTION.

THESIS ADVISOR : ASSOC. PROF. ANAN TONGRAAR, Ph.D. 77 PP.

METHYLAMMONIUM ION/ HYDROGEN BOND/ ONIOM-XS / STRUCTURE-
BREAKING

Sophisticate QM/MM MD technique based on the ONIOM-XS (Own N-layered Integrated Molecular Orbital and Molecular Mechanics – Extension to Solvation) method, ONIOM-XS has been employed to study the CH_3NH_3^+ -water hydrogen bonds (HBs) in aqueous solution. By the ONIOM-XS MD technique, the system is partitioned into a small QM treated region, *i.e.*, a sphere which contains the CH_3NH_3^+ ion and its surrounding water molecules, and the remaining MM region, *i.e.*, the bulk water. The interactions within the QM subsystem were treated at the HF level of accuracy using the DZP basis set, while the rest of the system was described by classical pair potentials. The HF method and the DZP basis set employed in this study are proved to be suitable choices, compromising between the quality of the simulation results and the requirement of the CPU time. The ONIOM-XS MD results clearly reveal a flexible CH_3NH_3^+ solvation, showing various numbers of water molecules, ranging from 3 to 8 and from 12 to 19, cooperatively involved in the primary region of the $-\text{NH}_3^+$ and $-\text{CH}_3$ species, respectively. In this respect, it is observed that the $-\text{NH}_3^+$ group participates in about 3.6 HBs with its nearest-neighbor waters, and the HBs between the $-\text{NH}_3^+$ hydrogen atoms and their nearest-neighbor waters are relatively weaker than the HBs of bulk water. In addition, it is evident that the “hydrophobic effect” of the $-\text{CH}_3$ species results in slightly more attractive water-water HB interactions in this region

Such phenomenon corresponds to a clear “structure-breaking” ability of CH_3NH_3^+ in aqueous solution.



ACKNOWLEDGEMENTS

First of all, I would like to express my deep gratitude to my thesis advisor, Assoc. Prof. Dr. Anan Tongraar, who gave me a great opportunity to do this wonderful project along with my Ph.D. study at the Suranaree University of Technology (SUT). I am very much appreciate on his guidance and supports throughout the course of my graduate. I am also very thankful to the thesis examining committee for their useful comments and suggestions.

In addition to my thesis advisor, I would like to express my special thanks to Prof. Dr. Kritsana Sagarik and all instructors at the School of Chemistry, SUT, for their helps and guidance with useful and constructive comments. I would also like to thank my friends at SUT for their friendship. Although I cannot name all of them, but of course, I will always remember them.

I am very grateful to Prof. Dr. Debbie C. Crans for her valuable guidance and encouragement when I visited her research group at the Colorado State University, United States of America. Moreover, I am really thankful to my friends in the Crans's research group for their sincere and helpful research collaboration.

Furthermore, I would like to acknowledge the financial support from the Thailand Research Fund (TRF) under the Royal Golden Jubilee Ph.D. Program (Contact number PHD/0126/2552), and SUT.

Finally, I am deeply grateful to my parents and relatives, for their understanding, support, encouragement, and love.

Prangthong Chaiyasit

CONTENTS

	Page
ABSTRACT IN THAI	I
ABSTRACT IN ENGLISH	II
ACKNOWLEDGEMENTS	IV
CONTENTS	V
LIST OF TABLES	VII
LIST OF FIGURES	VIII
LIST OF ABBREVIATIONS	XII
CHAPTER	
I INTRODUCTION.....	1
1.1 Literature reviews	1
1.2 Research objectives	4
1.3 Scope and limitation of the study	4
1.4 References	5
II COMPUTATIONAL METHODS AND RESEARCH PROCEDURES.....	9
2.1 Introduction to molecular dynamics (MD) simulation	9
2.2 Periodic boundary conditions	11
2.3 Cut-off and minimum image convention	11
2.4 Non-bonded neighbor lists	15
2.5 Long-range interactions	16
2.6 The QM/MM MD based on ONIOM-XS method.....	17

CONTENTS (Continued)

	Page
2.7 Construction of pair potential functions.....	20
2.8 Selection of QM size, QM method and basis set.....	23
2.9 Simulation details.....	27
2.10 References.....	28
III RESULTS AND DISCUSSION	32
3.1 Structural properties	32
3.2 Dynamical properties.....	48
3.3 References	57
IV CONCLUSIONS	60
APPENDICES	62
APPENDIX A THEORETICAL OBSERVATIONS	63
APPENDIX B LIST OF PRESENTATION	65
APPENDIX C MANUSCRIPT	66
CURRICULUM VITAE	77

LIST OF TABLES

Table	Page
2.1 Optimized parameters of the analytical pair potentials for the interaction of water with CH_3NH_3^+	23
2.2 Stabilization energies and some selected structural parameters of the optimized $\text{CH}_3\text{NH}_3^+(\text{H}_2\text{O})_3$ complex, calculated at the HF, B3LYP, MP2 and CCSD levels of accuracy using the DZP and 6-311++G(d,p) (data in parentheses) basis sets	26
3.1 D values of water molecules in the bulk and in the hydration shells of CH_3NH_3^+ , as obtained by the ONIOM-XS MD simulation.	49
3.2 Mean residence times ($\tau_{\text{H}_2\text{O}}^{t^*}$) of water molecules in the vicinity of CH_3NH_3^+ , calculated within first minimum of the ONIOM-XS MD's N- O_w and H $_N$ - O_w RDFs.....	54
3.3 Vibrational frequencies of water molecules in the hydration shells of CH_3NH_3^+ , K^+ , Ca^{2+} , Na^+ and in the bulk water. (Q_1 , Q_2 and Q_3 corresponding to symmetric stretching, bending, and asymmetric stretching vibrations, respectively).....	57

LIST OF FIGURES

Figure	Page
2.1 The scheme of molecular dynamics simulation	10
2.2 The periodic boundary conditions in two dimensions.....	11
2.3 The spherical cut-off and the minimum image convention.....	12
2.4 A discontinuity of cut-off	13
2.5 The effect of a switching function applied to the Lennard-Jones potential	14
2.6 The non-bonded neighbor list.....	15
2.7 Schematic diagram of the ONIOM-XS method	18
2.8 Movement of H ₂ O around CH ₃ NH ₃ ⁺	21
2.9 Variation of water's orientations	21
2.10 Requirements of CPU times for HF, B3LYP, MP2 and CCSD force calculations of (H ₂ O) _n , n = 1-15, complexes using DZP basis set. All calculations were performed on CCRL cluster with Intel Core ^{TM2} Quad of CPU and 4GB of Ram.....	24
2.11 Requirements of CPU times for HF force calculations of (H ₂ O) _n , n = 1-15, complexes using DZP and aug-cc-pVDZ basis sets. All calculations were performed on CCRL cluster with Intel Core ^{TM2} Quad of CPU and 4GB of Ram.	25

LIST OF FIGURES (Continued)

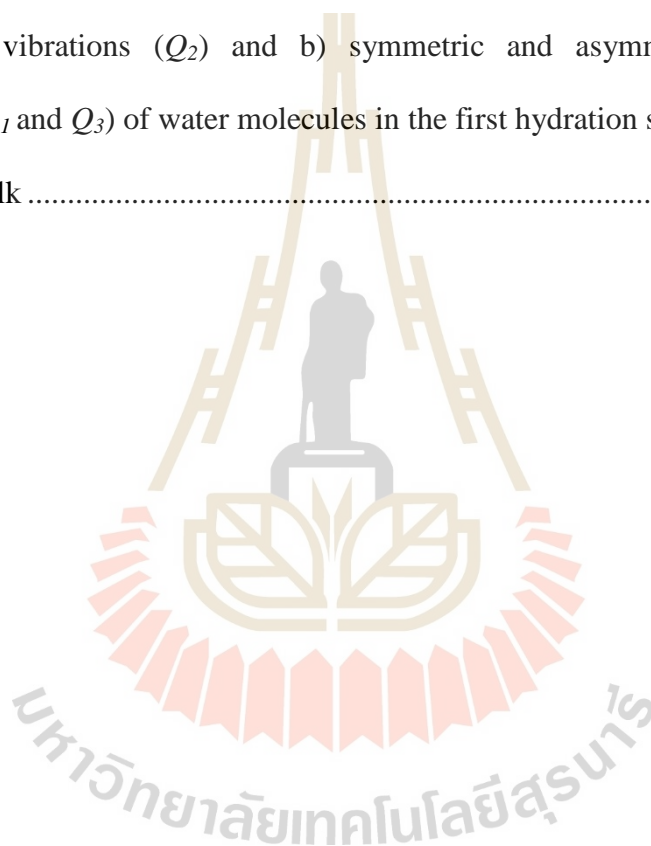
Figure	Page
3.1 a) N-O _w , b) N-H _w , c) H _N -O _w and d) H _N -H _w radial distribution functions and their corresponding integration numbers, as obtained by ONIOM-XS MD simulation.....	34
3.2 a) O-O, b) O-H, c) H-O and d) H-H radial distribution functions and their corresponding integration numbers, as obtained by ONIOM-XS MD simulation of liquid water	36
3.3 a) C-O _w , b) C-H _w , c) H _C -O _w and d) H _C -H _w radial distribution functions and their corresponding integration numbers, as obtained by ONIOM-XS MD simulation.....	38
3.4 Distributions of the coordination numbers of CH ₃ NH ₃ ⁺ , calculated within the first minimum of a) N-O _w and b) C-O _w RDFs.....	40
3.5 Distributions of numbers of HBs at each of -NH ₃ ⁺ hydrogens, calculated within the H _N ...O _w distance of 2.5 Å.....	41
3.6 Distributions of numbers of HBs at hydrophilic side, calculated within the H _N ...O _w distance of 2.5 Å.....	42
3.7 Some selected geometrical arrangements of the CH ₃ NH ₃ ⁺ -water complexes, showing the HB interactions between the -NH ₃ ⁺ hydrogen atoms and their nearest-neighbor waters located within the H _N -O _w distance of 2.5 Å.....	43
3.8 N-H _N ...O _w angular distributions, calculated up to the H _N ...O _w distances of 2.0 and 2.5 Å, respectively.....	44

LIST OF FIGURES (Continued)

Figure	Page
3.9 $H_N-N...O_W$ angular distributions, calculated within the first minimum of the H_N-O_W RDF.....	45
3.10 Probability distributions of θ angle, calculated within the first minimum of the H_N-O_W RDF.....	46
3.11 Distributions of N- H_N , C- H_C and C-N bond lengths of $CH_3NH_3^+$	47
3.12 Distributions of H_N-N-H_N , H_C-C-H_C , H_C-C-N and H_N-N-C angles of $CH_3NH_3^+$	47
3.13 Water exchange in the first solvation shell of each hydrogen atom of $-NH_3^+$, selected only for the first 10 ps of the ONIOM-XS MD simulation.....	50
3.14 Time dependence of the number of water molecules in the first solvation shell of each hydrogen atom of $-NH_3^+$, calculated within the $H_N...O_W$ distance of 2.5 Å and selected only for the first 10 ps of the ONIOM-XS MD simulation	51
3.15 Selected geometrical arrangements of the $CH_3NH_3^+$ -water complexes, showing the HB formations between the $-NH_3^+$ hydrogens and their nearest-neighbor waters (<i>i.e.</i> , the dash lines highlighted in “red”), as well as the HB formations among the first-shell waters (<i>i.e.</i> , the dash lines highlighted in “blue”) and between the first-shell waters and the bulk (<i>i.e.</i> , the dash lines highlighted in “green”). Note that water molecules located outside the $H_N...O_W$ distance of 2.5 Å are colored in “green”	52

LIST OF FIGURES (Continued)

Figure	Page
3.16 Fourier transforms of the hydrogen velocity autocorrelation functions of a) bending vibrations (Q_2) and b) symmetric and asymmetric stretching vibrations (Q_1 and Q_3) of water molecules in the first hydration shell of CH_3NH_3^+ and in the bulk	56



LIST OF ABBREVIATIONS

Å	=	Ångström
ADF	=	Angular distribution function
au	=	Atomic unit
Aug-cc-pVDZ	=	Additional diffuse basis function and correlation consistent polarized valence double zeta
B3LYP	=	Becke three-parameter hybrid functional combined with Lee-Yang-Parr correlation function
BJH	=	Flexible water model developed by Bopp, Jancsó and Heinzinger
BLYP	=	Becke hybrid functional combined with Lee-Yang-Parr correlation function
CH ₃ NH ₃ ⁺	=	Methylammonium ion
CCSD	=	Coupled cluster calculations using both single and double substitutions from Hartree-Fock determinant
cm ⁻¹	=	Wavenumber
CN	=	Coordination number
CPMD	=	Car-Parrinello molecular dynamics

LIST OF ABBREVIATIONS (Continued)

CPU	=	Central processing unit
D	=	Self-diffusion coefficient
DFT	=	Density functional theory
DZP	=	Double zeta plus polarization
e	=	Electron charge
E_{tot}	=	Total interaction energy
E_{MM}	=	Interactions within MM region
E_{QM-MM}	=	Interactions between QM and MM regions
$E^{ONIOM-XS}$	=	The potential energy of the entire system for ONIOM-XS
<i>etc</i>	=	et cetera
F_i	=	Force acting on each particle
F_{MM}	=	MM force
F_{QM}	=	QM force
fs	=	Femtosecond
HF	=	Hartree-Fock
K	=	Kelvin
kcal/mol	=	Kilocalorie per mole
l	=	Number of particles in the switching layer
MC	=	Monte Carlo
MD	=	Molecular dynamics

LIST OF ABBREVIATIONS (Continued)

MM	=	Molecular mechanics
MO	=	Molecular orbital
MP2	=	Second-order Møller-Plesset
MRT	=	Mean residence times
m	=	Mass
m_e	=	Mass of electron
m_k	=	Mass of nucleus
n_1	=	Number of particles in the QM sphere
n_2	=	Number of particle in the MM region
N_{ex}	=	Number of exchange events
ONIOM	=	Own N-layered Integrated molecular Orbital and molecular Mechanics
ps	=	Picosecond
QM	=	Quantum mechanics
QM/MM	=	Combined quantum mechanics/molecular mechanics
RDF	=	Radial distribution function
RHF	=	Restricted Hartree-Fock
r_0	=	Distance characterizing the start of QM region
r_1	=	Distance characterizing the end of QM region
r_{min}	=	First minimum of RDF peak

LIST OF ABBREVIATIONS (Continued)

r_{max}	=	First maximum of RDF peak
SCF	=	Self-consistent field
SPC/E	=	Simple point charge effective pair water model
VACF	=	Velocity autocorrelation functions
μ	=	Chemical potential
Φ	=	Trial function
o	=	Degree
τ_{H_2O}	=	MRT of water molecules
λ	=	Wavelength
t^*	=	Time for observing the number of exchange water
t_{sim}	=	Simulation time
$\chi(x)$	=	Spin orbital
∇^2	=	Laplacian operator

CHAPTER I

INTRODUCTION

1.1 Literature reviews

Methylammonium ion (CH_3NH_3^+) have a relationship in the methyltransferases which are enzymes that facilitate the transfer of methyl group to specific nucleophilic site on protein, nucleic acids and other biomolecules. Moreover CH_3NH_3^+ has been used to light adsorbent in the perovskite photovoltaic cell. Protonated amino groups ($-\text{NH}_3^+$) are the most common positively charged moieties in many biologically important molecules, such as amino acids and peptides (Andrade, O'Donoghue and Rost, 1998; Wolff, 1979). With regard to the protonated amines (RNH_3^+), CH_3NH_3^+ can be considered as a simple model in which the details with respect to the CH_3NH_3^+ -water hydrogen bonds (HBs) are essential in order to understand many biological processes that involve the $-\text{NH}_3^+$ species (Alagona, Ghio and Kollman, 1986; Chuev, Valiev and Fedotova, 2012; Fedotova and Kruchinin, 2012; Hesske and Gloe, 2007; Jorgensen and Gao, 1986; Kim, Cho and Boo, 2001; Kim, Han, Cho, Lee and Boo, 2006; Meng, Caldwell and Kollman, 1996; van Mourik and van Duijneveldt, 1995). Of particular interest, according to the amphiphilic nature of CH_3NH_3^+ which consists of hydrophilic ($-\text{NH}_3^+$) and hydrophobic ($-\text{CH}_3$) moieties, it is expected that the HB networks formed around the CH_3NH_3^+ ion are somewhat different from those of hydrophilic ion cores, such as ammonium (NH_4^+) or hydronium (H_3O^+) ions. Basically, when ions interact with the surrounding water molecules, the effects of the ions on the local structure and dynamics of the solvent's HB networks are usually discussed with respect to the "structure-making" and "structure-breaking" of the ions. In general, ions with small size and high charge density are usually defined as "structure-maker", while those with larger

size and more polarizable charge density are classified as “structure-breaker”, *i.e.*, they are regarded as a perturbation of the water’s HB networks.

In the literature, most of the published data regarding the determination of CH_3NH_3^+ in aqueous solution were obtained from Monte Carlo (MC) and molecular dynamics (MD) simulations. For example, an early MC simulation of CH_3NH_3^+ in aqueous solution using the TIP4P potential for water and analogous potentials for the ion (Thaomola, Tongraar and Kerdcharoen, 2012) has reported that the $-\text{NH}_3^+$ group has an average coordination number (CN) of 3.5, which corresponds to one water molecule closely attached to each H atom. In this respect, water molecules in the first solvation shell have both lone pairs directed toward the $-\text{NH}_3^+$ group, *i.e.*, implying that only their hydrogen atoms are available for coordinating to bulk water. The average number of HBs to bulk water of each first-shell water molecule is 1.88. For the hydrophobic side, the numbers of water molecules near the $-\text{CH}_3$ group can be varied from 12 to 15 (depending on the choice of the minimum position). In the meantime, another MC simulation using the OPLS potential functions (Jorgensen and Gao, 1986) has suggested that the CH_3NH_3^+ species participated in 4 strong HBs with water molecules, consisting of about 1.24 primary water molecules for each H atom of $-\text{NH}_3^+$, while the primary region around the $-\text{CH}_3$ group contains about 8.6 water molecules. Later, according to the MD simulations of aqueous CH_3NH_3^+ solution using a pairwise additive SPC/E model and a related polarizable model (POL3) for water (Meng and Kollman, 1996), the average hydration numbers of 3.67 and 3.60 were found for the hydrophilic group of CH_3NH_3^+ , respectively. This corresponds to the average numbers of 1.22 and 1.20 water molecules at each H atom of the $-\text{NH}_3^+$ group, respectively. In the hydrophobic region, the $-\text{CH}_3$ group contains about 9.33 and 9.36 water molecules, respectively. With regard to the earlier MC and MD studies, the observed discrepancies could be ascribed to the use of different molecular mechanical (MM) potentials, most of which were constructed with respect to the simplified effects of many-body interactions.

Thus, more sophisticated simulation techniques which take into account the importance of “quantum effects” seem to be necessary in order to obtain more accurate descriptions of such condensed-phase systems.

Based on the *ab initio* MD frameworks, a Car-Parrinello (CP) MD simulation study of aqueous CH_3NH_3^+ solution (Hesske and Gloe, 2007) has reported that the first hydration shell of the $-\text{NH}_3^+$ group contains 4.2 water molecules. In this respect, oxygen atoms of three water molecules are localized along the direction of the N-H bond and form HBs, while another nearest-neighbor water molecule is weakly bound and is not fixed within the first hydration shell. The CP-MD approach has a major advantage over the MM-based MC and MD techniques since the overall system’s interactions can directly be obtained from quantum mechanics (QM) calculations, and hence it can produce more reliable results. However, some methodical limitations of the CP-MD technique stem from the use of simple generalized gradient approximation (GGA) functionals, such as BLYP, and of the relatively small system size. It has been well demonstrated that the use of simple density functionals in the CP-MD scheme could result in improper structural and dynamical properties even for the pure liquid water (Grossman, Schwegler, Draeger, Gygi and Galli, 2003; Todorova, Seitsonen, Hutter, Kuo and Mundy, 2006; Yoo, Zeng and Xantheas, 2009). In particular, it has been shown that the use of the BLYP functional leads to a strongly decreased self-diffusion coefficient of this peculiar liquid (Todorova, Seitsonen, Hutter, Kuo and Mundy, 2006). Besides the full *ab initio* MD techniques, an alternative approach is to apply a so-called combined QM/MM MD technique based on the ONIOM-XS (Own N-layered Integrated Molecular Orbital and Molecular Mechanics – Extension to Solvation) method, called briefly ONIOM-XS MD (Kerdcharoen and Morokuma, 2003, 2002). This technique has been successfully applied for studying various condensed phase systems (Kabbalee, Sripa, Tongraar and Kerdcharoen, 2015; Kabbalee, Tongraar and Kerdcharoen, 2015; Kerdcharoen and Morokuma, 2003, 2002; Sripa, Tongraar and

Kerdcharoen, 2016, 2013, 2015; Sripradite, Tongraar and Kerdcharoen, 2015; Thaomola, Tongraar and Kerdcharoen, 2012; Wanprakhon, Tongraar and Kerdcharoen, 2011). Of particular interest, in the case of liquid water, the results obtained by the ONIOM-XS MD simulation (Thaomola, Tongraar and Kerdcharoen, 2012) have provided more insights into the multiple HB species among water molecules which correspond to the experimental XAS data for the arrangement of one strong and one weak (for both donor and acceptor), rather than the equivalent two donors and two acceptors tetrahedral structure. Recently, the ONIOM-XS MD technique has been successfully applied for characterizing the “structure-making” and “structure-breaking” abilities of some essential metal ions in water (Sripa, Tongraar and Kerdcharoen, 2016, 2013, 2015; Wanprakhon, Tongraar and Kerdcharoen, 2011), showing its capability in predicting more reliable results, especially when compared to those derived by the conventional QM/MM MD scheme. In this study, it is of particular interest, therefore, to apply the high-level ONIOM-XS MD technique for studying the characteristics of CH_3NH_3^+ in aqueous solution.

1.2 Research objectives

1. To apply the high-level ONIOM-XS MD technique for studying the solvation structure and dynamics of CH_3NH_3^+ in aqueous electrolyte solution.
2. To test the validity of the ONIOM-XS MD technique for studying such complicated system, namely the amphiphilic species which consist of hydrophilic and hydrophobic moieties solvated in aqueous electrolyte solution.

1.3 Scope and limitation of the study

In this work, the high-level ONIOM-XS MD technique will be applied to the system of CH_3NH_3^+ in liquid water. The system will be partitioned into a small (most important)

QM region, *i.e.*, a sphere which contains the CH_3NH_3^+ ion and its surrounding water molecules, and the MM region, *i.e.*, the bulk water. Within the QM region, all interactions will be evaluated by performing *ab initio* calculations at the Hartree-Fock (HF) level of accuracy using the DZP basis set (Dunning and Hay, 1977), whereas the interactions within the MM and between the QM and MM regions will be described by means of MM force fields. In this work, the MM potentials for describing the interactions between the CH_3NH_3^+ ion and water molecules will be newly developed, while the water-water interactions are described by means of the flexible BJH-CF2 model (Bopp, Jancsó and Heinzinger, 1983). The structural properties of the CH_3NH_3^+ hydrates will be analyzed through the plots of radial distribution functions (RDFs) and their corresponding integration numbers, together with the angular distribution functions (ADFs) of the ion-water complexes and the dipole-oriented arrangements of water molecules surrounding the ion. The dynamics details will be characterized through self-diffusion coefficient (D), mean residence times (MRTs) of water molecules and the water exchange processes at the ion.

1.4 References

- Alagona, G., Ghio, C. and Kollman, P. (1986). Monte Carlo simulation studies of the solvation of ions. 1. Acetate anion and methylammonium cation. **Journal of the American Chemical Society**. 108: 185-191.
- Andrade, M. A., O'Donoghue, S. I. and Rost, B. (1998). Adaptation of protein surfaces to subcellular location. **Journal of Molecular Biology**. 276: 517-525.
- Bopp, P., Jancsó, G. and Heinzinger, K. (1983). An improved potential for non-rigid water molecules in the liquid phase. **Chemical Physics Letters**. 98: 129-133.
- Chuev, G. N., Valiev, M. and Fedotova, M. V. (2012). Integral equation theory of molecular solvation coupled with quantum mechanical/molecular mechanics

- method in NWChem package. **Journal of Chemical Theory and Computation**. 8: 1246-1254.
- Dunning, J. T. H. and Hay, P. J. (1977). Methods of electronic structure theory. **III, Plenum, New York.**
- Fedotova, M. V. and Kruchinin, S. E. (2012). Hydration of methylamine and methylammonium ion: Structural and thermodynamic properties from the data of the integral equation method in the RISM approximation. **Russian Chemical Bulletin**. 61: 240-247.
- Grossman, J. X., Schwegler, E., Draeger, E. W., Gygi, F. and Galli, G. (2003). Towards an assessment of the accuracy of density functional theory for first principles simulations of water. **The Journal of Chemical Physics**. 120: 300-311.
- Hesske, H. and Gloe, K. (2007). Hydration behavior of alkyl amines and their corresponding protonated forms. 1. Ammonia and methylamine. **The Journal of Physical Chemistry A**. 111: 9848-9853.
- Jorgensen, W. L. and Gao, J. (1986). Monte Carlo simulations of the hydration of ammonium and carboxylate ions. **The Journal of Physical Chemistry**. 90: 2174-2182.
- Kabbalee, P., Tongraar, A. and Kerdcharoen, T. (2015). Preferential solvation and dynamics of Li^+ in aqueous ammonia solution: An ONIOM-XS MD simulation study. **Chemical Physics**. 446: 70-75.
- Kabbalee, P., Sripan, P., Tongraar, A. and Kerdcharoen, T. (2015). Solvation structure and dynamics of K^+ in aqueous ammonia solution: Insights from an ONIOM-XS MD simulation. **Chemical Physics Letters**. 633: 152-157.
- Kerdcharoen, T. and Morokuma, K. (2002). ONIOM-XS: An extension of the ONIOM method for molecular simulation in condensed phase. **Chemical Physics Letters**. 355: 257-262.

- Kerdcharoen, T. and Morokuma, K. (2003). Combined quantum mechanics and molecular mechanics simulation of Ca^{2+} /ammonia solution based on the ONIOM-XS method: Octahedral coordination and implication to biology. **The Journal of Chemical Physics**. 118: 8856-8862.
- Kim, K.-Y., Cho, U.-I. and Boo, D. W. (2001). *Ab initio* study on structures, energies and vibrations of methylammonium-(water)_n (n=1-3) complexes. **Bulletin of the Korean Chemical Society**. 22: 597-604.
- Kim, K.-Y., Han, W.-H., Cho, U.-I., Lee, Y. T. and Boo, D. W. (2006). *Ab initio* and vibrational predissociation studies on methylammonium-(water)₄ complex: evidence for multiple cyclic and non-cyclic hydrogen-bonded structures. **Bulletin of the Korean Chemical Society**. 27: 2028-2036.
- Meng, E. C. and Kollman, P. A. (1996). Molecular dynamics studies of the properties of water around simple organic solutes. **The Journal of Physical Chemistry**. 100: 11460-11470.
- Meng, E. C., Caldwell, J. W. and Kollman, P. A. (1996). Investigating the anomalous solvation free energies of amines with a polarizable potential. **The Journal of Physical Chemistry**. 100: 2367-2371.
- Sripa, P., Tongraar, A. and Kerdcharoen, T. (2013). "Structure-making" ability of Na^+ in dilute aqueous solution: An ONIOM-XS MD simulation study. **The Journal of Physical Chemistry A**. 117: 1826-1833.
- Sripa, P., Tongraar, A. and Kerdcharoen, T. (2015). Structure and dynamics of the Li^+ hydrates: A comparative study of conventional QM/MM and ONIOM-XS MD simulations. **Journal of Molecular Liquids**. 208: 280-285.
- Sripa, P., Tongraar, A. and Kerdcharoen, T. (2016). Characteristics of K^+ and Rb^+ as "structure-breaking" ions in dilute aqueous solution: Insights from ONIOM-XS MD simulations. **Chemical Physics**. 479: 72-80.

- Sripradite, J., Tongraar, A. and Kerdcharoen, T. (2015). Solvation structure and dynamics of Na^+ in liquid ammonia studied by ONIOM-XS MD simulations. **Chemical Physics**. 463: 88-94.
- Thaomola, S., Tongraar, A. and Kerdcharoen, T. (2012). Insights into the structure and dynamics of liquid water: A comparative study of conventional QM/MM and ONIOM-XS MD simulations. **Journal of Molecular Liquids**. 174: 26-33.
- Todorova, T., Seitsonen, A. P., Hutter, J., Kuo, F. W. and Mundy, C. J. (2006). Molecular dynamics simulation of liquid water: Hybrid density functionals. **The Journal of Physical Chemistry B**. 110: 3685 - 3691.
- van Mourik, T. and van Duijneveldt, F. B. (1995). *Ab initio* calculations on the C-H...O hydrogen-bonded systems $\text{CH}_4\text{-H}_2\text{O}$, $\text{CH}_3\text{NH}_2\text{-H}_2\text{O}$ and $\text{CH}_3\text{NH}_3^+\text{-H}_2\text{O}$. **Journal of Molecular Structure: THEOCHEM**. 341: 63-73.
- Wanprakhon, S., Tongraar, A. and Kerdcharoen, T. (2011). Hydration structure and dynamics of K^+ and Ca^{2+} in aqueous solution: Comparison of conventional QM/MM and ONIOM-XS MD simulations. **Chemical Physics Letters**. 517: 171-175.
- Wolff, M. (1979). The Basis of Medicinal Chemistry, **Burger's Medicinal Chemistry**, 4th Ed., Wiley, New York.
- Yoo, S., Zeng, X. C. and Xantheas, S. S. (2009). On the phase diagram of water with density functional theory potentials: The melting temperature of ice I_h with the Perdew–Burke–Ernzerhof and Becke–Lee–Yang–Parr functionals. **The Journal of Chemical Physics**. 130: 221102-221104.

CHAPTER II

COMPUTATIONAL METHODS AND RESEARCH PROCEDURES

2.1 Introduction to molecular dynamics (MD) simulation

In general, the simulation techniques can be classified into 2 types, namely, Monte Carlo (MC) and molecular dynamics (MD). The MD technique is widely used, especially for the study of condensed phase systems, since this technique can provide microscopic details related to time-dependent system's behaviors. The performance of the MD simulation is based on Newton's second law, $F = ma$, where F is the force on the particle, m is its mass, and a is its acceleration. According to the schematic details of the MD simulation shown in Figure 2.1, the simulation starts with reading in the starting configurations, velocities, accelerations and forces. In practice, since there are no explicitly time-dependent or velocity dependent forces that shall act on the system, the time integration algorithms will be employed to obtain the details of positions, velocities and accelerations of two successive time steps. The energy of the system can be obtained from either molecular mechanics (MM) or quantum mechanics (QM) calculations. The force on each atom in the system can be derived from the derivative of the energy with respect to the change in the atom's position. All particles in the system will be moved by their new forces to the new configurations. This process will be repeated until the system reaches its equilibrium. After that, the coordinates, velocities, accelerations, forces and so on of all particles in the system will be collected for further structural and dynamical property calculations.

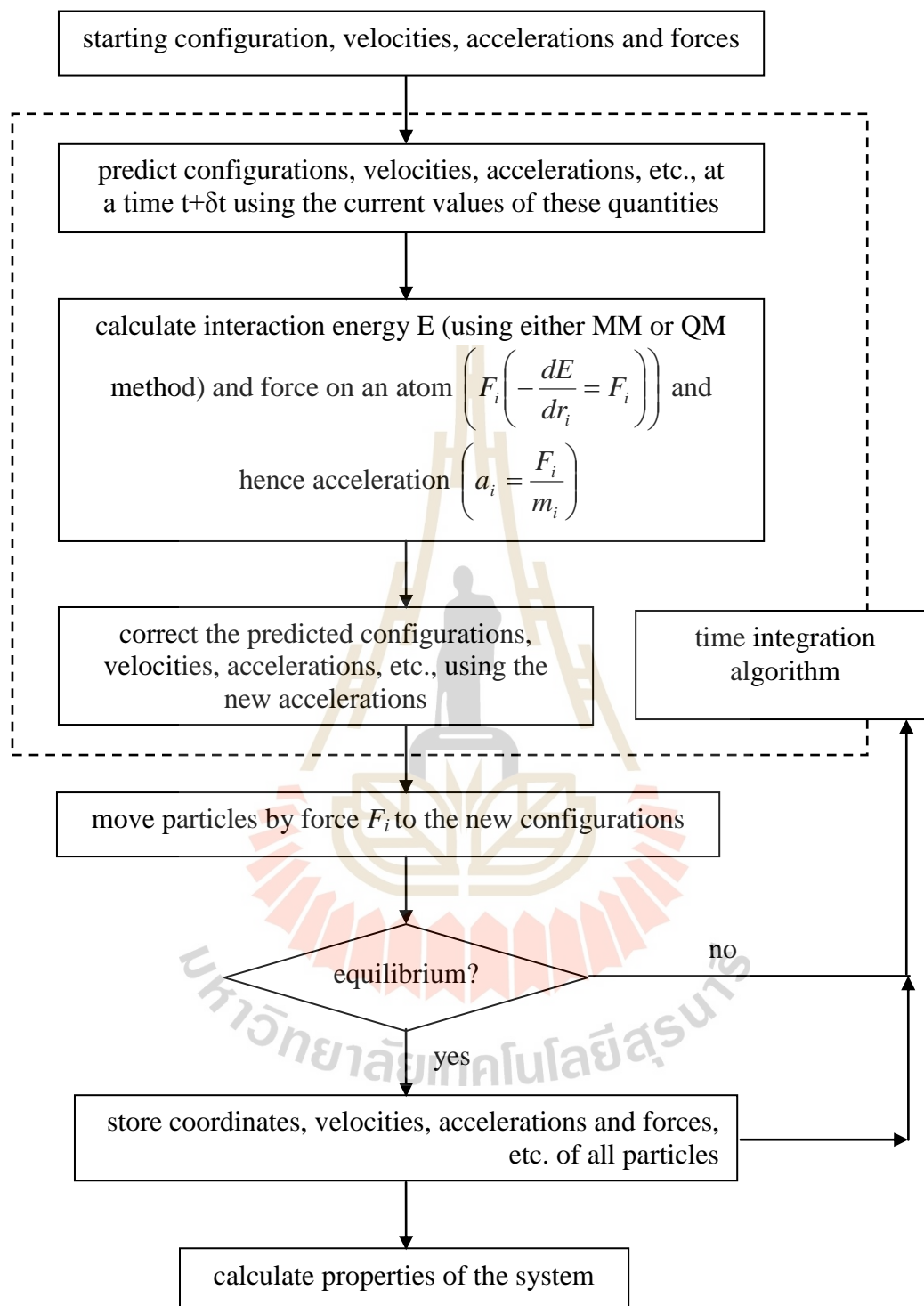


Figure 2.1 The scheme of molecular dynamics simulation.

2.2 Periodic boundary conditions

Since most of computer simulations make use of a small system size, this leads to the surface effects, *i.e.*, the interactions occur between the particles and the wall, and thus this reflects in wrong systems' properties. Such problem can be solved by using the periodic boundary (PB) conditions, as depicted in Figure 2.2.

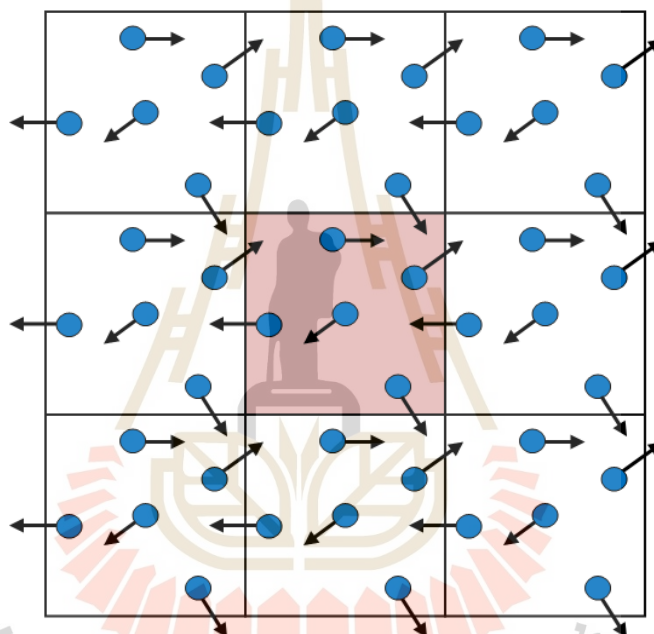


Figure 2.2 The periodic boundary conditions in two dimensions.

The main advantage of the PB condition is that the number of particles within the central box remains constant. According to the PB conditions, when the particle leaves the central box, its duplicate particle will enter from the opposite side at the same time.

2.3 Cut-off and minimum image convention

With regard to the system energy's calculations, the non-bonded interactions are conceptually calculated between every pair of atoms in the system. Hence, the most time

consuming of the simulation refers to the calculations of the non-bonded energies and forces. To solve this problem, the minimum image convention is introduced in which only the nearest images of the distinguishable particles are taken into account, as shown in Figure 2.3.

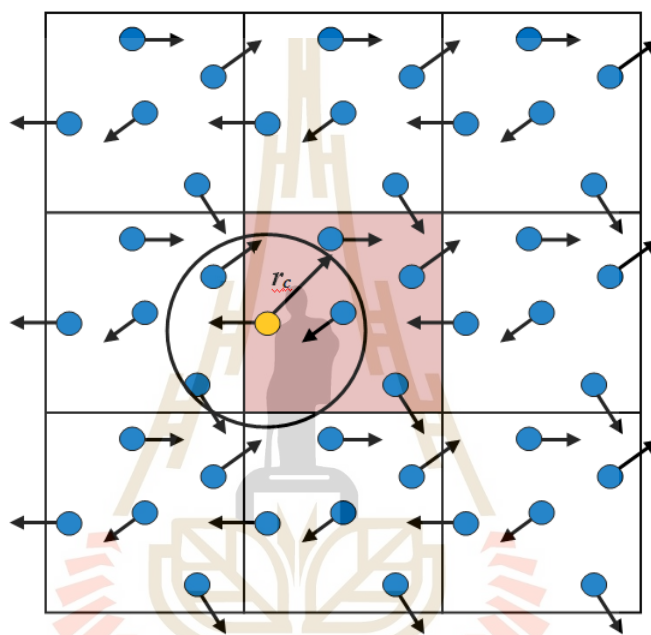


Figure 2.3 The spherical cut-off and the minimum image convention.

By using the cut-off, the interactions between all pairs of atoms that are further apart from the cut-off value are set to zero. In general, the cut-off distance should not be greater than half of the length of their image. Nevertheless, the use of cut-off leads to another serious problem in the simulation.

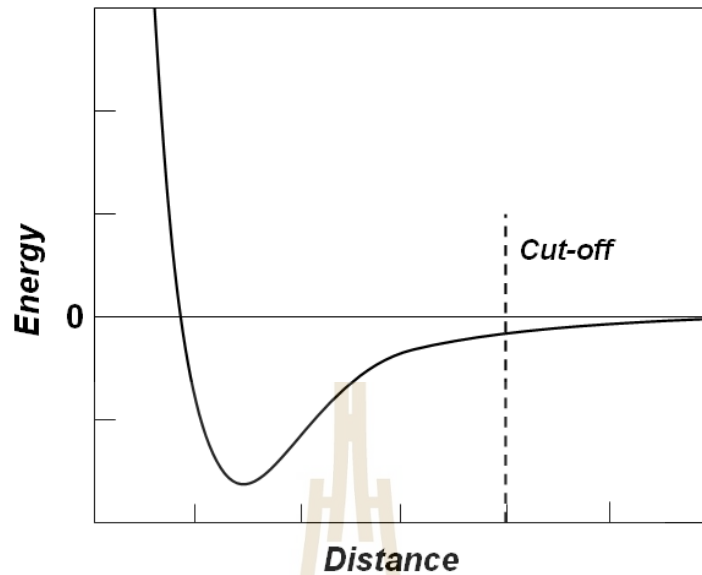


Figure 2.4 A discontinuity of cut-off.

According to the use of cut-off limit, this results in the discontinuity in both the potential energy and the force beyond the cut-off distance, as depicted in Figure 2.4. This problem can be solved by shifting the potential function by an amount V_c ,

$$V'(r) = \begin{cases} V(r) - V_c & \text{if } r \leq r_c \\ 0 & \text{if } r > r_c \end{cases}, \quad (2.1)$$

where r_c is the cut-off distance and V_c corresponds to the value of the potential at the cut-off distance. Note that, although the energy conservation can be improved by the shifted potential, the discontinuity in the force due to the shifted potential still exists. At the cut-off distance, since the force will have a finite value, a suitable shifted potential would be of the form

$$V'(r) = \begin{cases} V(r) - V_c - \left(\frac{dV(r)}{dr} \right)_{r=r_c} (r - r_c) & \text{if } r \leq r_c \\ 0 & \text{if } r > r_c \end{cases} \quad (2.2)$$

In practice, the application of shifted potential is not easy for inhomogeneous systems containing many different types of atom. Thus, an alternative way is to eliminate discontinuities in the energy and force by using a *switching function*. The switched potential ($V^{SF}(r)$) is related to the true potential ($V(r)$) as

$$V'(r) = V(r)S(r). \quad (2.3)$$

Several switching functions are applied to the entire range of the potential up to the cut-off point. In general, the switching function has a value of 1 at $r = 0$ and a value of 0 at $r = r_c$, while the switching function values between two cut-offs are varied. The example of a switching function applied to the Lennard-Jones potential is shown in Figure 2.5.

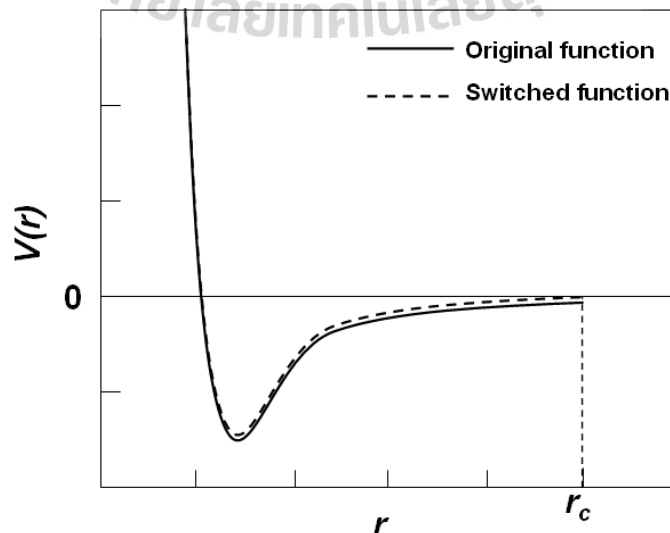


Figure 2.5 The effect of a switching function applied to the Lennard-Jones potential.

2.4 Non-bonded neighbor lists

With regard to the system energy's calculations, since the distance between every pair of atoms still have to be calculated in each simulation step, the use of cut-off and minimum image convention is not actually reduce the time for calculating the non-bonded interactions. According to the fact that most of atoms move within a time step of less than 0.2 \AA , *i.e.*, the local neighbors of a given atom remain almost the same for many time steps, the *non-bonded neighbor list* as shown in Figure 2.6 is employed. The first non-bonded neighbor list has been proposed by Verlet (Verlet, 1967). The Verlet neighbor list stores all atoms within the cut-off distance (r_c) and atoms are slightly further away than the cut-off distance (r_m). The neighbor list will frequently be updated throughout the simulation. With regard to this point, the distance used to calculate each atom's neighbors should be slightly larger than the actual cut-off distance in order to ensure that the atoms outside the cut-off will not move closer than the cut-off distance before the neighbor list is updated again.

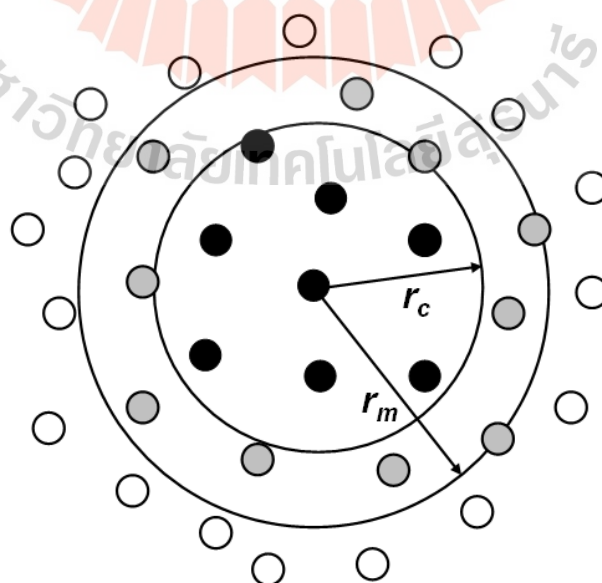


Figure 2.6 The non-bonded neighbor list.

2.5 Long-range interactions

The neglect of interactions beyond the cut-off distance, especially for the strong interacting systems, may result in an incorrect description of molecular properties. One simple way to treat the long-range interactions is to use a large simulation cell, but this reflects in more time-consuming. There are many suitable methods for the treatment of long-range interactions. The first method is the Ewald summation method, which was derived by Ewald in 1921 (Ewald, 1921). This method has been applied to study the energetic of ionic crystals, *i.e.*, a particle interacts with all the other particles in the simulation box and with all of their images in an infinite array of periodic cells. The charge-charge contribution to the potential energy of the Ewald summation method could be of the form

$$V = \frac{1}{2} \sum'_{\mathbf{n}=0} \sum_{i=1}^N \sum_{j=1}^N \frac{q_i q_j}{4\pi\epsilon_0 |r_{ij} + \mathbf{n}|}, \quad (2.4)$$

where the prime on the first summation indicates that the series does not include the interaction $i = j$ for $\mathbf{n} = 0$, q_i and q_j are charges and \mathbf{n} is a cubic lattice point. The Ewald summation method is the most correct way to accurately include all the effects of long-range forces in the computer simulation. Nevertheless, this method is rather expensive to implement since the equation (2.4) converges extremely slowly.

Another method for the treatment of long-range interactions is the *reaction field method* (Foulkes and Haydock, 1989). This method constructs the sphere around the molecule with a radius equal to the cut-off distance. By this scheme, all interactions within the sphere are calculated explicitly, while those outside of the sphere are modeled as a homogeneous medium of dielectric constant (ϵ_s). The electrostatic field due to the surrounding dielectric is given by

$$E_i = \frac{2(\varepsilon_s - 1)}{\varepsilon_s + 1} \left(\frac{1}{r_c^3} \right) \sum_{j; r_{ij} \leq r_c} \mu_j, \quad (2.5)$$

where μ_j are the dipoles of the neighboring molecules that are located within the cut-off distance (r_c) of the molecules i . The interaction between molecule i and the reaction field equals to $E_i \cdot \mu_i$.

2.6 The QM/MM MD based on ONIOM-XS method

The ONIOM-XS (Own N-layered Integrated Molecular Orbital and Molecular Mechanics – Extension to Solvation) MD technique (Kerdcharoen and Morokuma, 2003, 2002) has been successfully applied for studying various condensed phase systems (Kabbalee, Sripa, Tongraar and Kerdcharoen, 2015; Kabbalee, Tongraar and Kerdcharoen, 2015; Kerdcharoen and Morokuma, 2003, 2002; Sripa, Tongraar and Kerdcharoen, 2016, 2013, 2015; Sripradite, Tongraar and Kerdcharoen, 2015; Thaomola, Tongraar and Kerdcharoen, 2012; Wanprakhon, Tongraar and Kerdcharoen, 2011). By the ONIOM-XS MD technique, the system is divided into a “high-level” QM region, *i.e.*, a sphere which contains the CH_3NH_3^+ ion and its surrounding water molecules, and the “low-level” MM region, *i.e.*, the bulk water. A thin switching shell located between the QM and MM regions is introduced to ensure a smooth transition due to the solvent exchange. (cf. Figure 2.7)

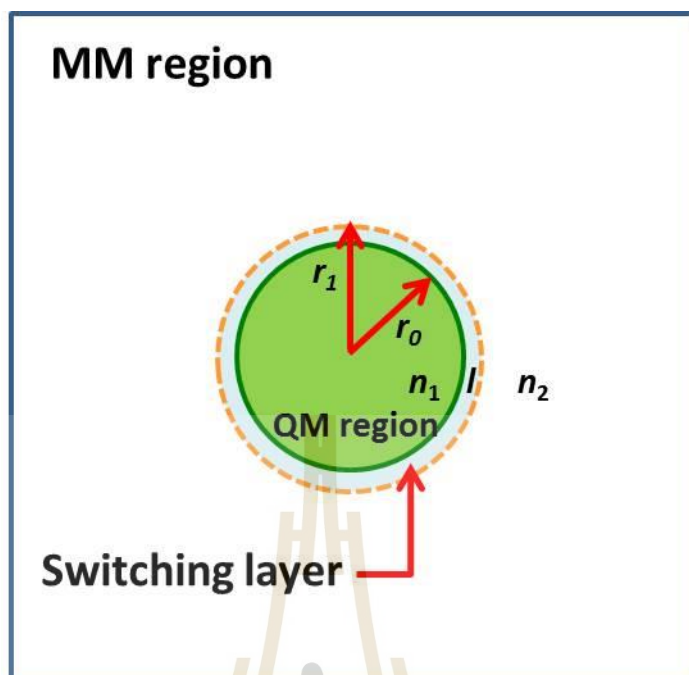


Figure 2.7 Schematic diagram of the ONIOM-XS method
(Kerdcharoen and Morokuma, 2002).

Given n_1 , l and n_2 as the number of particles in the QM region, the switching shell and the MM region, respectively, and $N (=n_1+l+n_2)$ is the total number of particles, the potential energy of the system can be written in two ways according to the ONIOM extrapolation scheme (Svensson, Humbel, Froese, Matsubara, Sieber and Morokuma, 1996). If the switching layer is included into the high-level QM sphere, the energy expression is defined as

$$E^{\text{ONIOM}}(n_1+l; N) = E^{\text{QM}}(n_1+l) - E^{\text{MM}}(n_1+l) + E^{\text{MM}}(N). \quad (2.6)$$

Otherwise, if the switching layer is considered as part of the low-level MM subsystem, the energy expression is written as

$$E^{\text{ONIOM}}(n_1; N) = E^{\text{QM}}(n_1) - E^{\text{MM}}(n_1) + E^{\text{MM}}(N). \quad (2.7)$$

In Equations (2.6) and (2.7), the E^{QM} and E^{MM} terms represent the interactions derived by the QM calculations and by the classical MM force fields, respectively. In this respect, since the interactions between the QM and MM regions are also described by means of the MM potentials, these contributions are already included in the $E^{\text{MM}}(N)$. In the performance of the ONIOM-XS MD simulation, when a particle moves into the switching layer (either from the QM or MM region), both Equations (2.6) and (2.7) will be evaluated. The potential energy of the entire system is taken as a hybrid between both energy terms (2.6) and (2.7),

$$E^{\text{ONIOM-XS}}(\{r_i\}) = (1 - \bar{s}(\{r_i\})) \cdot E^{\text{ONIOM}}(n_1 + l; N) + \bar{s}(\{r_i\}) \cdot E^{\text{ONIOM}}(n_1; N), \quad (2.8)$$

where $\bar{s}(\{r_i\})$ is an average over a set of switching functions for individual exchanging particle in the switching shell $s_i(x_i)$ (Tasaki, McDonald and Brady, 1993),

$$\bar{s}(\{r_i\}) = \frac{1}{l} \sum_{i=1}^l s_i(x_i). \quad (2.9)$$

In general, the switching function applied in Equation (2.9) can be of any form. In this study, a polynomial expression is employed,

$$s_i(x_i) = 6\left(x_i - \frac{1}{2}\right)^5 - 5\left(x_i - \frac{1}{2}\right)^3 + \frac{15}{8}\left(x_i - \frac{1}{2}\right) + \frac{1}{2}, \quad (2.10)$$

where $x_i = ((r_i - r_0)/(r_1 - r_0))$, and r_0 and r_1 are the radius of inner and outer surfaces of the switching shell, respectively, and r_i is the distance between the center of mass of the exchanging particle and the center of the QM sphere. Finally, the gradient of the energy can be written as

$$\begin{aligned} \nabla_R E^{ONIOM-XS}(\{r_i\}) = & (1 - \bar{s}(\{r_i\})) \cdot \nabla_R E^{ONIOM}(n_i + l; N) + \bar{s}(\{r_i\}) \\ & \cdot \nabla_R E^{ONIOM}(n_i; N) + \frac{1}{(r_1 - r_0)} \nabla \bar{s}(\{r_i\}) \\ & \cdot (E^{ONIOM}(n_i; N) - E^{ONIOM}(n_i + l; N)). \end{aligned} \quad (2.11)$$

2.7 Construction of pair potential functions

In this study, the pair potential functions for describing $\text{CH}_3\text{NH}_3^+ - \text{H}_2\text{O}$ interactions were newly constructed. A set of $\text{CH}_3\text{NH}_3^+ - \text{H}_2\text{O}$ configurations was generated by moving water molecule around the CH_3NH_3^+ ion according to the variations of θ (*i.e.* between 0° and 180°) and Φ (*i.e.* between 0° and 360°) angles, as depicted in Figure 2.8. Along with the variations of θ and Φ angles, 30 different types of water's orientations were employed (see Figure 2.9).

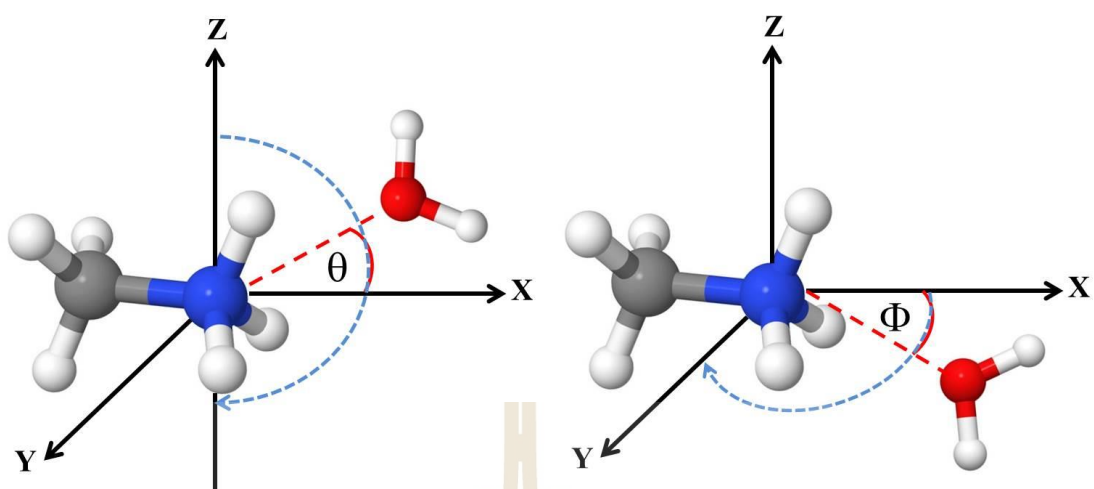


Figure 2.8 Movement of H_2O around CH_3NH_3^+ .

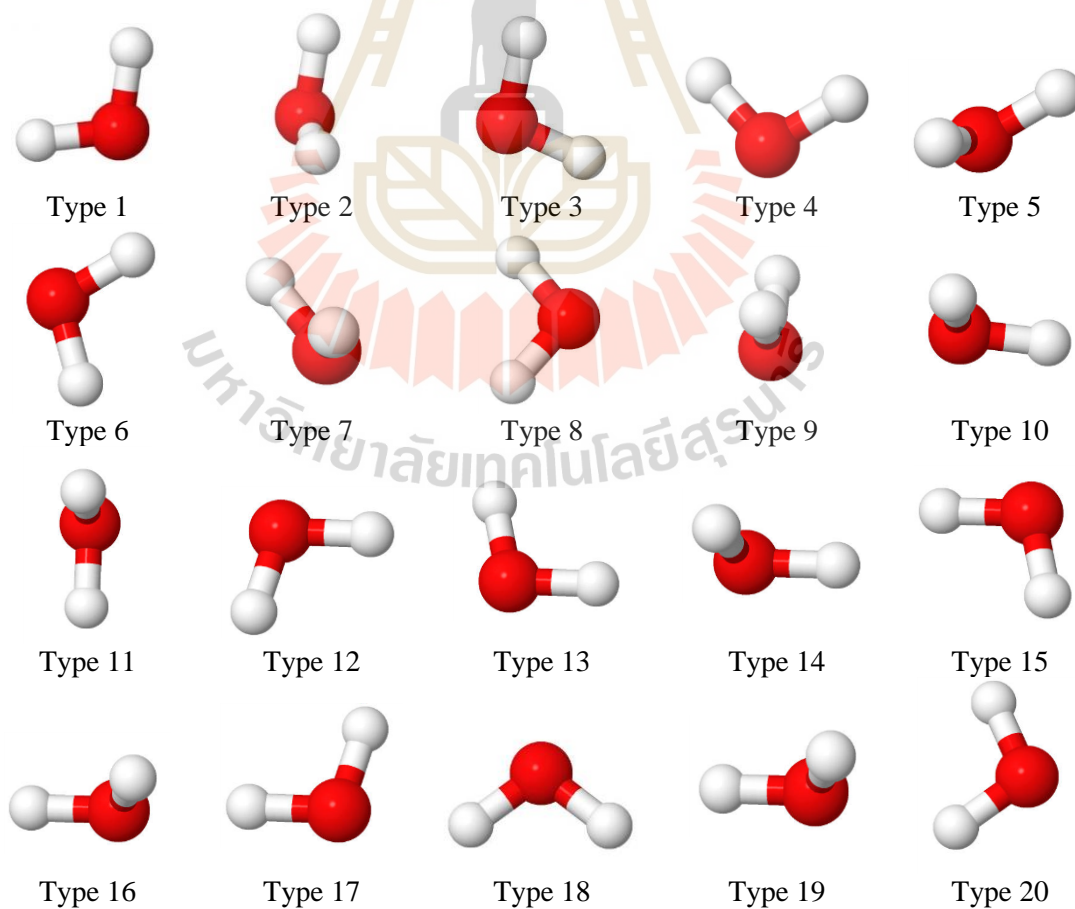


Figure 2.9 Variation of water's orientations.

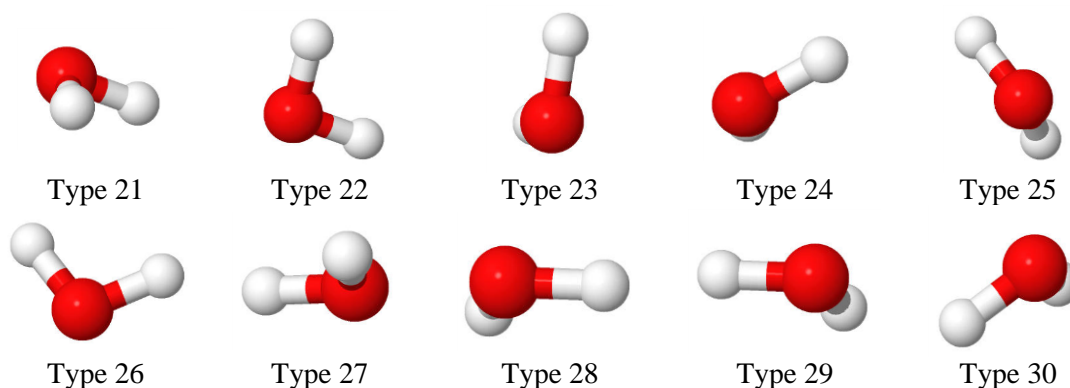


Figure 2.9 (Continued) Variation of water's orientations.

The 57,034 HF interaction energy points for various $\text{CH}_3\text{NH}_3^+-\text{H}_2\text{O}$ configurations, obtained from Gaussian03 calculations (Frisch et al., 2005), using the DZP basis set (Dunning, 1989) for water and CH_3NH_3^+ were fitted to the analytical forms of

$$\Delta E_{\text{CH}_3\text{NH}_3^+-\text{H}_2\text{O}} = \sum_{i=1}^7 \sum_{j=1}^3 \left[\frac{A_{ij}}{r_{ij}^4} + \frac{B_{ij}}{r_{ij}^5} + \frac{C_{ij}}{r_{ij}^6} + \frac{D_{ij}}{r_{ij}^{12}} + \frac{q_i q_j}{r_{ij}} \right] \quad (2.12)$$

where A , B , C and D are the fitting parameters (see Table 2.1), r_{ic} denotes the distances between the ion and the i -th atom of water, and q_i and q_j are the atomic net charges. In this work, the charges on C, H_C , N and H_N of CH_3NH_3^+ were obtained from Natural Bond Orbital (NBO) analysis (Alan, Larry and Frank 1988; Alan, Robert and Frank 1985; Carpenter and Weinhold, 1988) of the corresponding HF calculations, being of 0.6950, -0.0062, -0.2431 and 0.1890, respectively. The charges on O and H of water molecules were adopted from the BJH-CF2 water model (Stillinger and Rahman, 1978) as -0.6598 and 0.3299, respectively.

Table 2.1 Optimized parameters of the analytical pair potentials for the interaction of water with CH_3NH_3^+ .

pair	A ($\text{kcal}\cdot\text{mol}^{-1}\text{ \AA}^4$)	B ($\text{kcal}\cdot\text{mol}^{-1}\text{ \AA}^5$)	C ($\text{kcal}\cdot\text{mol}^{-1}\text{ \AA}^6$)	D ($\text{kcal}\cdot\text{mol}^{-1}\text{ \AA}^{12}$)
C-O_w	3.294261×10^2	-1.284494×10^4	2.867797×10^4	-2.736493×10^5
H_C-O_w	4.392700×10^2	-9.795945×10^2	7.804262×10^2	-2.978830×10^2
N-O_w	2.549314×10^3	-1.595213×10^4	2.601125×10^4	-1.219681×10^5
H_N-O_w	2.270976×10^1	-1.316456×10^2	2.245271×10^2	-8.618788×10^1
C-H_w	1.213528×10^2	2.935896×10^2	-6.708478×10^2	1.881890×10^3
H_C-H_w	-1.270316×10^2	3.009217×10^2	-1.720691×10^2	6.140965×10^0
N-H_w	-1.668167×10^2	1.272809×10^3	-1.472421×10^3	2.316114×10^3
H_N-H_w	-1.357481×10^2	3.091070×10^2	-1.726506×10^2	4.979114×10^0

2.8 Selection of QM size, QM method and basis set

By means of the ONIOM-XS MD simulation, the selection of QM size, as well as the QM method and basis set, is crucial in order to obtain reliable results. Basically, the energy and force calculations using correlated QM method and large basis set can provide high quality simulation data. In practice, however, these parameters must be optimized, compromising between the quality of the simulation results and the requirement of the CPU time. Figures 2.10 and 2.11 provide detailed information regarding the requirements of CPU time for the QM calculations of water clusters using different QM methods and basis sets (Thaomola, Tongraar and Kerdcharoen, 2012). It is apparent that the correlated QM calculations using relatively large basis sets are very time-consuming, *i.e.*, when compared to the HF calculations using moderate-size basis set.

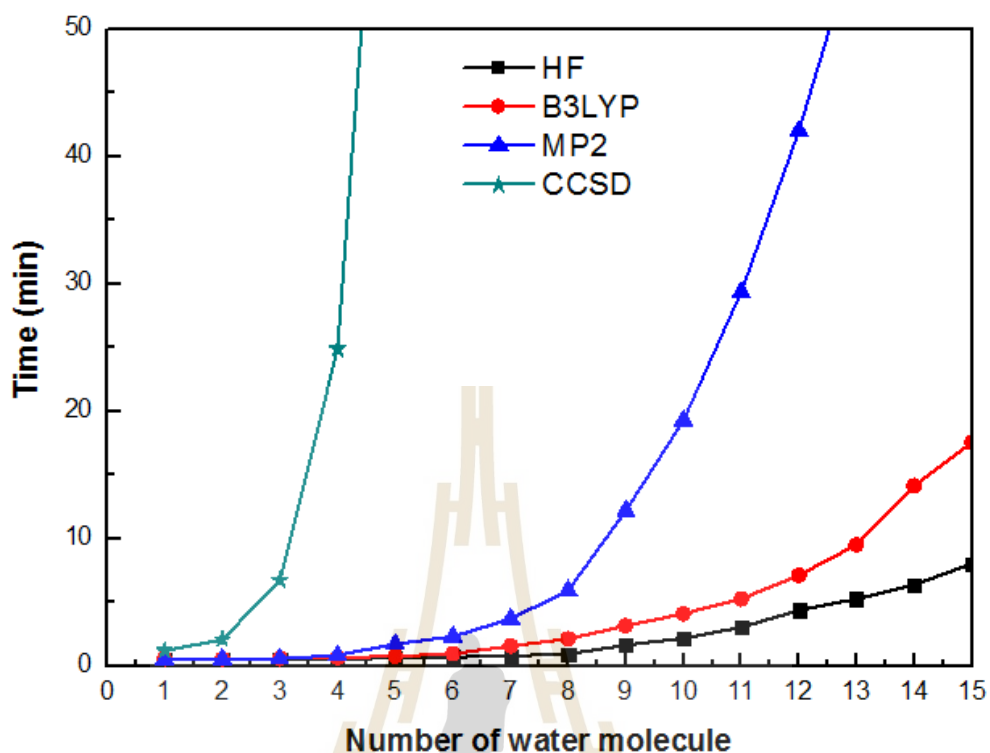


Figure 2.10 Requirements of CPU times for HF, B3LYP, MP2 and CCSD force calculations of $(\text{H}_2\text{O})_n$, $n = 1-15$, complexes using DZP basis set. All calculations were performed on CCRL cluster with Intel CoreTM2 Quad of CPU and 4GB of Ram (Thaomola, Tongraar and Kerdcharoen, 2012).

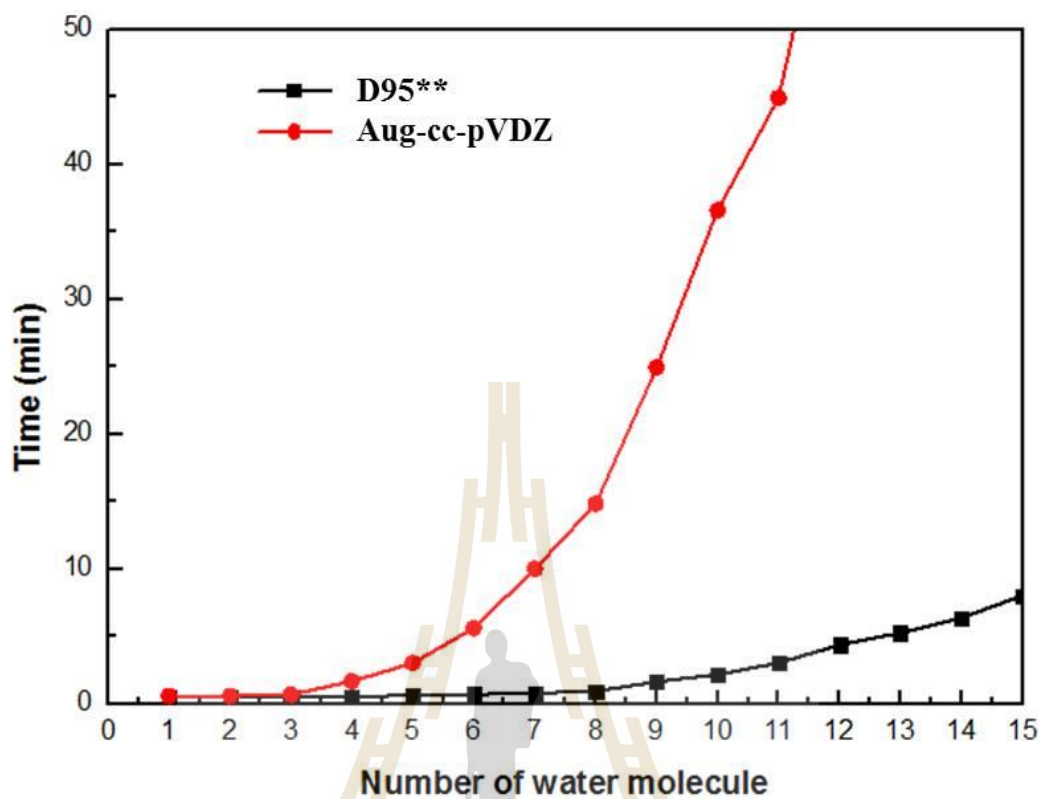


Figure 2.11 Requirements of CPU times for HF force calculations of $(\text{H}_2\text{O})_n$, $n = 1-15$, complexes using DZP and aug-cc-pVDZ basis sets. All calculations were performed on CCRL cluster with Intel CoreTM2 Quad of CPU and 4GB of Ram (Thaomola, Tongraar and Kerdcharoen, 2012).

In this study, the nitrogen atom of CH_3NH_3^+ was set as the center of the QM region, and a QM radius of 4.4 Å and a switching width of 0.2 Å were chosen, which correspond to the ONIOM-XS parameters r_0 and r_1 of 4.2 and 4.4 Å, respectively. This QM size is considered to be large enough to include most of the many-body interactions and the polarization effects, *i.e.*, at least within the whole first solvation shell of $-\text{NH}_3^+$ and the major part of the solvation sphere of $-\text{CH}_3$, and the remaining interactions beyond the QM region are assumed to be well accounted for by the MM potentials. Since the correlated QM calculations, even at the simple MP2, are rather too time-consuming for our current computational feasibility, all interactions within the QM region were evaluated by

performing *ab initio* calculations at the Hartree-Fock (HF) level of accuracy using the DZP basis set. It is known that the electron correlation and the charge transfer effects are not typically well-described by the HF theory, and that the use of the DZP basis set could result in a high basis set superposition error and an exaggeration of the ligand-to-metal charge transfer. To simply check the validity of the HF method and the DZP basis set employed for this particular system, the geometry optimizations of the $\text{CH}_3\text{NH}_3^+(\text{H}_2\text{O})_3$ complex have been carried at the HF, B3LYP, MP2 and CCSD levels of accuracy using the DZP and 6-311++G(d,p) basis sets, as summarized in Table 2.2. It is apparent that the HF calculations using the DZP basis set can predict the structure and stabilization energy of the $\text{CH}_3\text{NH}_3^+(\text{H}_2\text{O})_3$ complex in good accord with the correlated methods, implying that the effects of electron correlation are marginal and that the use of the HF method is assumed to be good enough to sufficiently provide reliable results.

Table 2.2 Stabilization energies and some selected structural parameters of the optimized $\text{CH}_3\text{NH}_3^+(\text{H}_2\text{O})_3$ complex, calculated at the HF, B3LYP, MP2 and CCSD levels of accuracy using the DZP and 6-311++G(d,p) (data in parentheses) basis sets.

Method	HF	B3LYP	MP2	CCSD
ΔE (kcal·mol ⁻¹)	-16.12 (-15.44)	-18.61 (-16.89)	-16.23 (-15.50)	-16.36 (-15.53)
C-N (Å)	1.4866 (1.4858)	1.4974 (1.4953)	1.4918 (1.4897)	1.4953 (1.4932)
N-H _N (Å)	1.0160 (1.0148)	1.0422 (1.0363)	1.0347 (1.0329)	1.0320 (1.0309)
C-H _C (Å)	1.0799 (1.0798)	1.0917 (1.0883)	1.0882 (1.0887)	1.0894 (1.0908)
∠ N-C-H _C (deg)	108.95 (108.91)	109.30 (109.14)	108.90 (108.91)	108.82 (108.84)
∠ C-N-H _N (deg)	110.51 (110.79)	110.25 (110.75)	110.04 (110.40)	110.07 (110.44)
O _W -H _W (Å)	0.9467 (0.9440)	0.9678 (0.9641)	0.9657 (0.9622)	0.9644 (0.9604)

Table 2.2 (Continued) Stabilization energies and some selected structural parameters of the optimized $\text{CH}_3\text{NH}_3^+(\text{H}_2\text{O})_3$ complex, calculated at the HF, B3LYP, MP2 and CCSD levels of accuracy using the DZP and 6-311++G(d,p) (data in parentheses) basis sets.

Method	HF	B3LYP	MP2	CCSD
$\angle \text{H}_\text{W}-\text{O}_\text{W}-\text{H}_\text{W}$ (deg)	106.59 (106.35)	105.96 (105.88)	105.11 (104.48)	105.17 (104.64)
$\text{H}_\text{N}\cdots\text{O}_\text{W}$ (Å)	1.8926 (1.9109)	1.7738 (1.8161)	1.7978 (1.8115)	1.8255 (1.8347)
$\angle \text{N}-\text{H}_\text{N}\cdots\text{O}_\text{W}$ (deg)	174.39 (176.07)	176.25 (177.29)	172.53 (174.37)	172.22 (174.46)

2.9 Simulation details

The ONIOM-XS MD simulation of CH_3NH_3^+ in aqueous electrolyte solution will be performed in a canonical ensemble at 298 K with periodic boundary conditions. The system's temperature will be kept constant using the Berendsen algorithm (Berendsen, Postma, van Gunsteren, DiNola and Haak, 1984). A periodic box, with a box length of 18.17 Å, contains one CH_3NH_3^+ and 199 water molecules, corresponding to the experimental density of pure water. For the QM size, a QM radius of 4.4 Å and a switching width of 0.2 Å will be chosen, corresponding to the ONIOM-XS parameters r_0 and r_1 of 4.2 and 4.4 Å, respectively. The interactions within the QM region will be evaluated by performing *ab initio* calculations at the Hartree-Fock (HF) level of accuracy using the DZP basis set (Dunning and Hay, 1977). All QM calculations were carried out using the Gaussian03 program (Frisch et al., 2005). The reaction-field method (Tironi, Sperb, Smith and van Gunsteren, 1995) will be employed for the treatment of long-range interactions. The Newtonian equations of motions will be treated by a general predictor-corrector algorithm. The time step size was set to 0.2 fs, which allows for the explicit movement of

the hydrogen atoms of water molecules. The ONIOM-XS MD simulation will be started with the system's re-equilibration for 30,000 time steps, followed by another 200,000 time steps to collect configurations every 10th step.

2.10 References

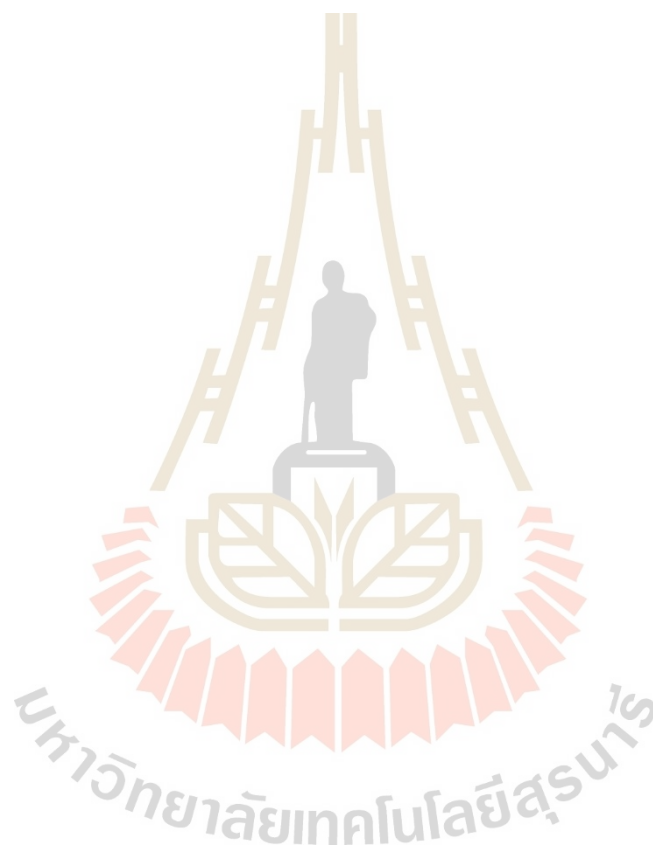
- Alan, E. R., Robert, B. W. and Frank, W. (1985). Natural population analysis. **The Journal of Chemical Physics**. 83: 735-746.
- Alan, E. R., Larry, A. C. and Frank, W. (1988). Intermolecular interactions from a natural bond orbital, donor-acceptor viewpoint. **Chemical Reviews**. 88: 899-926.
- Berendsen, H. J. C., Postma, J. P. M., van Gunsteren, W. F., DiNola, A. and Haak, J. R. (1984). Molecular dynamics with coupling to an external bath. **The Journal of Chemical Physics**. 81: 3684-3690.
- Carpenter, J. E. and Weinhold, F. (1988). Analysis of the geometry of the hydroxymethyl radical by the "different hybrids for different spins" natural bond orbital procedure. **Journal of Molecular Structure: THEOCHEM**. 169: 41-62.
- Dunning, J. T. H. (1989). Gaussian basis sets for use in correlated molecular calculations. I. The atoms boron through neon and hydrogen. **The Journal of Chemical Physics**. 90: 1007-1023.
- Dunning, J. T. H. and Hay, P. J. (1977). Methods of electronic structure theory. **III, Plenum, New York**.
- Ewald, P. P. (1921). Die berechnung optischer und elektrostatischer gitterpotentiale. **Annalen der Physik**. 369: 253-287.
- Foulkes, W. M. C. and Haydock, R. (1989). Tight-binding models and density-functional theory. **Physical Review B**. 39: 12520-12536.
- Frisch, M. J., Trucks, G. W., Schlegel, H. B., Scuseria, G. E., Robb, M. A., Cheeseman, J. R., Zakrzewski, V. G., Montgomery, J. A., Stratmann, R. E., Burant, J. C.,

- Dapprich, S., Millam, J. M., Daniel, A. D., Kudin, K. N., Strain, M. C., Farkas, O., Tomasi, J., Barone, V., Cossi, M., Cammi, R., Mennucci, B., Pomelli, C., Adamo, C., Clifford, S., Ochterski, J., Petersson, G. A., P.Y. Ayala, Q. C., Morokuma, K., Salvador, P., Dannenberg, J. J., Malick, D. K., Rabuck, A. D., Raghavachari, K., J. B. Foresman, Cioslowski, J., Ortiz, J. V., Baboul, A. G., Stefanov, B. B., Liu, G., Liashenko, A., Piskorz, P., Komaromi, I., Gomperts, R., Martin, R. L., Fox, D. J., T. Keith, M. A. A. L., Peng, C. Y., Nanayakkara, A., Challacombe, M., Gill, B. J., Chen, W., Wong, M. W., Gonzalez, C., Pople, J. A. (2005). Gaussian 03 (Revision D.1) [Computer Software]. Wallingford, CT, USA: Gaussian.
- Kabbalee, P., Tongraar, A. and Kerdcharoen, T. (2015). Preferential solvation and dynamics of Li^+ in aqueous ammonia solution: An ONIOM-XS MD simulation study. **Chemical Physics**. 446: 70-75.
- Kabbalee, P., Sripa, P., Tongraar, A. and Kerdcharoen, T. (2015). Solvation structure and dynamics of K^+ in aqueous ammonia solution: Insights from an ONIOM-XS MD simulation. **Chemical Physics Letters**. 633: 152-157.
- Kerdcharoen, T. and Morokuma, K. (2002). ONIOM-XS: An extension of the ONIOM method for molecular simulation in condensed phase. **Chemical Physics Letters**. 355: 257-262.
- Kerdcharoen, T. and Morokuma, K. (2003). Combined quantum mechanics and molecular mechanics simulation of Ca^{2+} /ammonia solution based on the ONIOM-XS method: Octahedral coordination and implication to biology. **The Journal of Chemical Physics**. 118: 8856-8862.
- Sripa, P., Tongraar, A. and Kerdcharoen, T. (2013). "Structure-making" ability of Na^+ in dilute aqueous solution: An ONIOM-XS MD simulation study. **The Journal of Physical Chemistry A**. 117: 1826-1833.

- Sripa, P., Tongraar, A. and Kerdcharoen, T. (2015). Structure and dynamics of the Li^+ hydrates: A comparative study of conventional QM/MM and ONIOM-XS MD simulations. **Journal of Molecular Liquids**. 208: 280-285.
- Sripa, P., Tongraar, A. and Kerdcharoen, T. (2016). Characteristics of K^+ and Rb^+ as “structure-breaking” ions in dilute aqueous solution: Insights from ONIOM-XS MD simulations. **Chemical Physics**. 479: 72-80.
- Sripradite, J., Tongraar, A. and Kerdcharoen, T. (2015). Solvation structure and dynamics of Na^+ in liquid ammonia studied by ONIOM-XS MD simulations. **Chemical Physics**. 463: 88-94.
- Stillinger, F. H. and Rahman, A. (1978). Revised central force potentials for water. **The Journal of Chemical Physics**. 68: 666-670.
- Svensson, M., Humbel, S., Froese, R. D. J., Matsubara, T., Sieber, S. and Morokuma, K. (1996). ONIOM: A multilayered integrated MO + MM method for geometry optimizations and single point energy predictions. A test for Diels–Alder reactions and $\text{Pt}(\text{P}(t\text{-Bu})_3)_2 + \text{H}_2$ oxidative addition. **The Journal of Physical Chemistry**. 100: 19357-19363.
- Tasaki, K., McDonald, S. and Brady, J. W. (1993). Observations concerning the treatment of long-range interactions in molecular dynamics simulations. **Journal of Computational Chemistry**. 14: 278-284.
- Thaomola, S., Tongraar, A. and Kerdcharoen, T. (2012). Insights into the structure and dynamics of liquid water: A comparative study of conventional QM/MM and ONIOM-XS MD simulations. **Journal of Molecular Liquids**. 174: 26-33.
- Tironi, I. G., Sperb, R., Smith, P. E. and van Gunsteren, W. F. (1995). A generalized reaction field method for molecular dynamics simulations. **The Journal of Chemical Physics**. 102: 5451-5459.

Verlet, L. (1967). Computer “experiments” on classical fluids. I. Thermodynamical properties of Lennard-Jones molecules. **Physical Review**. 159: 98-103.

Wanprakhon, S., Tongraar, A. and Kerdcharoen, T. (2011). Hydration structure and dynamics of K^+ and Ca^{2+} in aqueous solution: Comparison of conventional QM/MM and ONIOM-XS MD simulations. **Chemical Physics Letters**. 517: 171-175.



CHAPTER III

RESULTS AND DISCUSSION

3.1 Structural properties

Water molecules surrounding the CH_3NH_3^+ ion will be classified into two groups, namely at the hydrophilic $-\text{NH}_3^+$ and hydrophobic $-\text{CH}_3$ regions. The hydration structure of the hydrophilic group of CH_3NH_3^+ can be visualized from the N-O_w , N-H_w , $\text{H}_N\text{-O}_w$ and $\text{H}_N\text{-H}_w$ RDFs and their corresponding integration numbers, as depicted in Figures 3.1a to d, respectively. To reliably discuss the behavior of HBs between the $-\text{NH}_3^+$ group and its nearest-neighbor waters, the corresponding atom-atom RDFs for pure water obtained by the similar ONIOM-XS MD technique (Thaomola, Tongraar and Kerdcharoen, 2012) were utilized for comparison, as shown in Figure 3.2. With regard to Figure 3.1a, a pronounced first N-O_w peak is exhibited at 2.94 Å, together with a recognizable second N-O_w peak at around 4.23 Å. The characteristics of the N-O_w RDF, as compared to the O-O RDF of pure water (cf. Figure 3.2a), clearly supplies information that the hydration structure of the $-\text{NH}_3^+$ species is somewhat flexible, *i.e.*, water molecules in the primary region of the $-\text{NH}_3^+$ group are labile and they can exchange with water molecules in the outer region. The position of the first N-O_w minimum is roughly estimated to be 3.50 Å where the integration up to this N-O_w distance yields an average coordination number of 4.9 ± 0.1 . In Figure 3.1b, the first N-H_w peak is found at around 3.26 Å, implying that water molecules in the primary region tend to point their dipole moments toward the $-\text{NH}_3^+$ group. However, according to Figures 3.1a and b, the nonzero first minimum of the N-O_w RDF and the observed broad peak of the N-H_w RDF clearly suggest that water molecules in this region are labile and their hydrogen atoms would have considerable orientational freedom. In this

respect, the observed slight second peak of the N-O_W RDF (cf. Figure 3.1a) could also be assigned to oxygen atoms of some water molecules in the outer region that form HBs with hydrogen atoms of water molecules in the first hydration shell of -NH₃⁺.

The HB interactions between the -NH₃⁺ group and its surrounding water molecules can be analyzed from the H_N-O_W and H_N-H_W RDFs, as shown in Figures 3.1c and d, respectively. According to Figure 3.1c, the first H_N-O_W peak is exhibited at 1.94 Å, and the integration up to the corresponding first H_N-O_W minimum gives an average coordination number of 1.2±0.1. This implies that the -NH₃⁺ species participates in about 3.6 HBs with its nearest-neighbor waters, *i.e.*, consisting of about 1.2 water molecules for each H atom of -NH₃⁺. The slight pronounced second peak of the H_N-O_W RDF could be ascribed to the contributions of water molecules in the first hydration layer of other -NH₃⁺ hydrogen atoms and of water molecules in the outer region. In Figure 3.1d, the feature of the H_N-H_W RDF corresponds to the arrangements of primary water molecules forming HBs at each of the -NH₃⁺ hydrogens. As compared to the feature of the O-H and H-O RDFs (cf. Figures 3.2b and c) of pure water (Thaomola, Tongraar and Kerdcharoen, 2012), *i.e.*, in terms of shape and separation of the first and second H_N-O_W peaks, it is apparent that the HB interactions between the -NH₃⁺ hydrogens and their nearest-neighbor waters are relatively weaker than the HB networks of water molecules in the bulk. Consequently, this leads to more frequent and easy exchange of water molecules between the first shell and the outer region.

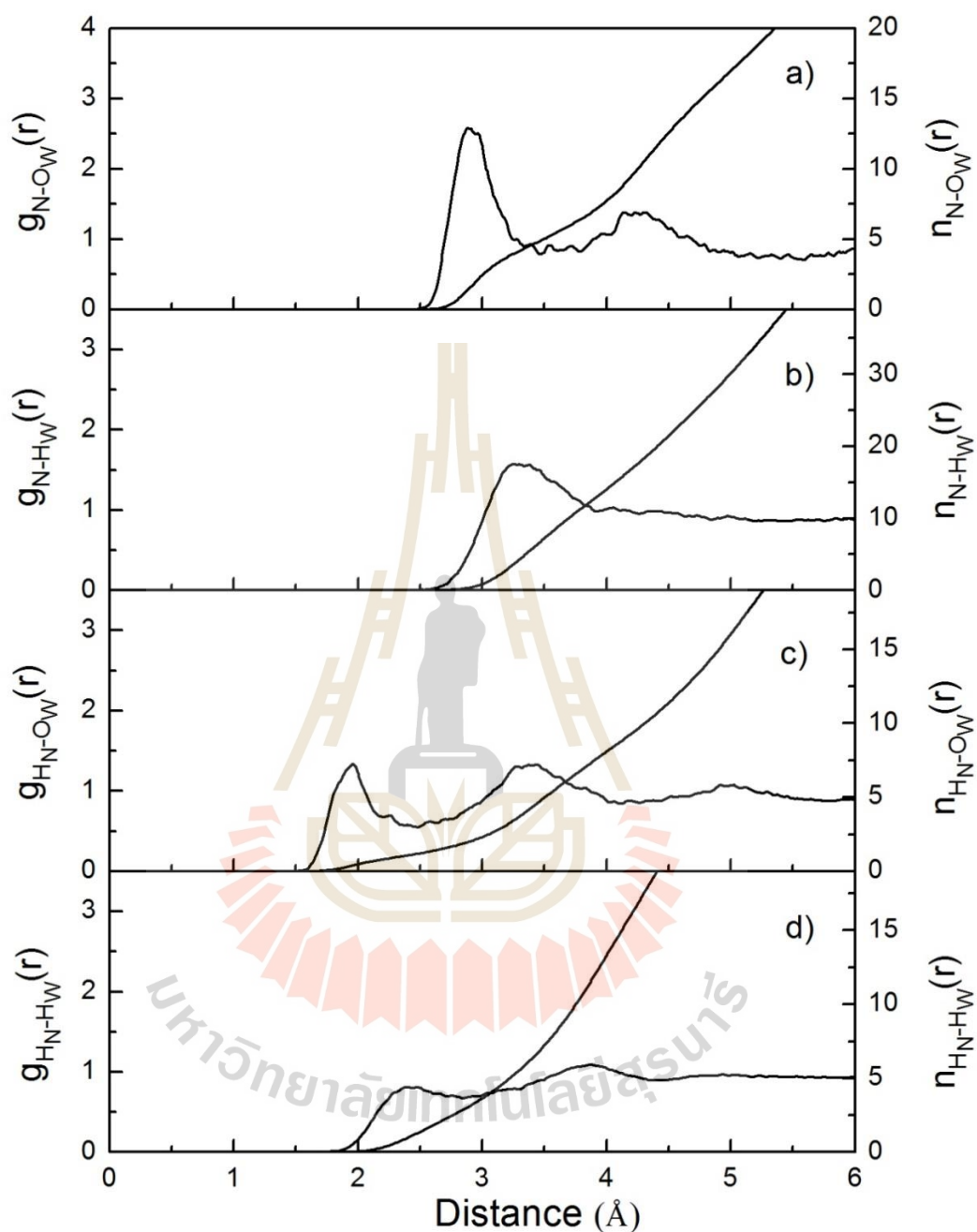


Figure 3.1 a) N-O_w, b) N-H_w, c) H_N-O_w and d) H_N-H_w radial distribution functions and their corresponding integration numbers, as obtained by ONIOM-XS MD simulation.

The hydration shell structure of the $-\text{NH}_3^+$ group, as obtained by the ONIOM-XS MD simulation, is comparable to that reported in the CPMD study (Hesske and Gloe, 2007). However, some observed differences between the ONIOM-XS and the CPMD

results could be discussed as follows. By means of the ONIOM-XS MD simulation, about 4.9 water molecules are found to be involved in the primary region of the $-\text{NH}_3^+$ group, compared to the average value of 4.2 of the CPMD study. In addition, according to the characteristics of the ONIOM-XS MD's N-H_w RDF, it is apparent that hydrogen atoms of water molecules in the first hydration shell of the $-\text{NH}_3^+$ group have rather high orientational freedom. In the CPMD study (Hesske and Gloe, 2007), the peaks of the partial distribution functions $g(\text{NO})$ and $g(\text{ND})$ (D denotes water hydrogen) are slightly better defined than the ONIOM-XS MD's N-O_w and N-H_w RDFs, which is explainable since the use of the BLYP functional could result in an overestimation of the solute-solvent interactions. Regarding the ONIOM-XS MD results, the observed hydration structure of the $-\text{NH}_3^+$ group is similar to the hydration structure of the spherical NH_4^+ species derived by means of the conventional QM/MM scheme (Intharathep, Tongraar and Sagarik, 2005). Note that, in the case of the spherical NH_4^+ , the QM/MM MD study has predicted a broad unsymmetrical first N-O_w RDF, which corresponds to the experimentally observed fast translation and rotation of NH_4^+ in water (Perrin and Gipe, 1986; Perrin and Gipe 1987). For the CH_3NH_3^+ species, the steric hindrance arising from the $-\text{CH}_3$ group could be expected to prevent such phenomenon, *i.e.*, the ONIOM-XS MD simulation clearly reveals a relatively more structured N-O_w RDF.

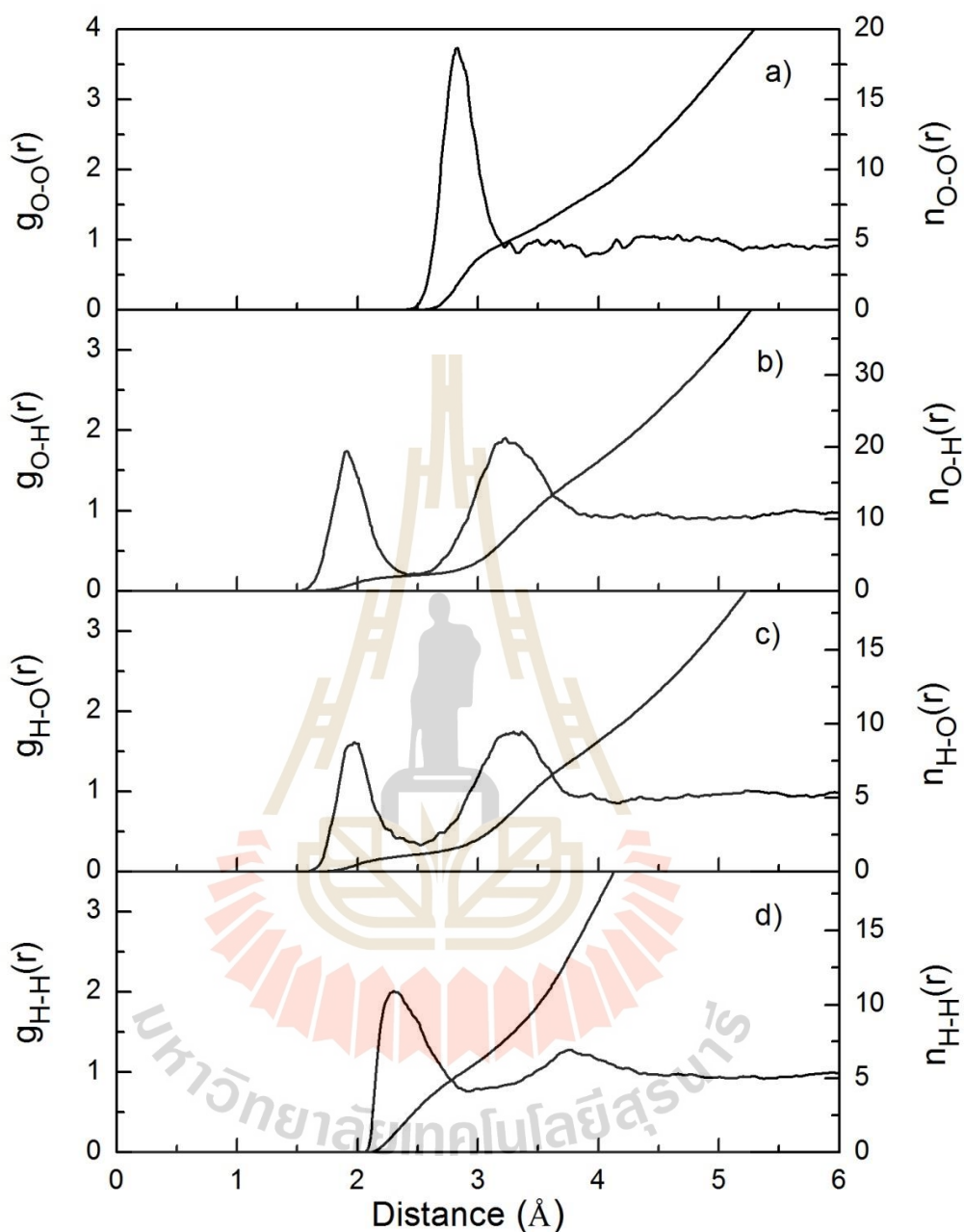


Figure 3.2 a) O-O, b) O-H, c) H-O and d) H-H radial distribution functions and their corresponding integration numbers, as obtained by ONIOM-XS MD simulation of liquid water.

At the hydrophobic site of CH_3NH_3^+ , the arrangements of water molecules around the $-\text{CH}_3$ group can be analyzed from a set of C-O_w , C-H_w , $\text{H}_c\text{-O}_w$ and $\text{H}_c\text{-H}_w$ RDFs and their corresponding integration numbers, as shown in Figures 3.3a to d, respectively. The

observed broad C-O_W and C-H_W peaks with maxima at around 3.48 and 3.67 Å, as well as the observed broad and less pronounced first H_C-O_W and H_C-H_W RDFs, clearly indicate weak interactions between the -CH₃ group and its surrounding water molecules. The integration up to a rough estimate of the first C-O_W minimum (*i.e.*, of around 4.90 Å) yields about 15.1±0.2 water molecules. Interestingly, it has been reported that, according to a more polar character of the -CH₃ group of CH₃NH₃⁺, *i.e.*, compared to that of CH₃COO⁻, the interactions between the -CH₃ group and its surrounding water molecules could play some roles in the nature of the CH₃NH₃⁺ solvation (Alagona, Ghio and Kollman, 1986). Based on the ONIOM-XS MD simulation, it is observed that the -CH₃ group in CH₃NH₃⁺ has a slight positive partial charge, which allows some nearest-neighbor water molecules to have their lone pair directed toward the -CH₃ species. However, according to the characteristics of the H_C-O_W and H_C-H_W RDFs, it could be demonstrated that water molecules in the hydrophobic region are arranged with respect to the strength of their water-water HB interactions, rather than by the influence of the -CH₃ group.

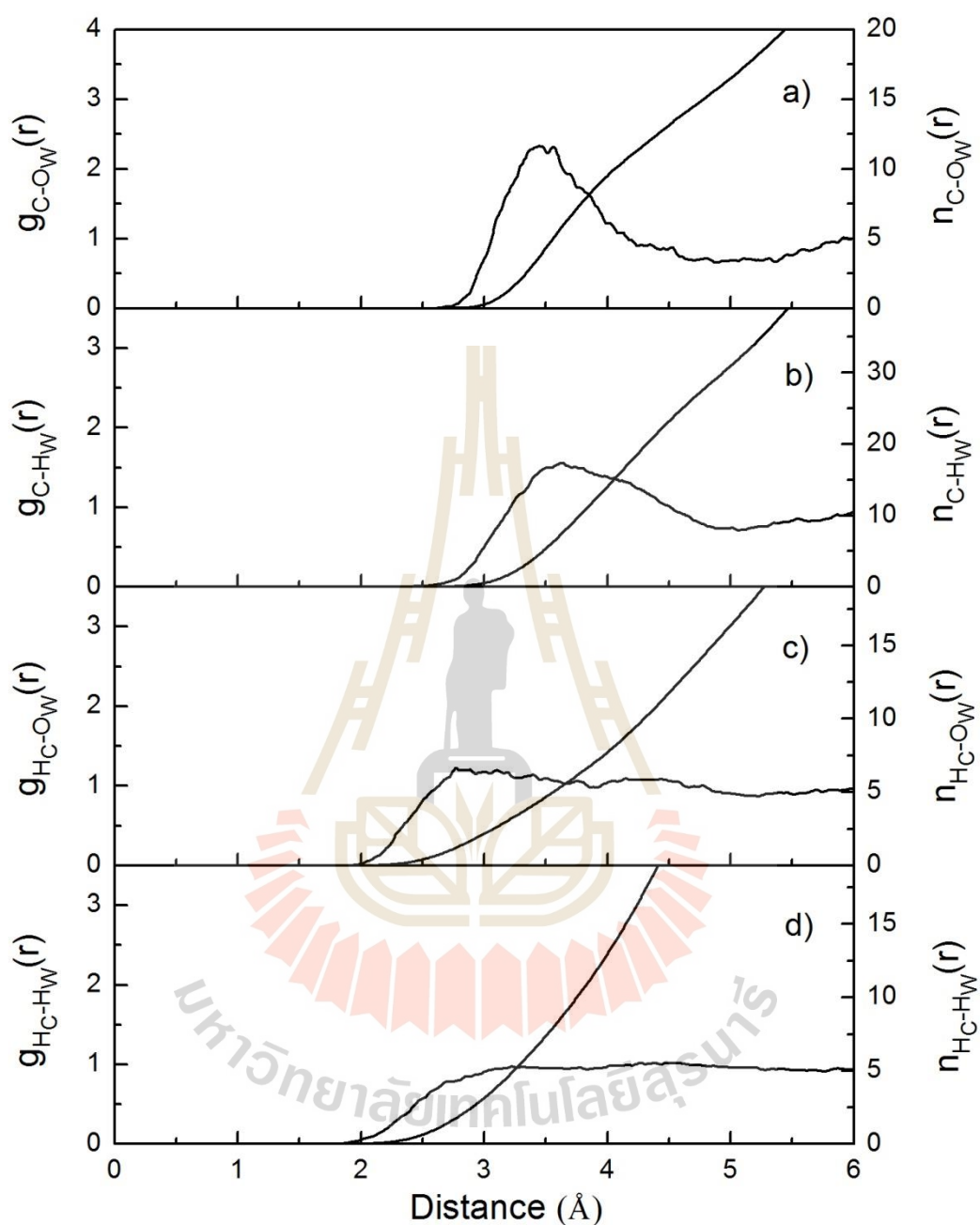


Figure 3.3 a) C-O_w, b) C-H_w, c) H_C-O_w and d) H_C-H_w radial distribution functions and their corresponding integration numbers, as obtained by ONIOM-XS MD simulation.

The probability distributions of the number of water molecules, calculated within the first minima of the N-O_w and C-O_w RDFs, respectively, are plotted in Figures 3.4a and b, respectively. With regard to Figure 3.4a, it is apparent that various numbers of water

molecules, varying from 3 to 8 with the prevalent value of 5, are cooperatively involved in the first hydration shell of the $-\text{NH}_3^+$ group. In this respect, it could be expected that these water molecules can mutually play a role in the HB formation with hydrogen atoms of the $-\text{NH}_3^+$ group. The numbers of HBs which are simultaneously formed at each of the $-\text{NH}_3^+$ hydrogens during the ONIOM-XS MD simulation can be evaluated with respect to the following geometrical criteria of the HB formation: (1) the HB distance is limited by the first minimum of the $\text{H}_\text{N}-\text{O}_\text{W}$ RDF and (2) the $\text{N}-\text{H}_\text{N}-\text{O}_\text{W}$ and $\text{H}_\text{N}-\text{O}_\text{W}-\text{H}_\text{W}$ HB angles $\geq 100^\circ$, as depicted in Figure 3.5. According to the detailed analysis of the ONIOM-XS MD trajectories, it is observed that most of the $-\text{NH}_3^+$ hydrogens favor to form a single HB with one of its nearest-neighbor water molecules, compared to about 12-13% of the remaining configurations which form two HBs with two nearest-neighbor waters. In Figure 3.4b, the number of water molecules around the $-\text{CH}_3$ group shows large variations, ranging from 11 to 20, which corresponds to the observed weak interactions between the $-\text{CH}_3$ group and its surrounding water molecules.

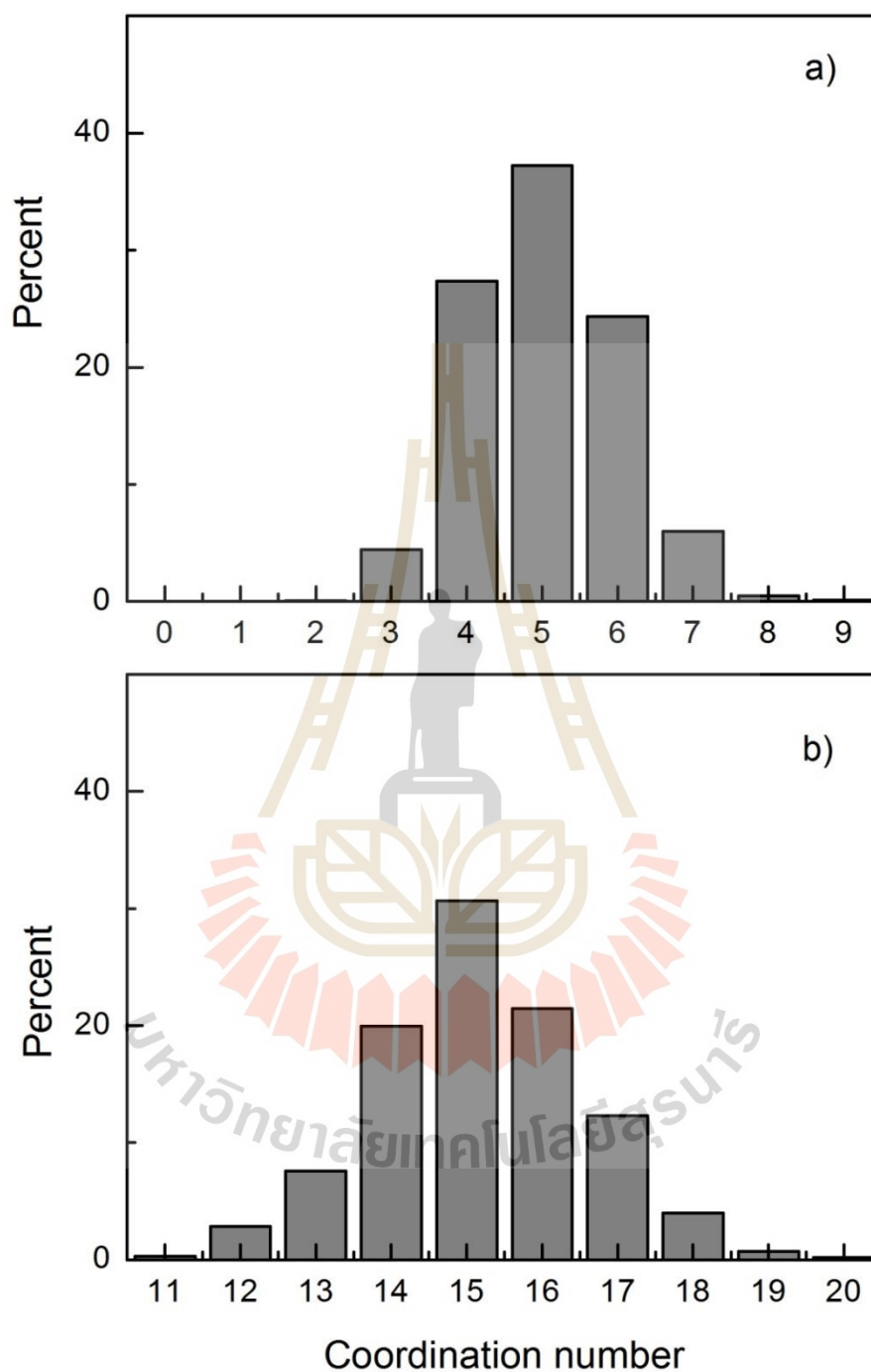


Figure 3.4 Distributions of the coordination numbers of CH_3NH_3^+ , calculated within the first minimum of a) N-O_w and b) C-O_w RDFs.

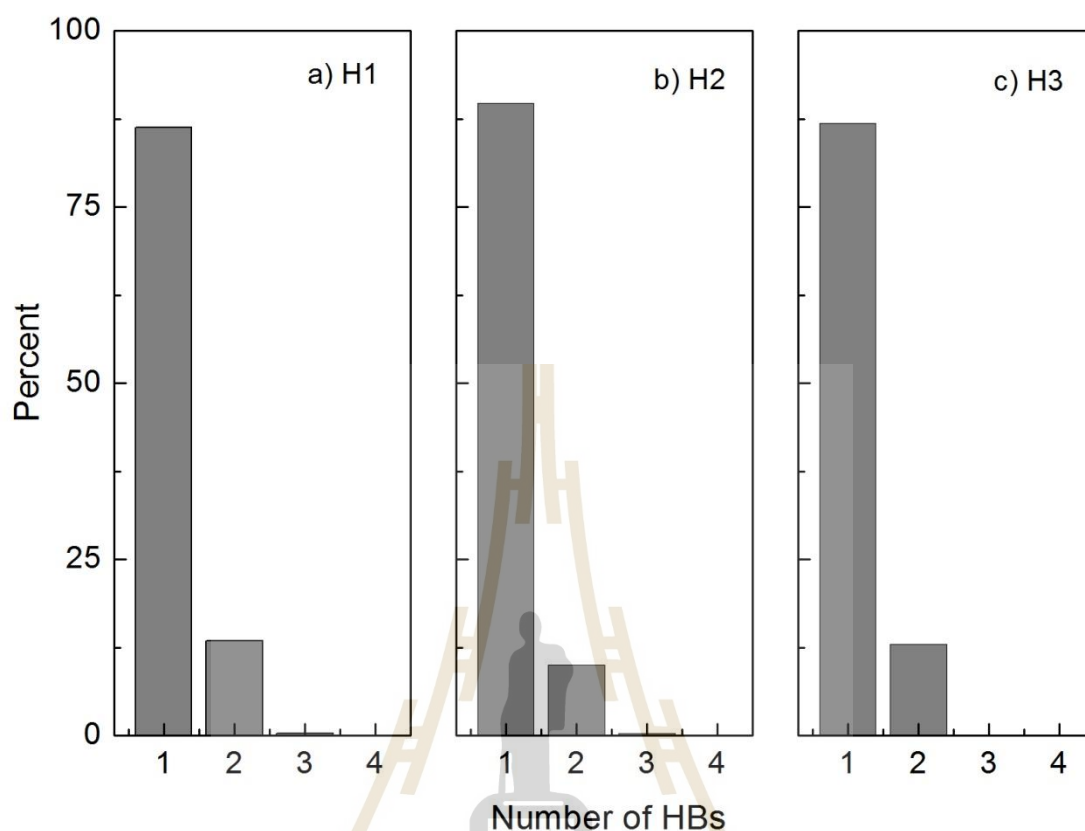


Figure 3.5 Distributions of numbers of HBs at each of $-\text{NH}_3^+$ hydrogens, calculated within the $\text{H}_\text{N}\cdots\text{O}_\text{W}$ distance of 2.5 Å.

Figure 3.6 displays the average numbers of HBs at the $-\text{NH}_3^+$ group, calculated within the $\text{H}_\text{N}\cdots\text{O}_\text{W}$ distance of 2.5 Å. By means of the ONIOM-XS MD simulation, it is observed that the hydrophilic side could form HBs with several water molecules, varying from 2 to 6 HBs with the prevalent value of 3. Some selected geometrical arrangements of the CH_3NH_3^+ -water complexes showing the HB interactions between the $-\text{NH}_3^+$ hydrogens and their nearest-neighbor waters are shown in Figure 3.7.

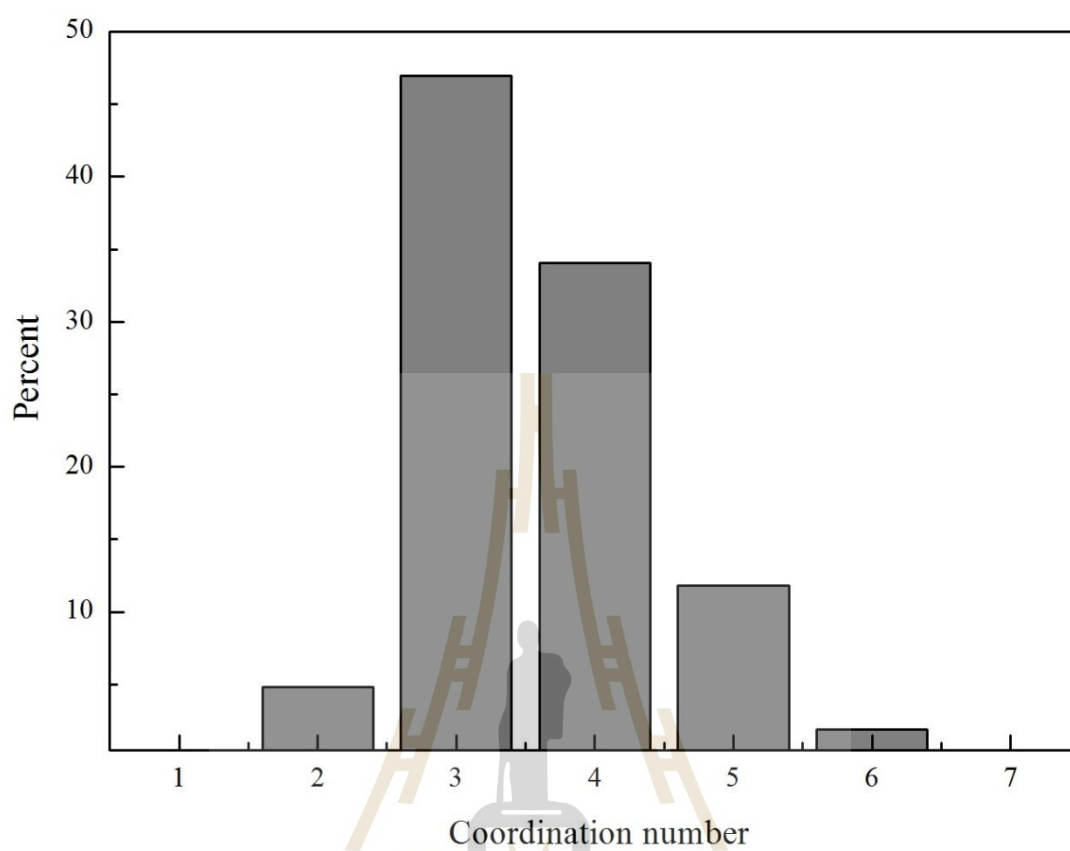


Figure 3.6 Distributions of numbers of HBs at the hydrophilic side, calculated within the $H_N \cdots O_W$ distance of 2.5 Å.

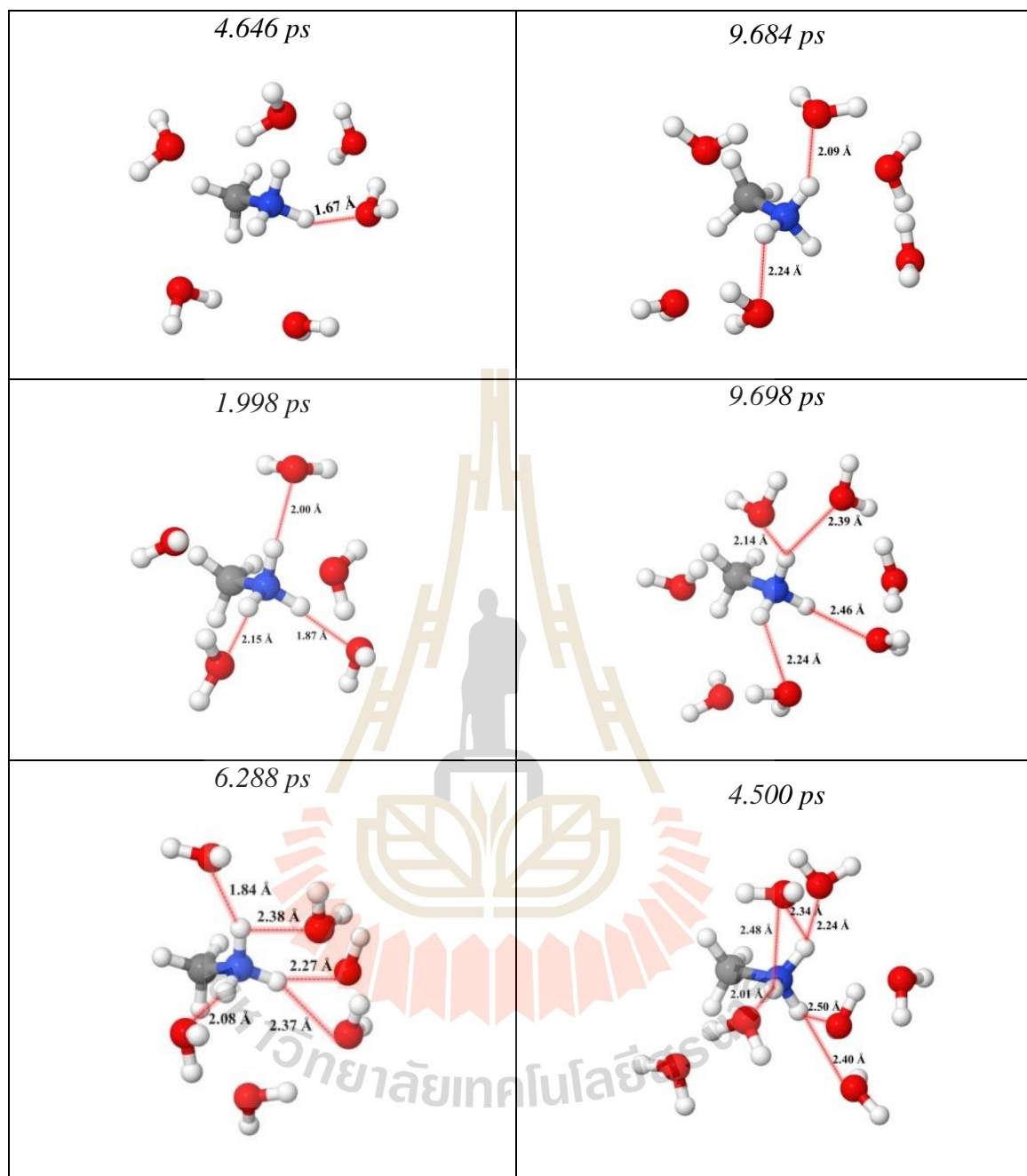


Figure 3.7 Some selected geometrical arrangements of the CH_3NH_3^+ -water complexes, showing the HB interactions between the $-\text{NH}_3^+$ hydrogen atoms and their nearest-neighbor waters located within the $\text{H}_\text{N}-\text{O}_\text{W}$ distance of 2.5 Å.

The details with respect to the HBs between the $-\text{NH}_3^+$ hydrogen atoms and their nearest-neighbor waters can be further analyzed from the distributions of the $\text{N}-\text{H}_\text{N}\cdots\text{O}_\text{W}$ angle, calculated within the $\text{H}_\text{N}\cdots\text{O}$ distances of 2.0 and 2.5 Å, respectively, as shown in

Figure 3.8. At the short $H_N \cdots O_W$ distance of 2.0 Å, it is apparent that the $N-H_N \cdots O_W$ HBs are nearly linear, with peak maxima around 160°. However, at the slightly longer $H_N \cdots O_W$ distance of 2.5 Å (*i.e.*, the first minimum of the H_N-O_W RDF), the probability of finding linear HBs apparently decreases, while the pronounced peak between 90-150° becomes more significant. This could be ascribed to the presence of multiple, non-linear HBs at each of the $-NH_3^+$ hydrogen atoms. Such phenomenon can be analyzed by plotting the $H_N-N \cdots O_W$ angular distributions, calculated within the $H_N \cdots O_W$ distance of 2.5 Å, as depicted in Figure 3.9. The two pronounced peaks around 0–30° and 90–120° correspond to the distributions of the three nearest-neighbor water molecules that are directly hydrogen bonded to each of $-NH_3^+$ hydrogen atoms, whereas the pronounced shoulder peak around 40–80° refers to the distributions of other nearest-neighbor waters that can possibly form additional HBs at some hydrogen atoms of the $-NH_3^+$ group.

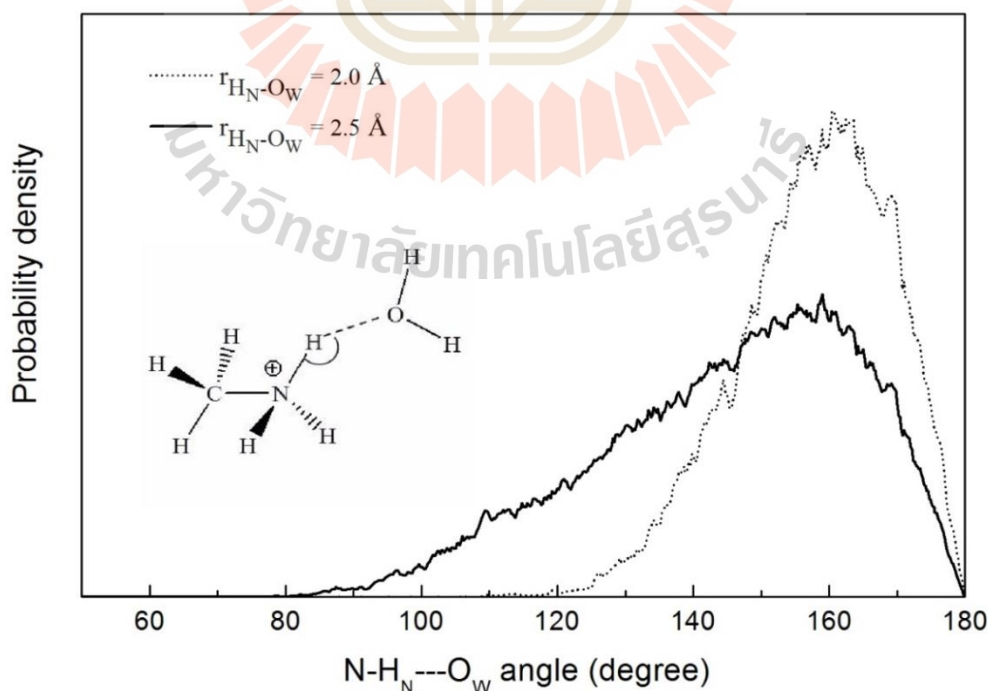


Figure 3.8 $N-H_N \cdots O_W$ angular distributions, calculated up to the $H_N \cdots O_W$ distances of 2.0 and 2.5 Å, respectively.

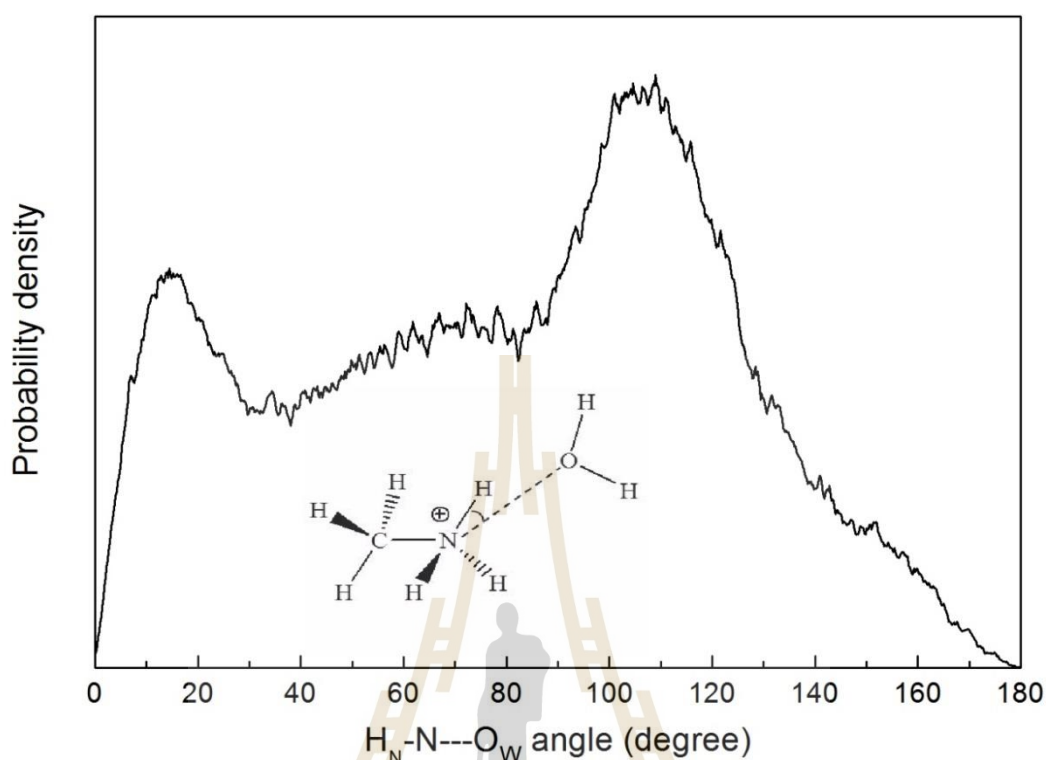


Figure 3.9 $H_N-N\cdots O_W$ angular distributions, calculated within the first minimum of the H_N-O_W RDF.

More insights into the HBs between the $-NH_3^+$ hydrogens and their nearest-neighbor waters can be visualized from the plot of water orientations within the $H_N\cdots O_W$ distance of 2.5 Å, as shown in Figure 3.10. The orientation of water molecules is described in terms of the distributions of angle θ , as defined by the $H_N\cdots O_W$ axis and the dipole vector of the water molecules. According to Figure 3.10, the observed broad distributions of θ angles, *i.e.*, between 80–160°, clearly suggest that water molecules which form HBs with the $-NH_3^+$ hydrogens have freely dipole-oriented arrangements.

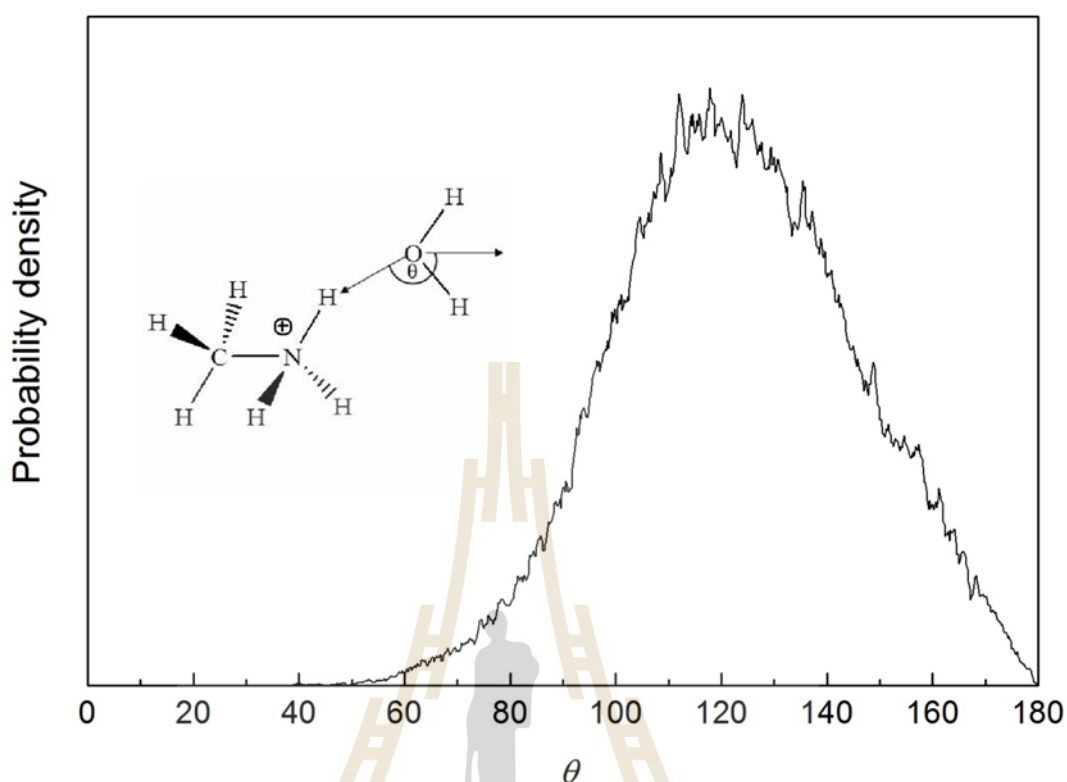


Figure 3.10 Probability distributions of θ angle, calculated within the first minimum of the $\text{H}_\text{N}\text{-O}_\text{W}$ RDF.

The geometrical arrangements of CH_3NH_3^+ in aqueous solution are described in terms of distributions of intramolecular bond lengths and bond angles, as shown in Figures 3.11 and 3.12, respectively. It is apparent that the structure of the CH_3NH_3^+ ion in water is somewhat flexible. As compared to the gas phase CH_3NH_3^+ structure, as well as the optimized $\text{CH}_3\text{NH}_3^+(\text{H}_2\text{O})_3$ complex (cf. Table 2.2), the ONIOM-XS MD simulation clearly reveals a significant change in the local structure of the CH_3NH_3^+ ion according to the influence of water environment.

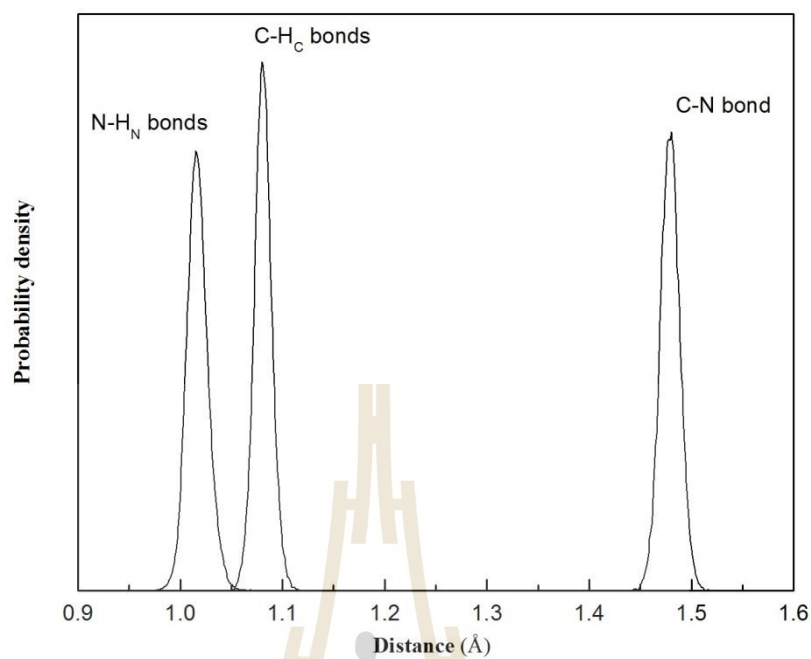


Figure 3.11 Distributions of N-H_N , C-H_C and C-N bond lengths of CH_3NH_3^+ .

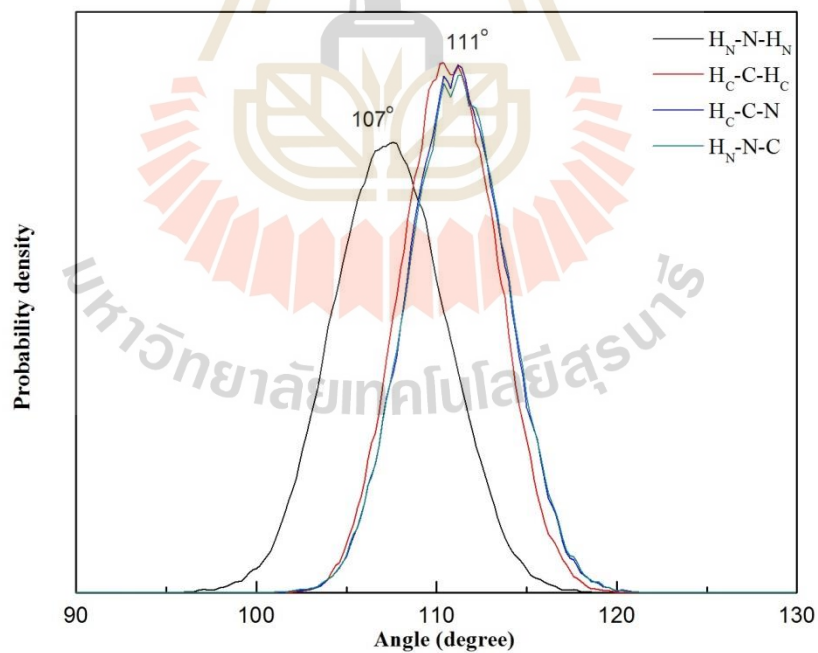


Figure 3.12 Distributions of $\text{H}_\text{N}\text{-N-H}_\text{N}$, $\text{H}_\text{C}\text{-C-H}_\text{C}$, $\text{H}_\text{C}\text{-C-N}$ and $\text{H}_\text{N}\text{-N-C}$ angles of CH_3NH_3^+ .

3.2 Dynamical properties

The lability of water molecules surrounding the -NH_3^+ and -CH_3 groups of CH_3NH_3^+ can be interpreted through the self-diffusion coefficient (D), which is calculated from the center-of-mass velocity autocorrelation functions (VACFs) of water molecules in the primary regions of the -NH_3^+ and -CH_3 groups using the Green-Kubo relation (MaQuarrie, 1976),

$$D = \frac{1}{3} \lim_{t \rightarrow \infty} \int_0^t C_v(t) dt. \quad (3.1)$$

By the ONIOM-XS MD simulation, the D values for water molecules in the vicinity of the -NH_3^+ and -CH_3 groups are estimated to be 2.28×10^{-5} and $1.93 \times 10^{-5} \text{ cm}^2 \cdot \text{s}^{-1}$, respectively (cf. Table 3.1), which are close to the value of $2.23 \times 10^{-5} \text{ cm}^2 \cdot \text{s}^{-1}$ of pure water derived by the similar ONIOM-XS MD scheme (Thaomola, Tongraar and Kerdcharoen, 2012). This supplies information that water molecules in the primary region of both the -NH_3^+ -CH_3 groups are quite labile, *i.e.*, they diffuse in a similar degree of lability of those in the bulk. In particular, it is evident that the “hydrophobic effect” of the -CH_3 group results in slightly more attractive water-water interactions in this region, *i.e.*, giving a lower D value when compared to that of bulk water. This corresponds to a scenario in which water molecules adjacent to a nonpolar group are less labile and their water-water HB interactions are (on the average) stronger than those in the bulk.

Table 3.1 D values of water molecules in the bulk and in the hydration shells of CH_3NH_3^+ , as obtained by the ONIOM-XS MD simulation.

Phase	D ($\text{cm}^2.\text{s}^{-1}$)
Hydration shell of CH_3NH_3^+	
At the $-\text{NH}_3^+$ group	2.28×10^{-5}
At the $-\text{CH}_3$ group	1.93×10^{-5}
Bulk water ^a	2.23×10^{-5}
H_2O around NH_4^+ ^b	3.23×10^{-5}

^a (Thaomola, Tongraar and Kerdcharoen, 2012)

^b (Intharathep, Tongraar and Sagarik, 2005)

Water exchange at each hydrogen atom of the $-\text{NH}_3^+$ group can be visualized from the plots of time dependence of the $\text{H}_\text{N}\cdots\text{O}_\text{W}$ distance, as depicted in Figure 3.13. During the ONIOM-XS MD simulation, it is observed that water molecules which formed HBs at each of the $-\text{NH}_3^+$ hydrogens are quite labile, *i.e.*, they can easily exchange with other nearest-neighbor waters. Figure 3.14 displays the plots of time dependence of the number of water molecules at each hydrogen atom of the $-\text{NH}_3^+$ group, calculated within the first minimum of the $\text{H}_\text{N}\cdots\text{O}_\text{W}$ RDF. According to Figures 3.13 and 3.14, it is apparent that each of the $-\text{NH}_3^+$ hydrogens can simultaneously form (either strong or weak) HBs to different numbers of water molecules, leading to various possible species of the CH_3NH_3^+ hydrates formed in aqueous solution. In Figure 3.15, some selected conformations of several hydrated CH_3NH_3^+ complexes are shown, which include all nearest-neighbor waters located within the $\text{H}_\text{N}\cdots\text{O}_\text{W}$ distance of 2.5 \AA and some water molecules from the outer region. Interestingly, it is observed that, besides the HB formation between the $-\text{NH}_3^+$ hydrogens and their nearest-neighbor waters, the HB interactions among the shell-shell waters as well

as between the first-shell waters and the bulk also exist. These observed phenomena clearly supply information that CH_3NH_3^+ acts as a “structure-breaking” ion in aqueous solution.

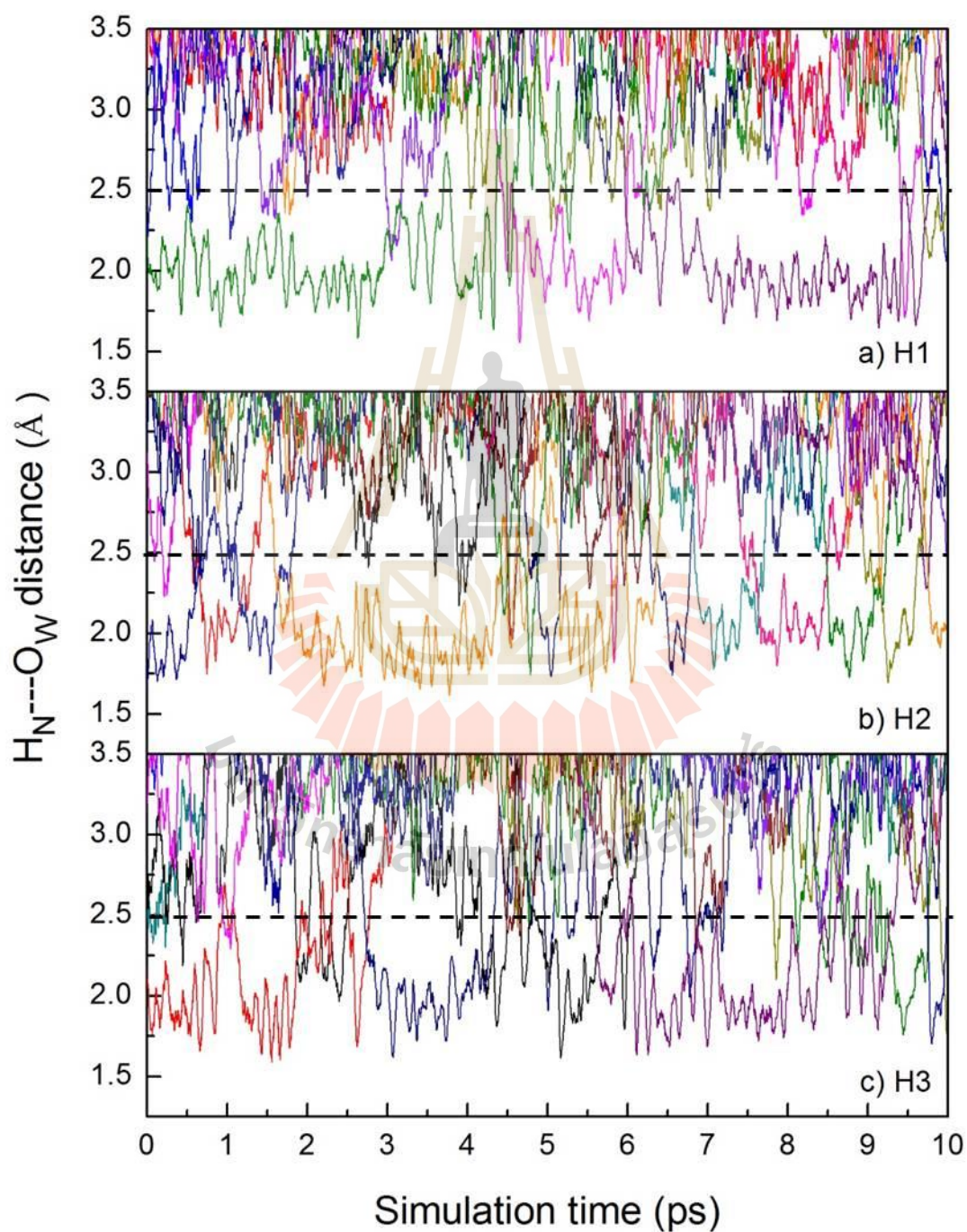


Figure 3.13 Water exchange in the first solvation shell of each hydrogen atom of $-\text{NH}_3^+$, selected only for the first 10 ps of the ONIOM-XS MD simulation.

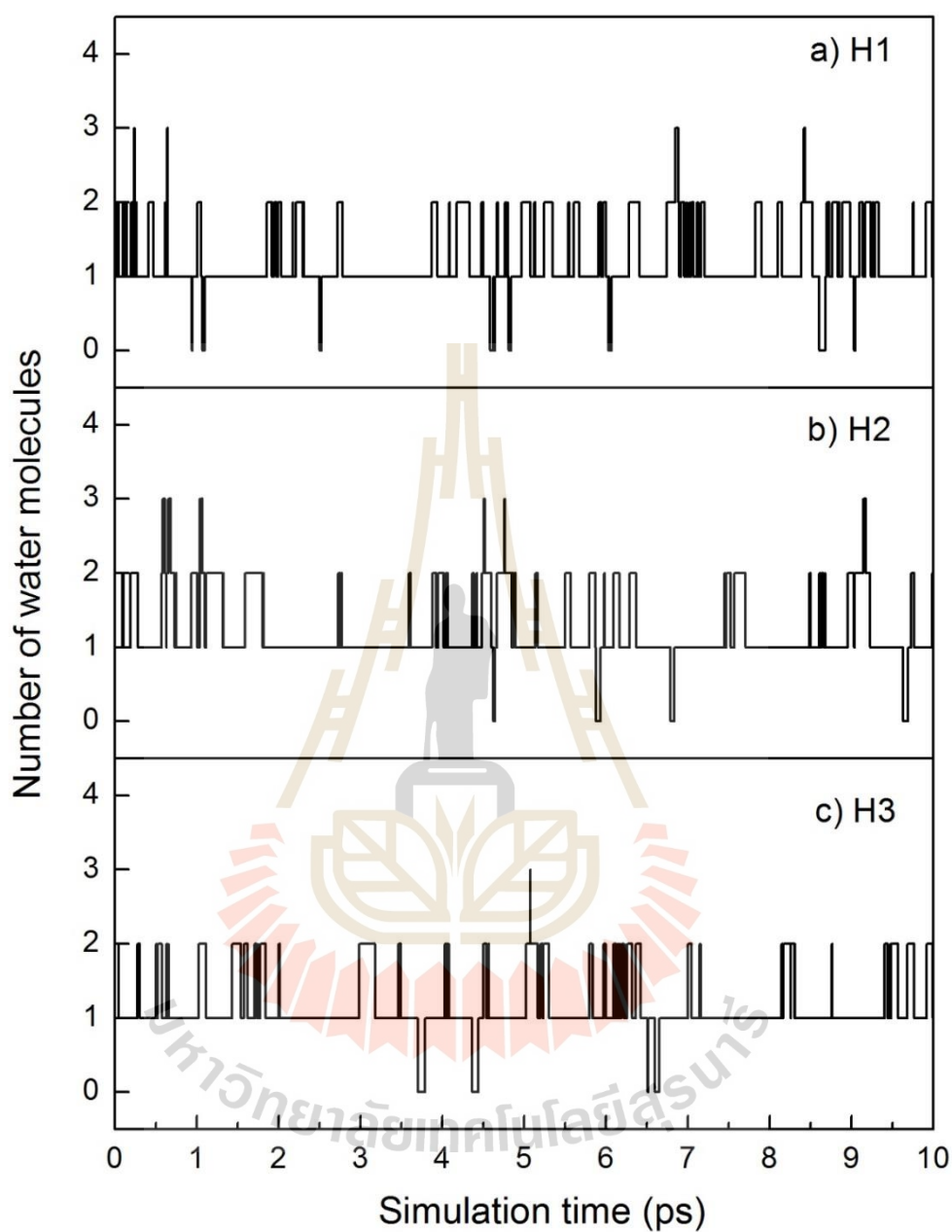


Figure 3.14 Time dependence of the number of water molecules in the first solvation shell of each hydrogen atom of $-\text{NH}_3^+$, calculated within the $\text{H}_\text{N}\cdots\text{O}_\text{W}$ distance of 2.5 Å and selected only for the first 10 ps of the ONIOM-XS MD simulation.

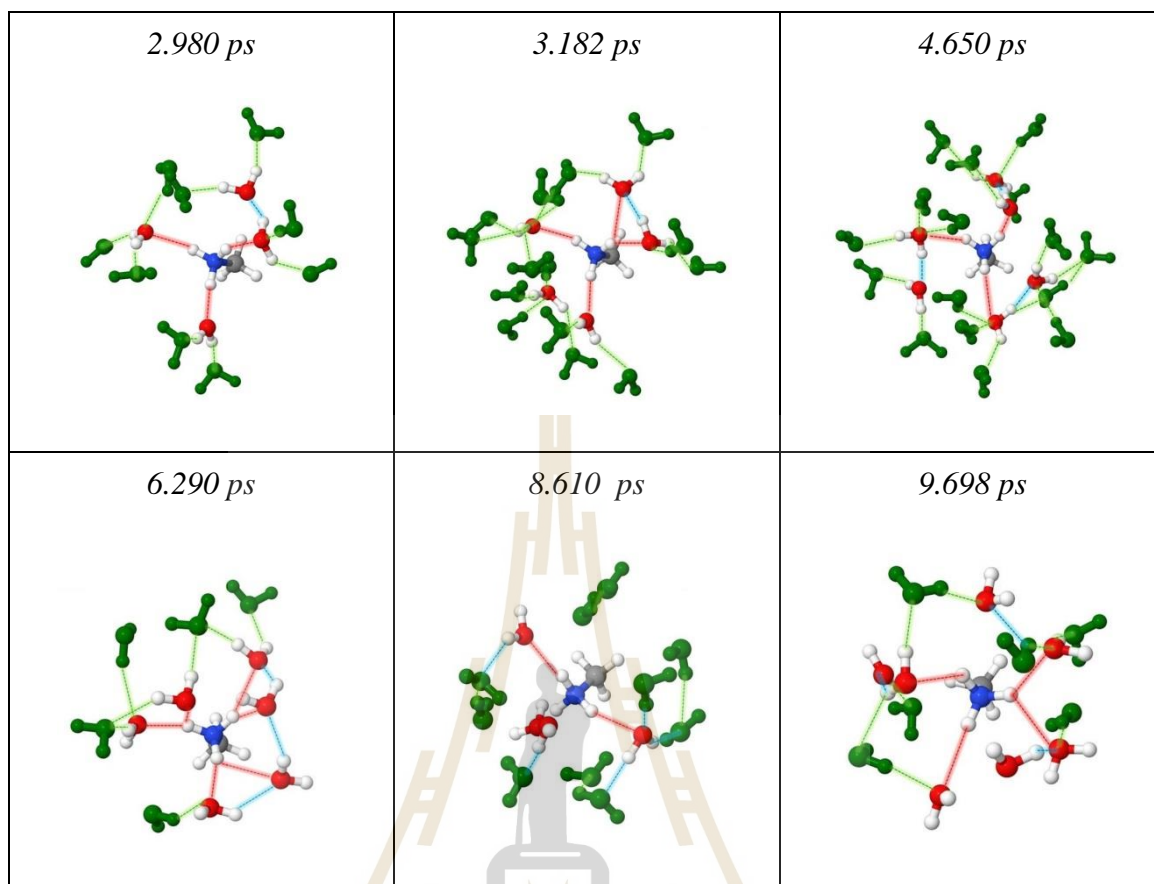


Figure 3.15 Selected geometrical arrangements of the CH_3NH_3^+ -water complexes, showing the HB formations between the $-\text{NH}_3^+$ hydrogens and their nearest-neighbor waters (*i.e.*, the dash lines highlighted in “red”), as well as the HB formations among the first-shell waters (*i.e.*, the dash lines highlighted in “blue”) and between the first-shell waters and the bulk (*i.e.*, the dash lines highlighted in “green”). Note that water molecules located outside the $\text{H}_\text{N} \cdots \text{O}_\text{W}$ distance of 2.5 Å are colored in “green”.

The rates of water exchange processes at the $-\text{CH}_3$ and $-\text{NH}_3^+$ species, as well as at each of the $-\text{NH}_3^+$ hydrogens, were evaluated by means of mean residence times (MRTs) of the water molecules. Using the “direct” method (Hofer, Tran, Schwenk and Rode, 2004), the MRT data were obtained from the product of the average number of nearest-neighbor water molecules located within the defined solvation shell with the duration of the ONIOM-

XS MD simulation, divided by the observed number of exchange events lasting a given time interval t^* ,

$$MRT(\tau) = \frac{CN \times t_{sim}}{N_{ex}} \quad (3.2)$$

With regard to the “direct” method (Hofer, Tran, Schwenk and Rode, 2004), a t^* value of 0.0 ps was proposed as a suitable choice for the estimation of HB lifetimes, while a t^* value of 0.5 ps was used as a good measure for water exchange processes. The calculated MRT data with respect to t^* values of 0.0 and 0.5 ps are summarized in Table 3.2. To provide a useful discussion with respect to the “structure-breaking” ability of CH_3NH_3^+ , the MRT data for pure water, as derived by the compatible ONIOM-XS MD scheme (Thaomola, Tongraar and Kerdcharoen, 2012), were also given for comparison. For both $t^* = 0.0$ and 0.5 ps, the MRT values of water molecules in the primary region of the $-\text{NH}_3^+$ group, as well as in the first solvation shell of each of $-\text{NH}_3^+$ hydrogens, are lower than those of bulk water, indicating that the HB interactions between the $-\text{NH}_3^+$ hydrogens and their nearest-neighbor waters are relatively weaker than the water-water HBs in the bulk. For the hydrophobic site, the observed larger MRT data for water molecules in this region correspond to the “hydrophobic effect” of the $-\text{CH}_3$ group, *i.e.*, the influence of the $-\text{CH}_3$ species could be regarded as a small perturbation to slightly strengthen the solvent’s HB structure. Based on the ONIOM-XS MD simulation, the observed flexible hydration structure and the relatively low MRT values of water molecules in the vicinity of the $-\text{NH}_3^+$ group, as well as the observed weak interactions between the $-\text{CH}_3$ group and its surrounding waters, clearly confirm the “structure-breaking” ability of CH_3NH_3^+ in aqueous solution.

Table 3.2 Mean residence times ($\tau_{H_2O}^{t^*}$) of water molecules in the vicinity of CH_3NH_3^+ , calculated within the first minimum of the ONIOM-XS MD's N-O_W and H_N-O_W RDFs.

Solute/ion	CN	t_{sim}	$t^* = 0.0$ ps		$t^* = 0.5$ ps		
			$N_{ex}^{0.0}$	$\tau_{H_2O}^{0.0}$	$N_{ex}^{0.5}$	$\tau_{H_2O}^{0.5}$	
ONIOM-XS MD*							
CH_3NH_3^+	N-O _W	5.02	40.96	744	0.276	129	1.593
	C-O _W	14.49	40.96	1139	0.521	221	2.685
	H _{N(1)} -O _W	1.219	40.96	510	0.098	41	1.218
	H _{N(2)} -O _W	1.178	40.96	439	0.110	38	1.270
	H _{N(3)} -O _W	1.187	40.96	549	0.089	44	1.352
H ₂ O ^a	O-O	4.7	30.0	607	0.23	65	2.17

* This work

^a (Thaomola, Tongraar and Kerdcharoen, 2012)

Additional details regarding the dynamics of water molecules in the vicinity of the CH_3NH_3^+ ion can be gained by computing the velocity autocorrelation functions (VACFs) of first-shell water molecules and their Fourier transformations. In this work, the normal-coordinate analysis developed by Bopp (Bopp, 1986; Spohr, Pálinkás, Heinzinger, Bopp and Probst, 1988) was used for obtaining three quantities Q_2 , Q_1 and Q_3 , which are defined for describing bending vibration, and symmetric and asymmetric stretching vibrations of water molecules, respectively, as depicted in Figure 3.16. By the ONIOM-XS MD technique, since all the atomic motions of first-shell water molecules are generated according to the QM force calculations, the calculated vibrational spectra are usually scaled by an empirical factor, *i.e.*, an approximate correction for errors in the force constants and

for anharmonic effects (Johnson, Irikura, Kacker and Kessel, 2010; Merrick, Moran and Radom, 2007; Scott and Radom, 1996). With regard to the systematic error of the HF frequency calculations, all frequencies obtained by the ONIOM-XS MD simulation were multiplied by an appropriate scaling factor of 0.905 (Scott and Radom, 1996). To reliably illustrate the “structure-breaking” ability of CH_3NH_3^+ in water, the corresponding Q_1 , Q_2 and Q_3 frequencies obtained from the ONIOM-XS MD simulation of liquid water (Thaomola, Tongraar and Kerdcharoen, 2012) were also utilized for comparison. All intramolecular vibrational frequencies (Q_1 , Q_2 and Q_3) of water molecules in the hydration shell of CH_3NH_3^+ and some simple alkali metal ions (Li^+ , Na^+ , K^+), as well as of the liquid water are given in Table 3.3. For liquid water, all the bending and stretching vibrational frequencies showed peaks with recognizable shoulders, especially for the symmetric and asymmetric vibrational modes. These observed spectra have been ascribed to the presence of several kinds, with varying strengths, of HBs formed in liquid water (Thaomola, Tongraar and Kerdcharoen, 2012). In the hydration shell of CH_3NH_3^+ , since water molecules are arranged with respect to the influence of the ion as well as to the HBs among the water molecules, the corresponding Q_2 , Q_1 and Q_3 frequencies are mostly found to be exhibited between the main peaks and the shoulders of the respective Q_2 , Q_1 and Q_3 frequencies of liquid water. These observed data are in good accord with the observed “structure-breaking” ability of the CH_3NH_3^+ ion in water. In this context, it could be demonstrated that the ONIOM-XS MD results can provide more insights into the behaviors of the CH_3NH_3^+ hydrates, which are very crucial in order to correctly understand the functionality and reactivity of this ion in aqueous solution.

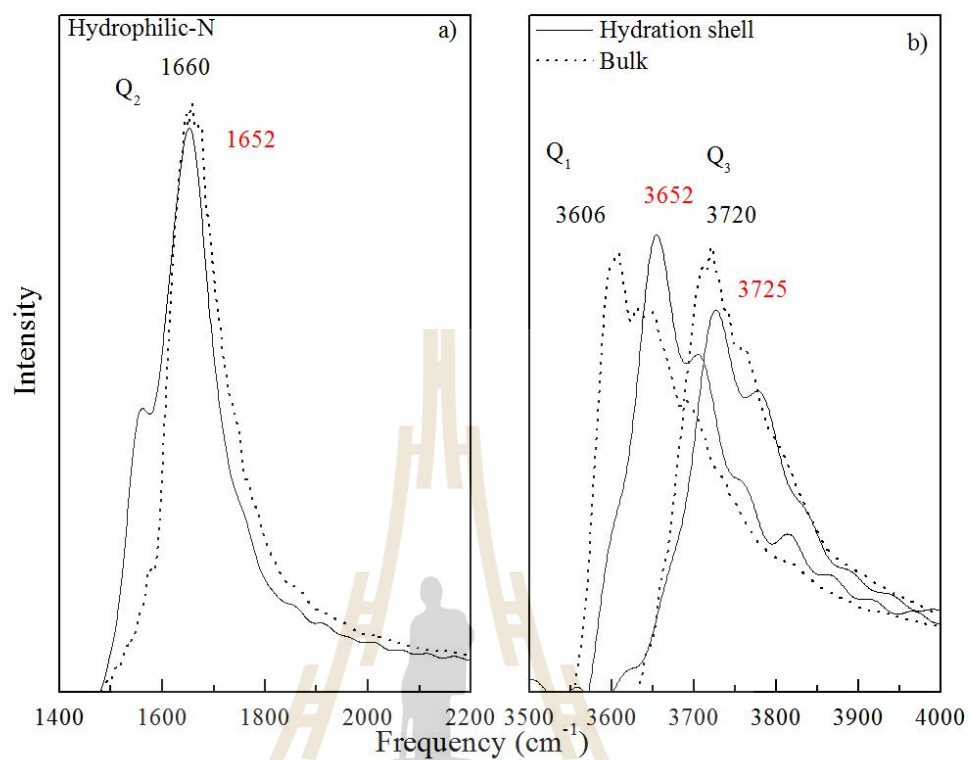


Figure 3.16 Fourier transforms of the hydrogen velocity autocorrelation functions of a) bending vibrations (Q_2) and b) symmetric and asymmetric stretching vibrations (Q_1 and Q_3) of water molecules in the first hydration shell of CH_3NH_3^+ and in the bulk.

Table 3.3 Vibrational frequencies of water molecules in the hydration shells of CH_3NH_3^+ , K^+ , Ca^{2+} , Na^+ and in the bulk water. (Q_1 , Q_2 and Q_3 corresponding to symmetric stretching, bending and asymmetric stretching vibrations, respectively).

Phase	Frequency (cm^{-1})		
	Q_2	Q_1	Q_3
NH_3^+ site	1650	3653	3726
CH_3 site	1658	3658	3731
H_N site	1655	3632	3712
Hydration shell of K^+ ^a	1674	3579	3667
Hydration shell of Ca^{2+} ^a	1634	3483	3605
Hydration shell of Na^+ ^b	1629	3628	3738
Pure water ^c	1660	3650 (3606)	3755 (3720)

^a (Wanprakhon, Tongraar and Kerdcharoen, 2011)

^b (Sripa, Tongraar and Kerdcharoen, 2013)

^c (Thaomola, Tongraar and Kerdcharoen, 2012)

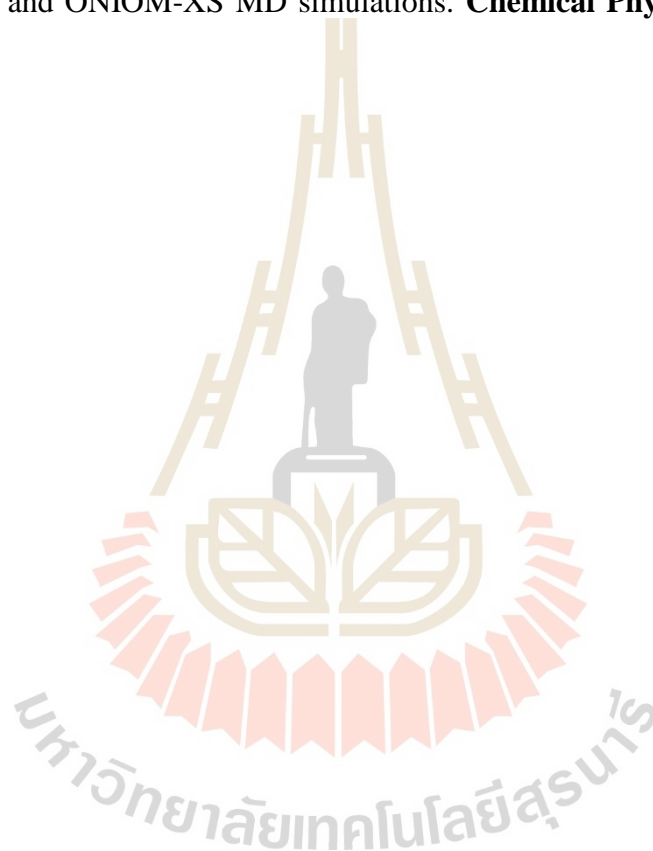
3.3 References

- Alagona, G., Ghio, C. and Kollman, P. (1986). Monte Carlo simulation studies of the solvation of ions. 1. Acetate anion and methylammonium cation. **Journal of the American Chemical Society**. 108: 185-191.
- Bopp, P. (1986). A study of the vibrational motions of water in an aqueous CaCl_2 solution. **Chemical Physics**. 106: 205-212.
- Hesske, H. and Gloe, K. (2007). Hydration behavior of alkyl amines and their corresponding protonated forms. 1. ammonia and methylamine. **The Journal of Physical Chemistry A**. 111: 9848-9853.

- Hofer, T. S., Tran, H. T., Schwenk, C. F. and Rode, B. M. (2004). Characterization of dynamics and reactivities of solvated ions by *ab initio* simulations. **Journal of Computational Chemistry**. 25: 211 - 217.
- Intharathep, P., Tongraar, A. and Sagarik, K. (2005). Structure and dynamics of hydrated NH_4^+ : An *ab initio* QM/MM molecular dynamics simulation. **Journal of Computational Chemistry**. 26: 1329-1338.
- Johnson, R. D., Irikura, K. K., Kacker, R. N. and Kessel, R. (2010). Scaling factors and uncertainties for *ab initio* anharmonic vibrational frequencies. **Journal of Chemical Theory and Computation**. 6: 2822-2828.
- MaQuarrie, D. A. (1976). in **statistical Mechanics; Harper & Row , New York**.
- Merrick, J. P., Moran, D. and Radom, L. (2007). An evaluation of harmonic vibrational frequency scale factors. **The Journal of Physical Chemistry A**. 111: 11683-11700.
- Perrin, C. L. and Gipe, R. K. (1986). Absence of stereoelectronic control in hydrolysis of cyclic amidines. **Journal of the American Chemical Society**. 108: 5997-6003.
- Perrin, C. L. and Gipe, R. K. (1987). Rotation and solvation of ammonium ion. **Science (New York, N.Y.)**. 238: 1393-1394.
- Scott, A. P. and Radom, L. (1996). Harmonic vibrational frequencies: An evaluation of hartree-fock, møller-plesset, quadratic configuration interaction, density functional theory, and semiempirical scale factors. **The Journal of Physical Chemistry**. 100: 16502-16513.
- Spohr, E., Pálinkás, G., Heinzinger, K., Bopp, P. and Probst, M. M. (1988). Molecular dynamics study of an aqueous SrCl_2 solution. **The Journal of Physical Chemistry**. 92: 6754-6761.
- Sripa, P., Tongraar, A. and Kerdcharoen, T. (2013). “Structure-making” ability of Na^+ in dilute aqueous solution: An ONIOM-XS MD simulation study. **The Journal of Physical Chemistry A**. 117: 1826-1833.

Thaomola, S., Tongraar, A. and Kerdcharoen, T. (2012). Insights into the structure and dynamics of liquid water: A comparative study of conventional QM/MM and ONIOM-XS MD simulations. **Journal of Molecular Liquids**. 174: 26-33.

Wanprakhon, S., Tongraar, A. and Kerdcharoen, T. (2011). Hydration structure and dynamics of K^+ and Ca^{2+} in aqueous solution: Comparison of conventional QM/MM and ONIOM-XS MD simulations. **Chemical Physics Letters**. 517: 171-175.

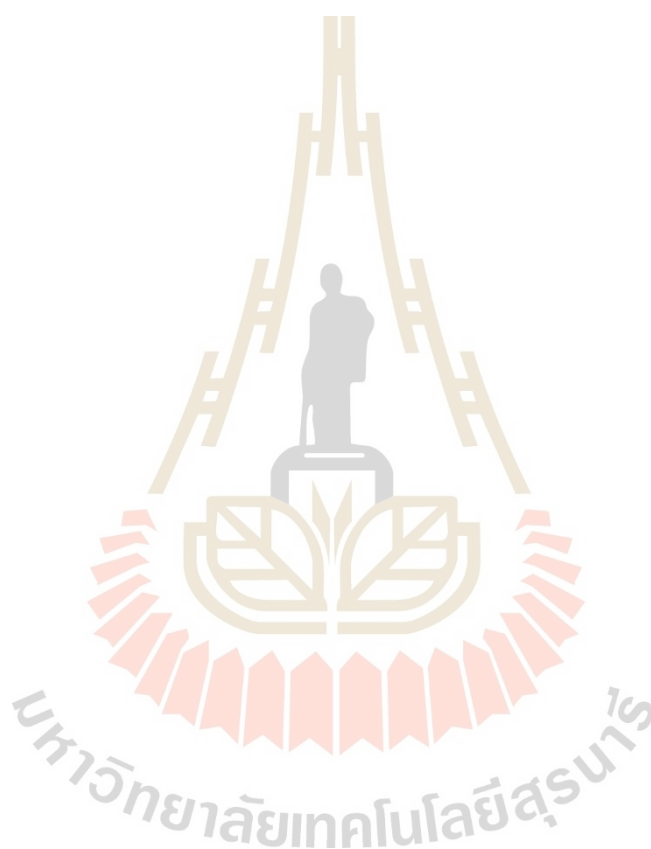


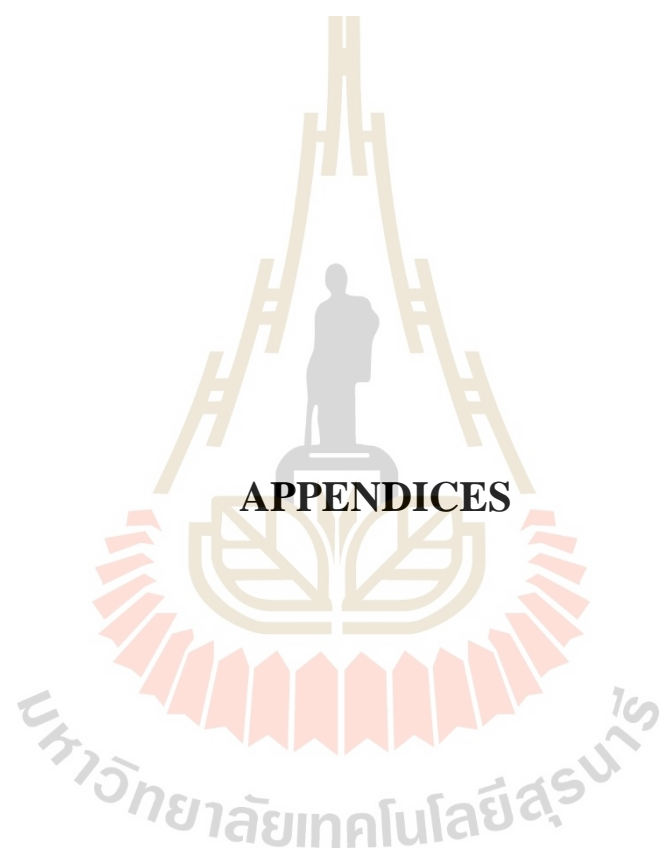
CHAPTER IV

CONCLUSIONS

In this work, the sophisticated ONIOM-XS MD technique has been applied for studying the solvation structure and dynamics of CH_3NH_3^+ in aqueous solution. By the ONIOM-XS MD technique, the system is divided into a small subsystem, *i.e.*, a sphere which contains the CH_3NH_3^+ ion and its nearest-neighbor waters, treated at the HF level of accuracy using the DZP basis set, and the remaining MM subsystem which described by means of classical pair potentials. The selection of the HF method and the DZP basis set employed for this particular system has been checked to be a suitable choice, compromising between the quality of the simulation results and the CPU time available. Based on the ONIOM-XS MD simulation, it is observed that the solvation structure of the CH_3NH_3^+ ion is somewhat flexible, in which various numbers of water molecules, ranging from 3 to 8 and from 12 to 19, are cooperatively involved in the primary region of the $-\text{NH}_3^+$ and $-\text{CH}_3$ groups, respectively. For the hydrophilic side, it is found that the $-\text{NH}_3^+$ group participates in about 3.6 HBs with its nearest-neighbor waters, *i.e.*, consisting of about 1.2 water molecules for each of the $-\text{NH}_3^+$ hydrogens. Interestingly, it is observed that the HB interactions between the $-\text{NH}_3^+$ hydrogens and their nearest-neighbor waters are not strong, *i.e.*, when compared to the water-water HBs in the bulk. Consequently, this allows several water exchange processes to frequently occur at each of the $-\text{NH}_3^+$ hydrogens. For the hydrophobic side, it is observed that water molecules in this region are labile and they are arranged according to their water-water HB networks, rather than by the influence of the $-\text{CH}_3$ group. In addition, it is evident that the “hydrophobic effect” of the $-\text{CH}_3$ species results in slightly more attractive water-water HB interactions in this region. Overall, the

ONIOM-XS MD results clearly reveal the characteristics of CH_3NH_3^+ as a “structure-breaking” ion in aqueous solution. In this context, the ONIOM-XS MD technique can be considered as an elegant simulation approach to obtain more detailed interpretation on the structure and dynamics of such amphiphilic species solvated in aqueous electrolyte solution.





APPENDICES

APPENDIX A

THEORETICAL OBSERVATIONS

Table A.1 Theoretical observations for CH_3NH_3^+ in aqueous solution.

RDF (Coordination numbers)					Number of HBs	Method	Year
$\text{C}\cdots\text{O}_w$	$\text{H}_\text{C}\cdots\text{O}_w$	$\text{N}\cdots\text{O}_w$	$\text{H}_\text{N}\cdots\text{O}_w$	$\text{H}_\text{N}\cdots\text{H}_w$			
n.a.	n.a.	2.80 (4.40)	≈ 1.9 (≈ 1.3)	n.a.	3.72	MC	1986
≈ 3.7 (≈ 10)	≈ 1.8 (≈ 1)	n.a.	n.a.	n.a.	3.67	MC	1986
n.a.	n.a.	2.85 (5.60)	n.a.	n.a.	3.67	MD	1996
n.a.	n.a.	3.45 (4.20)	n.a.	n.a.	≈ 3	CPMD	2007

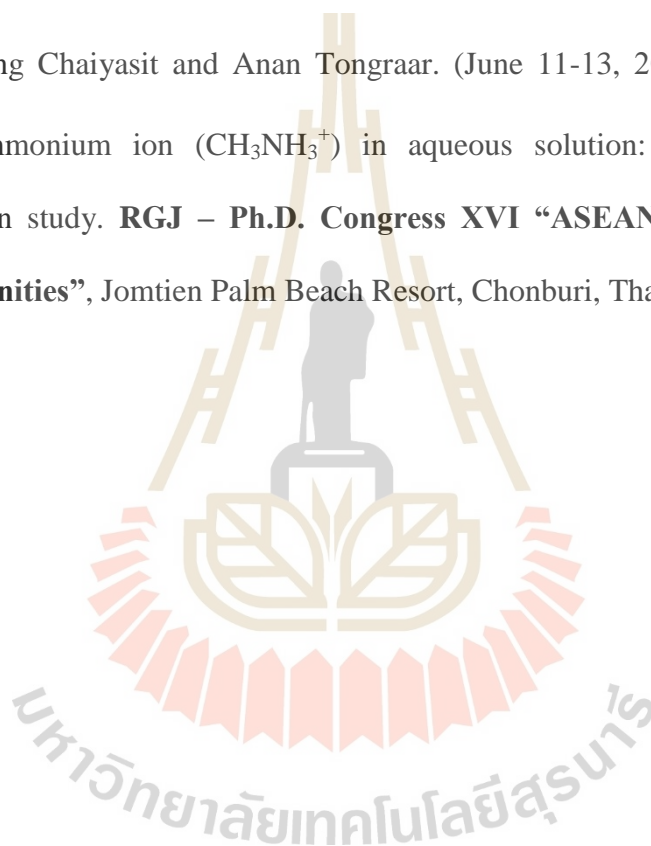
Table A.1 (Continued) Theoretical observations for CH_3NH_3^+ in aqueous solution.

RDF (Coordination numbers)					Number of HBs	Method	Year
$\text{C}\cdots\text{O}_w$	$\text{H}_\text{C}\cdots\text{O}_w$	$\text{N}\cdots\text{O}_w$	$\text{H}_\text{N}\cdots\text{O}_w$	$\text{H}_\text{N}\cdots\text{H}_w$			
3.10 (13.5)	1.80 (1.10)	3.00 (6.20)	n.a.	n.a.	1.00	GAFF/RISM	
3.20 (13.00)	1.90 (1.00)	2.90 (5.70)	n.a.	n.a.	1.00	QM/RISM	2012
3.50 (13.80)	1.90 (1.40)	2.90 (5.40)	n.a.	n.a.	1.40	QM/MM	
3.18 (12.70)	2.33 (1.91)	2.88 (5.58)	1.85 (1.00)	≈ 2.1 (≈ 0.9)	3.00	RISM	2012

APPENDIX B

LIST OF PRESENTATION

1. Prangthong Chaiyasit and Anan Tongraar. (June 11-13, 2015). Characteristics of methylammonium ion (CH_3NH_3^+) in aqueous solution: An ONIOM-XS MD simulation study. **RGJ – Ph.D. Congress XVI “ASEAN: Emerging Research Opportunities”**, Jomtien Palm Beach Resort, Chonburi, Thailand.



APPENDIX C

PUBLICATION

Chemical Physics 493 (2017) 91–101



Contents lists available at ScienceDirect

Chemical Physics

journal homepage: www.elsevier.com/locate/chemphys



Characteristics of methylammonium ion (CH_3NH_3^+) in aqueous electrolyte solution: An ONIOM-XS MD simulation study



Prangthong Chaityasit^a, Anan Tongraar^{a,*}, Teerakiat Kerdcharoen^b

^aSchool of Chemistry, Institute of Science, Suranaree University of Technology and NANOTEC-SUT Center of Excellence on Advanced Functional Nanomaterials, Nakhon Ratchasima 30000, Thailand

^bDepartment of Physics and NANOTEC Center of Excellence, Faculty of Science, Mahidol University, Bangkok 10400, Thailand

ARTICLE INFO

Article history:
Received 11 March 2017
In final form 25 June 2017
Available online 27 June 2017

Keywords:
ONIOM-XS MD
Methylammonium ion
Hydrogen bonds
Aqueous solution
Hartree-Fock

ABSTRACT

An ONIOM-XS MD simulation has been performed to characterize the CH_3NH_3^+ -water hydrogen bonds (HBs) in aqueous solution. The sphere which includes the CH_3NH_3^+ ion and its surrounding waters was treated by the HF/DZP method, while the rest was described by classical pair potentials. The ONIOM-XS MD results clearly reveal a flexible CH_3NH_3^+ solvation, showing various numbers of water molecules, ranging from 3 to 8 and from 12 to 19, cooperatively involved in the primary region of the $-\text{NH}_3^+$ and $-\text{CH}_3$ species, respectively. The $-\text{NH}_3^+$ group participates in about 3.6 HBs with its nearest-neighbor waters, and the HBs between the $-\text{NH}_3^+$ hydrogens and their nearest-neighbor waters are relatively weaker than the HBs of bulk water. It is evident that the “hydrophobic effect” of the $-\text{CH}_3$ species results in slightly more attractive water-water HB interactions in this region. Such phenomenon corresponds to a clear “structure-breaking” ability of CH_3NH_3^+ in aqueous solution.

© 2017 Elsevier B.V. All rights reserved.

1. Introduction

Protonated amino groups ($-\text{NH}_3^+$) are the most common positively charged moieties in many biologically important molecules, such as amino acids and peptides [1,2]. With regard to the protonated amines (RNH_3^+), methylammonium ion (CH_3NH_3^+) can be considered as a simple model in which the details with respect to the CH_3NH_3^+ -water hydrogen bonds (HBs) are essential in order to understand many biological processes that involve the $-\text{NH}_3^+$ species [3–11]. Of particular interest, according to the amphiphilic nature of CH_3NH_3^+ which consists of hydrophilic ($-\text{NH}_3^+$) and hydrophobic ($-\text{CH}_3$) moieties, it is expected that the HB networks formed around the CH_3NH_3^+ ion are somewhat different from those of hydrophilic ion cores, such as ammonium (NH_4^+) or hydronium (H_3O^+) ions. In the literature, most of the published data regarding the determination of CH_3NH_3^+ in aqueous solution were obtained from Monte Carlo (MC) and molecular dynamics (MD) simulations. For example, an early MC simulation of CH_3NH_3^+ in aqueous solution using the TIP4P potential for water and analogous potentials for the ion [8] has reported that the $-\text{NH}_3^+$ group has an average coordination number (CN) of 3.5, which corresponds to one water molecule closely attached to each H atom. In this respect, water

molecules in the first solvation shell have both lone pairs directed toward the $-\text{NH}_3^+$ group, i.e., implying that only their hydrogen atoms are available for coordinating to bulk water. The average number of HBs to bulk water of each first-shell water molecule is 1.88. For the hydrophobic side, the numbers of water molecules near the $-\text{CH}_3$ group can be varied from 12 to 15 (depending on the choice of the minimum position). In the meantime, another MC simulation using the OPLS potential functions [9] has suggested that the CH_3NH_3^+ species participated in 4 strong HBs with water molecules, consisting of about 1.24 primary water molecules for each H atom of $-\text{NH}_3^+$, while the primary region around the $-\text{CH}_3$ group contains about 8.6 water molecules. Later, according to the MD simulations of aqueous CH_3NH_3^+ solution using a pairwise additive SPC/E model and a related polarizable model (POL3) for water [10], the average hydration numbers of 3.67 and 3.60 were found for the hydrophilic group of CH_3NH_3^+ , respectively. This corresponds to the average numbers of 1.22 and 1.20 water molecules at each H atom of the $-\text{NH}_3^+$ group, respectively. In the hydrophobic region, the $-\text{CH}_3$ group contains about 9.33 and 9.36 water molecules, respectively. With regard to the earlier MC and MD studies, the observed discrepancies could be ascribed to the use of different molecular mechanical (MM) potentials, most of which were constructed with respect to the simplified effects of many-body interactions. Thus, more sophisticated simulation techniques which take into account the importance of “quantum

* Corresponding author.

E-mail address: anan_tongraar@yahoo.com (A. Tongraar).

effects" seem to be necessary in order to obtain more accurate descriptions of such condensed-phase systems.

Based on the *ab initio* MD frameworks, a Car-Parrinello (CP) MD simulation study of aqueous CH_3NH_3^+ solution [11] has reported that the first hydration shell of the $-\text{NH}_3^+$ group contains 4.2 water molecules. In this respect, oxygen atoms of three water molecules are localized along the direction of the N–H bond and form HBs, while another nearest-neighbor water molecule is weakly bound and is not fixed within the first hydration shell. The CP-MD approach has a major advantage over the MM-based MC and MD techniques since the overall system's interactions can directly be obtained from quantum mechanics (QM) calculations, and hence it can produce more reliable results. However, some methodical limitations of the CP-MD technique stem from the use of simple generalized gradient approximation (GGA) functionals, such as BLYP, and of the relatively small system size. It has been well demonstrated that the use of simple density functionals in the CP-MD scheme could result in improper structural and dynamical properties even for the pure liquid water [12–14]. In particular, it has been shown that the use of the BLYP functional leads to a strongly decreased self-diffusion coefficient of this peculiar liquid [14]. Besides the full *ab initio* MD techniques, an alternative approach is to apply a so-called combined QM/MM MD technique based on the ONIOM-XS (Own N-layered Integrated Molecular Orbital and Molecular Mechanics – Extension to Solvation) method, called briefly ONIOM-XS MD [15,16]. This technique has been successfully applied for studying various condensed phase systems [15–24]. Of particular interest, in the case of liquid water, the results obtained by the ONIOM-XS MD simulation [18] have provided more insights into the multiple HB species among water molecules which correspond to the experimental XAS data for the arrangement of one strong and one weak (for both donor and acceptor), rather than the equivalent two donors and two acceptors tetrahedral structure. Recently, the ONIOM-XS MD technique has been successfully applied for characterizing the "structure-making" and "structure-breaking" abilities of some essential metal ions in water [17,19,20,24], showing its capability in predicting more reliable results, especially when compared to those derived by the conventional QM/MM MD scheme. In this study, it is of particular interest, therefore, to apply the high-level ONIOM-XS MD technique for studying the characteristics of CH_3NH_3^+ in aqueous solution.

2. Method

With regard to the ONIOM-XS MD technique [15,16], the system is partitioned into a QM treated region, *i.e.*, a sphere which contains the CH_3NH_3^+ and its surrounding water molecules, and the remaining MM region, *i.e.*, the bulk waters. A thin switching layer, which is located between the QM and MM regions, is employed to detect the exchanging particles and assist in smoothing the energy and forces of the combined system. Based on the

ONIOM extrapolation scheme [25], the potential energy of the system can be expressed in two ways, *i.e.*, if the switching layer is included into the QM sphere, the energy expression is written as

$$E^{\text{ONIOM}}(n_1 + l; N) = E^{\text{QM}}(n_1 + l) - E^{\text{MM}}(n_1 + l) + E^{\text{MM}}(N), \quad (1)$$

and if the switching layer is considered as part of the MM region, the energy expression is

$$E^{\text{ONIOM}}(n_1; N) = E^{\text{QM}}(n_1) - E^{\text{MM}}(n_1) + E^{\text{MM}}(N). \quad (2)$$

In Eqs. (1) and (2), the n_1 , l and n_2 parameters refer to the number of particles involved in the QM region, the switching layer and the MM region, respectively, and N is the total number of particles (*i.e.*, $N = n_1 + l + n_2$), whereas the E^{QM} and E^{MM} terms represent the interactions obtained from the QM calculations and from the MM potentials, respectively. Note that, according to the ONIOM-XS MD approach, the interactions between the QM and MM regions are described by means of the MM potentials, and thus these terms are already included into the $E^{\text{MM}}(N)$. During the ONIOM-XS MD simulation, when a particle moves into the switching layer (either from the QM or MM region), both Eqs. (1) and (2) will be evaluated. In this respect, the potential energy of the entire system can be written as a hybrid between both energy terms (1) and (2),

$$E^{\text{ONIOM-XS}}(\{r_i\}) = (1 - \bar{s}(\{r_i\})) \cdot E^{\text{ONIOM}}(n_1 + l; N) + \bar{s}(\{r_i\}) \cdot E^{\text{ONIOM}}(n_1; N), \quad (3)$$

where $\bar{s}(\{r_i\})$ is an average over a set of switching functions for individual exchanging particles in the switching layer $s_i(x_i)$,

$$\bar{s}(\{r_i\}) = \frac{1}{l} \sum_{i=1}^l s_i(x_i), \quad (4)$$

For the switching function in Eq. (4), a polynomial expression is employed,

$$s_i(x_i) = 6 \left(x_i - \frac{1}{2} \right)^5 - 5 \left(x_i - \frac{1}{2} \right)^3 + \frac{15}{18} \left(x_i - \frac{1}{2} \right) + \frac{1}{2}, \quad (5)$$

where $x_i = ((r_i - r_0)/(r_1 - r_0))$, and r_0 and r_1 are the radius of the inner and outer surfaces of the switching layer, respectively, and r_i is the distance between the reference atom of the solute and the oxygen atom of the exchanging water molecule. Finally, the gradient of the energy can be expressed as

$$\begin{aligned} \nabla_{\mathbf{r}} E^{\text{ONIOM-XS}}(\{r_i\}) &= (1 - \bar{s}(\{r_i\})) \cdot \nabla_{\mathbf{r}} E^{\text{ONIOM}}(n_1 + l; N) \\ &+ \bar{s}(\{r_i\}) \cdot \nabla_{\mathbf{r}} E^{\text{ONIOM}}(n_1; N) \\ &+ \frac{1}{(r_1 - r_0)} \nabla \bar{s}(\{r_i\}) \cdot (E^{\text{ONIOM}}(n_1; N) - E^{\text{ONIOM}}(n_1 + l; N)). \end{aligned} \quad (6)$$

In this study, the nitrogen atom of CH_3NH_3^+ was set as the center of the QM region, and a QM radius of 4.4 Å and a switching width of 0.2 Å were chosen, which correspond to the ONIOM-XS

Table 1
Stabilization energies and some selected structural parameters of the optimized $\text{CH}_3\text{NH}_3^+(\text{H}_2\text{O})_3$ complex, calculated at the HF, B3LYP, MP2 and CCSD levels of accuracy using the DZP and 6-311++G(d,p) (data in parentheses) basis sets.

Method	HF	B3LYP	MP2	CCSD
ΔE (kcal mol ⁻¹)	-16.12 (-15.44)	-18.61 (-16.89)	-16.23 (-15.50)	-16.36 (-15.53)
C–N (Å)	1.4866 (1.4858)	1.4974 (1.4953)	1.4918 (1.4897)	1.4953 (1.4932)
N–H _N (Å)	1.0160 (1.0148)	1.0422 (1.0363)	1.0347 (1.0329)	1.0320 (1.0309)
C–H _C (Å)	1.0799 (1.0798)	1.0917 (1.0883)	1.0882 (1.0887)	1.0894 (1.0908)
∠ N–C–H _C (deg)	108.95 (108.91)	109.30 (109.14)	108.90 (108.91)	108.82 (108.84)
∠ C–N–H _N (deg)	110.51 (110.79)	110.25 (110.75)	110.04 (110.40)	110.07 (110.44)
O _W –H _W (Å)	0.9467 (0.9440)	0.9678 (0.9641)	0.9657 (0.9622)	0.9644 (0.9604)
∠ H _W –O _W –H _W (deg)	106.59 (106.35)	105.96 (105.88)	105.11 (104.48)	105.17 (104.64)
H _N ···O _W (Å)	1.8926 (1.9109)	1.7738 (1.8161)	1.7978 (1.8115)	1.8255 (1.8347)
∠ N–H _N ···O _W (deg)	174.39 (176.07)	176.25 (177.29)	172.53 (174.37)	172.22 (174.46)

parameters r_0 and r_1 of 4.2 and 4.4 Å, respectively. This QM size is considered to be large enough to include most of the many-body interactions and the polarization effects, *i.e.*, at least within the whole first solvation shell of $-\text{NH}_3^+$ and the major part of the solvation sphere of $-\text{CH}_3$, and the remaining interactions beyond the QM region are assumed to be well accounted for by the MM potentials. Since the correlated QM calculations, even at the simple MP2, are rather too time-consuming for our current computational feasibility, all interactions within the QM region were evaluated by performing *ab initio* calculations at the Hartree-Fock (HF) level of accuracy using the DZP [26] basis set. It is known that the electron correlation and the charge transfer effects are not typically well-described by the HF theory, and that the use of the DZP basis set

could result in a high basis set superposition error and an exaggeration of the ligand-to-metal charge transfer. To simply check the validity of the HF method and the DZP basis set employed for this particular system, the geometry optimizations of the $\text{CH}_3\text{NH}_3^+(\text{H}_2\text{O})_3$ complex have been carried at the HF, B3LYP, MP2 and CCSD levels of accuracy using the DZP and 6-311++G(d,p) basis sets, as summarized in Table 1. It is apparent that the HF calculations using the DZP basis set can predict the structure and stabilization energy of the $\text{CH}_3\text{NH}_3^+(\text{H}_2\text{O})_3$ complex in good accord with the correlated methods, implying that the effects of electron correlation are marginal and that the use of the HF method is assumed to be good enough to sufficiently provide reliable results. All the QM calculations were carried out using the Gaussian03 program [27]. For the

Table 2
Optimized parameters of the analytical pair potentials for the interactions of water with CH_3NH_3^+ (interaction energies in $\text{kcal}\cdot\text{mol}^{-1}$ and distances in Å).

Pair	A ($\text{kcal}\cdot\text{mol}^{-1}\cdot\text{Å}^4$)	B ($\text{kcal}\cdot\text{mol}^{-1}\cdot\text{Å}^5$)	C ($\text{kcal}\cdot\text{mol}^{-1}\cdot\text{Å}^6$)	D ($\text{kcal}\cdot\text{mol}^{-1}\cdot\text{Å}^{12}$)
C-O _w	3.294261×10^2	-1.284494×10^4	2.867797×10^4	-2.736493×10^5
H _c -O _w	4.392700×10^2	-9.795945×10^2	7.804262×10^2	-2.978830×10^2
N-O _w	2.549314×10^3	-1.595213×10^4	2.601125×10^4	-1.219681×10^5
H _N -O _w	2.270976×10^1	-1.316456×10^2	2.245271×10^2	-8.618788×10^1
C-H _w	1.213528×10^2	2.935896×10^2	-6.708478×10^2	1.881890×10^3
H _c -H _w	-1.270316×10^2	3.009217×10^2	-1.720691×10^2	6.140965×10^0
N-H _w	-1.668167×10^2	1.272809×10^3	-1.472421×10^3	2.316114×10^3
H _N -H _w	-1.357481×10^2	3.091070×10^2	-1.726506×10^2	4.979114×10^0

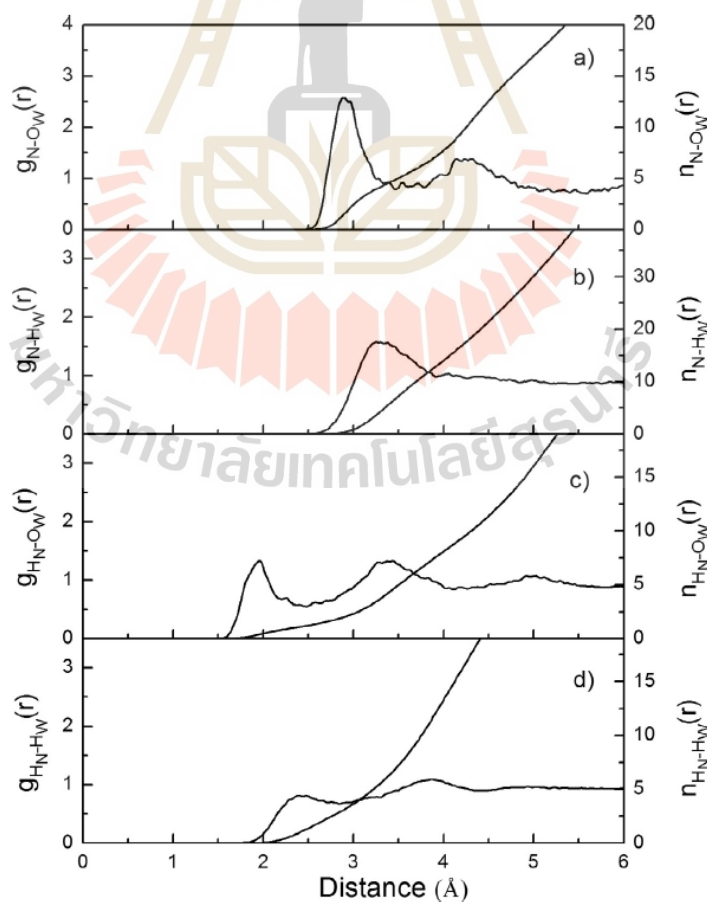


Fig. 1. a) N-O_w, b) N-H_w, c) H_N-O_w and d) H_N-H_w RDFs and their corresponding integration numbers.

interactions within the MM and between the QM and MM regions, a flexible BJH-CF2 model, which describes intermolecular [28] and intramolecular [29] interactions, was employed for water. This flexible water model allows explicit hydrogen movements, and thus ensures a smooth transition when water molecules move from the QM region with its full flexibility to the MM region and *vice versa*. The pair potential functions for describing the $\text{CH}_3\text{NH}_3^+-\text{H}_2\text{O}$ interactions were newly constructed. The 57,034 HF interaction energy points for various $\text{CH}_3\text{NH}_3^+-\text{H}_2\text{O}$ configurations as obtained from Gaussian03 [27] calculations using the DZP [26] basis set were fitted to the analytical form of

$$\Delta E_{\text{CH}_3\text{NH}_3^+-\text{H}_2\text{O}} = \sum_{i=1}^7 \sum_{j=1}^3 \left[\frac{A_{ij}}{r_{ij}^4} + \frac{B_{ij}}{r_{ij}^5} + \frac{C_{ij}}{r_{ij}^6} + \frac{D_{ij}}{r_{ij}^{12}} + \frac{q_i q_j}{r_{ij}} \right], \quad (7)$$

where A , B , C and D are the fitting parameters (see Table 2), r_{ij} denotes the distances between the i -th atoms of CH_3NH_3^+ and the j -th atoms of water molecules and q are atomic net charges. In the present study, the charges on C, H_C, N, H_N of CH_3NH_3^+ were obtained from Natural Bond Orbital (NBO) analysis [30–32] of the corresponding HF calculations, being of 0.6950, –0.0062, –0.2431

and 0.1890, respectively. The charges on O and H of water molecules were adopted from the BJH-CF2 water model [28] as –0.6598 and 0.3299, respectively.

The ONIOM-XS MD simulation was performed in a canonical ensemble at 298 K with periodic boundary conditions. The system's temperature was kept constant using the Berendsen algorithm [33]. A periodic box, with a box length of 18.17 Å, contains one CH_3NH_3^+ and 199 water molecules, corresponding to the experimental density of pure water. The reaction-field method [34] was employed for the treatment of long-range interactions. The Newtonian equations of motions were treated by a general predictor-corrector algorithm. The time step size was set to 0.2 fs, which allows for the explicit movement of the hydrogen atoms of water molecules. The ONIOM-XS MD simulation was started with the system's re-equilibration for 30,000 time steps, followed by another 200,000 time steps to collect configurations every 10th step.

3. Results and discussion

Water molecules surrounding the CH_3NH_3^+ ion will be classified into two groups, namely at the hydrophilic $-\text{NH}_3^+$ and hydrophobic

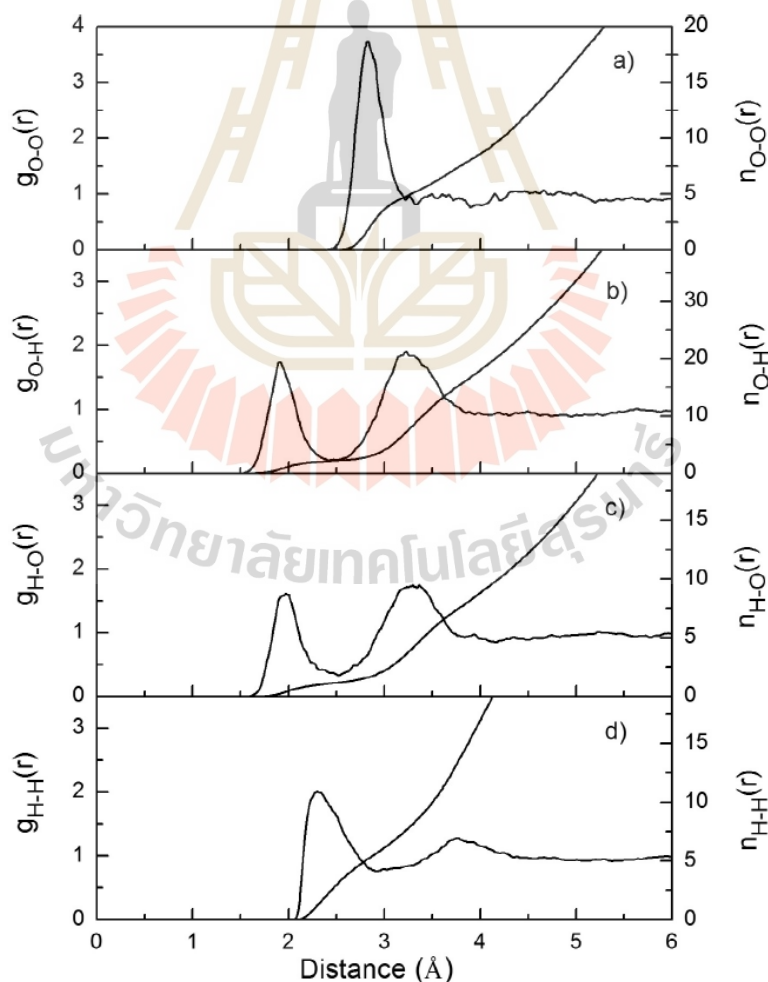


Fig. 2. a) O–O, b) O–H, c) H–O and d) H–H RDFs and their corresponding integration numbers, as obtained from the previous ONIOM-XS MD simulation of liquid water [18].

—CH₃ regions. The hydration structure of the hydrophilic group of CH₃NH₃⁺ can be visualized from the N-O_W, N-H_W, H_N-O_W and H_N-H_W radial distribution functions (RDFs) and their corresponding integration numbers, as depicted in Fig. 1 a–d, respectively. To reliably discuss the behavior of HBs between the —NH₃⁺ group and its nearest-neighbor waters, the corresponding atom-atom RDFs for pure water obtained by the similar ONIOM-XS MD technique [18] were utilized for comparison, as shown in Fig. 2. With regard to Fig. 1a, a pronounced first N-O_W peak is exhibited at 2.94 Å, together with a recognizable second N-O_W peak at around 4.23 Å. The characteristics of the N-O_W RDF, as compared to the O—O RDF of pure water (cf. Fig. 2a), clearly supplies information that the hydration structure of the —NH₃⁺ species is somewhat flexible, i.e., water molecules in the primary region of the —NH₃⁺ group are labile and they can exchange with water molecules in the outer region. The position of the first N-O_W minimum is roughly estimated to be 3.50 Å where the integration up to this N-O_W distance yields an average coordination number of 4.9 ± 0.1. In Fig. 1b, the first N-H_W peak is found at around 3.26 Å, implying that water molecules in the primary region tend to point their dipole moments toward the —NH₃⁺ group. However, according to Fig. 1a and b, the nonzero first minimum of the N-O_W RDF and

the observed broad peak of the N-H_W RDF clearly suggest that water molecules in this region are labile and their hydrogen atoms would have considerable orientational freedom. In this respect, the observed slight second peak of the N-O_W RDF (cf. Fig. 1a) could also be assigned to oxygen atoms of some water molecules in the outer region that form HBs with hydrogen atoms of water molecules in the first hydration shell of —NH₃⁺.

The HB interactions between the —NH₃⁺ group and its surrounding water molecules can be analyzed from the H_N-O_W and H_N-H_W RDFs, as shown in Fig. 1c and d, respectively. According to Fig. 1c, the first H_N-O_W peak is exhibited at 1.94 Å, and the integration up to the corresponding first H_N-O_W minimum gives an average coordination number of 1.2 ± 0.1. This implies that the —NH₃⁺ species participates in about 3.6 HBs with its nearest-neighbor waters, i.e., consisting of about 1.2 water molecules for each H atom of —NH₃⁺. The slight pronounced second peak of the H_N-O_W RDF could be ascribed to the contributions of water molecules in the first hydration layer of other —NH₃⁺ hydrogen atoms and of water molecules in the outer region. In Fig. 1d, the feature of the H_N-H_W RDF corresponds to the arrangements of primary water molecules forming HBs at each of the —NH₃⁺ hydrogens. As compared to the feature of the O—H and H—O RDFs (cf. Fig. 2b and c) of pure water

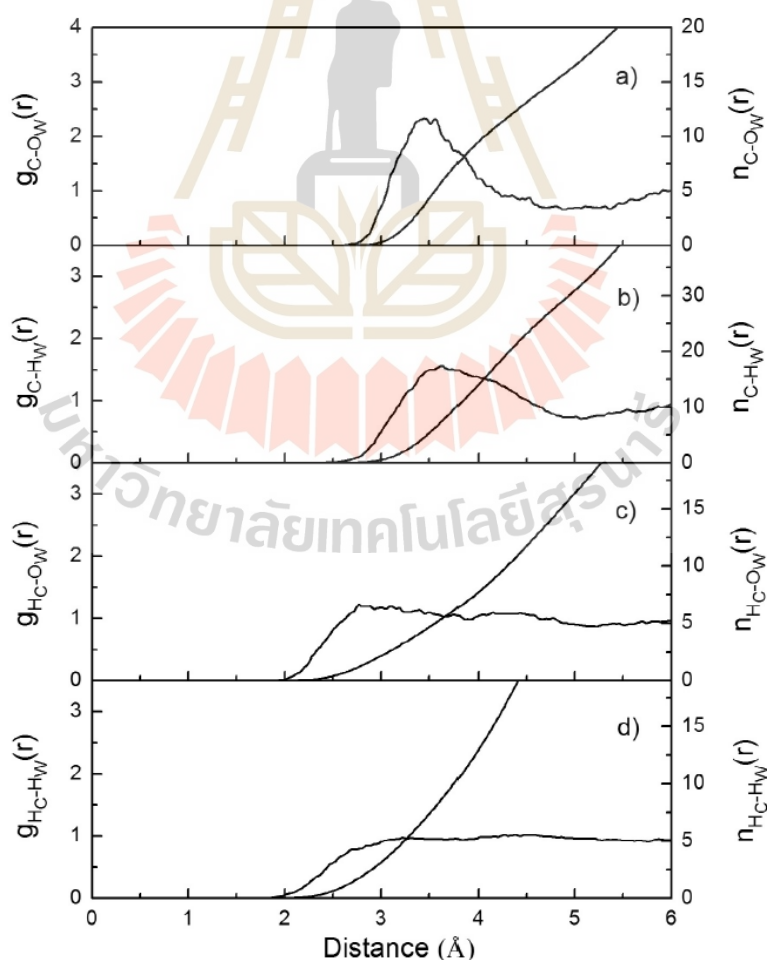


Fig. 3. a) C-O_W, b) C-H_W, c) H_C-O_W and d) H_C-H_W RDFs and their corresponding integration numbers.

[18], i.e., in terms of shape and separation of the first and second $H_N\cdots O_W$ peaks, it is apparent that the HB interactions between the $-NH_3^+$ hydrogens and their nearest-neighbor waters are relatively weaker than the HB networks of water molecules in the bulk. Consequently, this leads to more frequent and easy exchange of water molecules between the first shell and the outer region.

The hydration shell structure of the $-NH_3^+$ group, as obtained by the ONIOM-XS MD simulation, is comparable to that reported in the CPMD study [11]. However, some observed differences between the ONIOM-XS and the CPMD results could be discussed as follows. By means of the ONIOM-XS MD simulation, about 4.9 water molecules are found to be involved in the primary region of the $-NH_3^+$ group, compared to the average value of 4.2 of the CPMD study. In addition, according to the characteristics of the ONIOM-XS MD's N- H_W RDF, it is apparent that hydrogen atoms of water molecules in the first hydration shell of the $-NH_3^+$ group have rather high orientational freedom. In the CPMD study [11], the peaks of the partial distribution functions $g(NO)$ and $g(ND)$ (D denotes water hydrogen) are slightly better defined than the ONIOM-XS MD's N- O_W and N- H_W RDFs, which is explainable since the use of the BLYP functional could result in an overestimation of the solute-solvent interactions. Regarding the ONIOM-XS MD results, the observed hydration structure of the $-NH_3^+$ group is similar to the hydration structure of the spherical NH_4^+ species derived by means of the conventional QM/MM scheme [35]. Note that, in the case of the spherical NH_4^+ , the QM/MM MD study has predicted a broad unsymmetrical first N- O_W RDF, which corresponds to the experimentally observed fast translation and rotation of NH_4^+ in water [36,37]. For the $CH_3NH_3^+$ species, the steric hindrance arising from the $-CH_3$ group could be expected to prevent such phenomenon, i.e., the ONIOM-XS MD simulation clearly reveals a relatively more structured N- O_W RDF.

At the hydrophobic site of $CH_3NH_3^+$, the arrangements of water molecules around the $-CH_3$ group can be analyzed from a set of C- O_W , C- H_W , $H_C\cdots O_W$ and $H_C\cdots H_W$ RDFs and their corresponding integration numbers, as shown in Fig. 3a to d, respectively. The observed broad C- O_W and C- H_W peaks with maxima at around 3.48 and 3.67 Å, as well as the observed broad and less pronounced first $H_C\cdots O_W$ and $H_C\cdots H_W$ RDFs, clearly indicate weak interactions between the $-CH_3$ group and its surrounding water molecules. The integration up to a rough estimate of the first C- O_W minimum (i.e., of around 4.90 Å) yields about 15.1 ± 0.2 water molecules. Interestingly, it has been reported that, according to a more polar character of the $-CH_3$ group of $CH_3NH_3^+$, i.e., compared to that of CH_3COO^- , the interactions between the $-CH_3$ group and its surrounding water molecules could play some roles in the nature of the $CH_3NH_3^+$ solvation [8]. Based on the ONIOM-XS MD simulation, it is observed that the $-CH_3$ group in $CH_3NH_3^+$ has a slight positive partial charge, which allows some nearest-neighbor water molecules to have their lone pair directed toward the $-CH_3$ species. However, according to the characteristics of the $H_C\cdots O_W$ and $H_C\cdots H_W$ RDFs, it could be demonstrated that water molecules in the hydrophobic region are arranged with respect to the strength of their water-water HB interactions, rather than by the influence of the $-CH_3$ group.

The probability distributions of the number of water molecules, calculated within the first minima of the N- O_W and C- O_W RDFs, respectively, are plotted in Fig. 4a and b, respectively. With regard to Fig. 4a, it is apparent that various numbers of water molecules, varying from 3 to 8 with the prevalent value of 5, are cooperatively involved in the first hydration shell of the $-NH_3^+$ group. In this respect, it could be expected that these water molecules can mutually play a role in the HB formation with hydrogen atoms of the $-NH_3^+$ group. The numbers of HBs which are simultaneously formed at each of the $-NH_3^+$ hydrogens during the ONIOM-XS MD simulation can be evaluated with respect to the following geo-

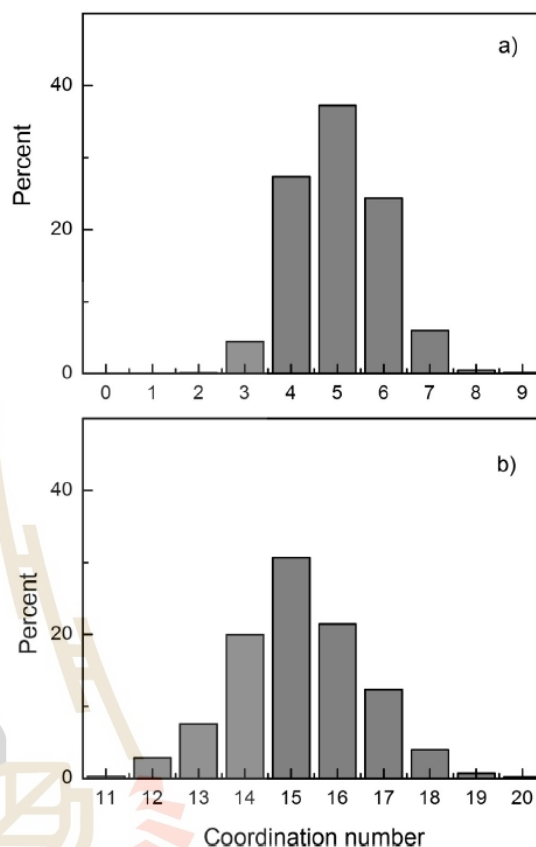


Fig. 4. Probability distributions of the coordination numbers, calculated within the first minimum of a) N- O_W and b) C- O_W RDFs.

metrical criteria of the HB formation: (1) the HB distance is limited by the first minimum of the $H_N\cdots O_W$ RDF and (2) the N- $H_N\cdots O_W$ and $H_N\cdots O_W\cdots H_W$ HB angles $\geq 100^\circ$, as depicted in Fig. 5. According to the detailed analysis of the ONIOM-XS MD trajectories, it is observed that most of the $-NH_3^+$ hydrogens favor to form a single HB with one of its nearest-neighbor water molecules, compared to about 12–13% of the remaining configurations which form two HBs with two nearest-neighbor waters. In Fig. 4b, the number of water molecules around the $-CH_3$ group shows large variations, ranging from 11 to 20, which corresponds to the observed weak interactions between the $-CH_3$ group and its surrounding water molecules.

The details with respect to the HBs between the $-NH_3^+$ hydrogen atoms and their nearest-neighbor waters can be further analyzed from the distributions of the N- $H_N\cdots O_W$ angle, calculated within the $H_N\cdots O$ distances of 2.0 and 2.5 Å, respectively, as shown in Fig. 6. At the short $H_N\cdots O_W$ distance of 2.0 Å, it is apparent that the N- $H_N\cdots O_W$ HBs are nearly linear, with peak maxima around 160° . However, at the slightly longer $H_N\cdots O_W$ distance of 2.5 Å (i.e., the first minimum of the $H_N\cdots O_W$ RDF), the probability of finding linear HBs apparently decreases, while the pronounced peak between 90 and 150° becomes more significant. This could be ascribed to the presence of multiple, non-linear HBs at each of the $-NH_3^+$ hydrogen atoms. Such phenomenon can be analyzed by plotting the $H_N\cdots O_W$ angular distributions, calculated within

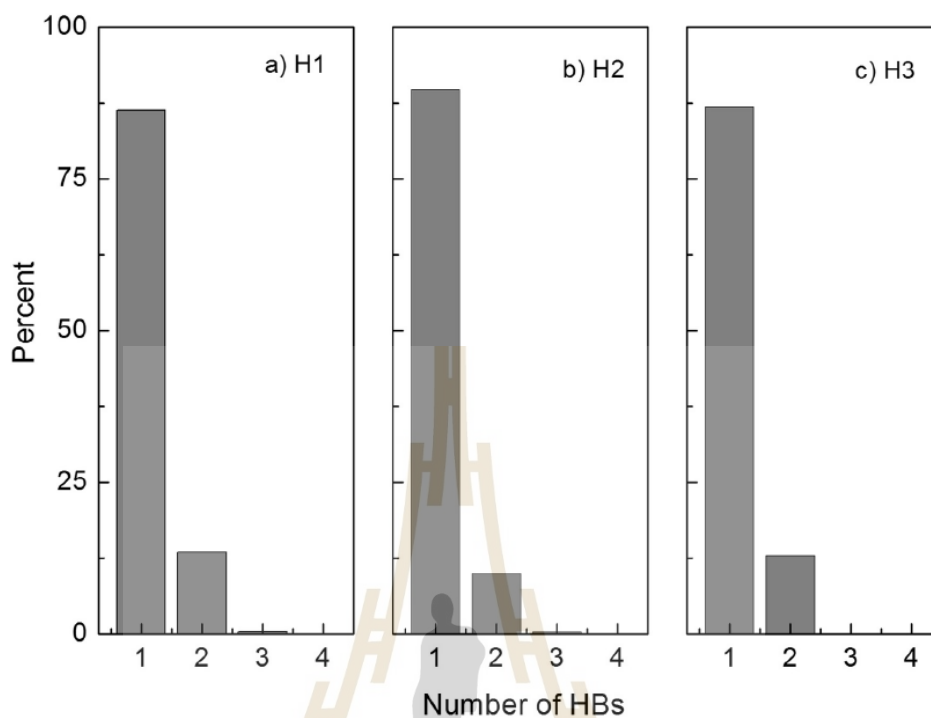


Fig. 5. Probability distributions of the number of HBs at each of $-\text{NH}_3^+$ hydrogens, calculated within the $\text{H}_\text{N}\cdots\text{O}_\text{W}$ distance of 2.5 Å.

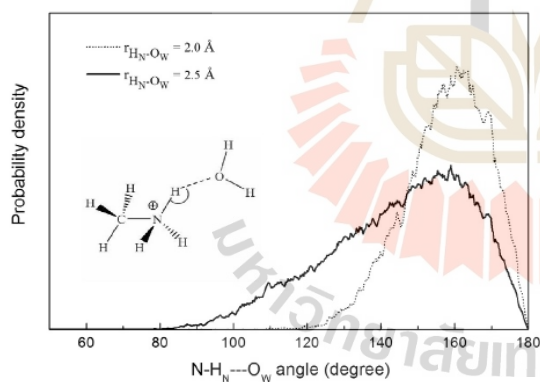


Fig. 6. $\text{N}-\text{H}_\text{N}\cdots\text{O}_\text{W}$ angular distributions, calculated up to the $\text{H}_\text{N}\cdots\text{O}_\text{W}$ distances of 2.0 and 2.5 Å, respectively.

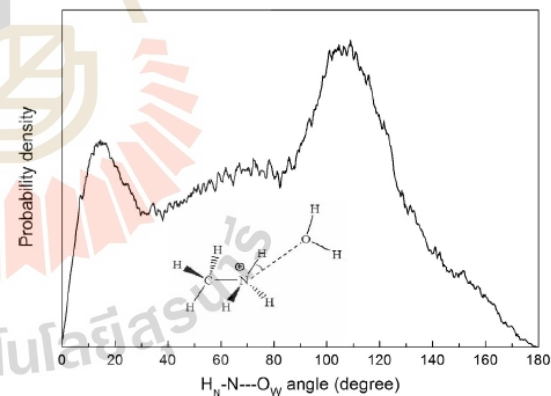


Fig. 7. $\text{H}_\text{N}\cdots\text{O}_\text{W}$ angular distributions, calculated within the first minimum of the $\text{H}_\text{N}\cdots\text{O}_\text{W}$ RDF.

the $\text{H}_\text{N}\cdots\text{O}_\text{W}$ distance of 2.5 Å, as depicted in Fig. 7. The two pronounced peaks around 0–30° and 90–120° correspond to the distributions of the three nearest-neighbor water molecules that are directly hydrogen bonded to each of $-\text{NH}_3^+$ hydrogen atoms, whereas the pronounced shoulder peak around 40–80° refers to the distributions of other nearest-neighbor waters that can possibly form additional HBs at some hydrogen atoms of the $-\text{NH}_3^+$ group. More insights into the HBs between the $-\text{NH}_3^+$ hydrogens and their nearest-neighbor waters can be visualized from the plot of water orientations within the $\text{H}_\text{N}\cdots\text{O}_\text{W}$ distance of 2.5 Å, as

shown in Fig. 8. The orientation of water molecules is described in terms of the distributions of angle θ , as defined by the $\text{H}_\text{N}\cdots\text{O}_\text{W}$ axis and the dipole vector of the water molecules. According to Fig. 8, the observed broad distributions of θ angles, *i.e.*, between 80 and 160°, clearly suggest that water molecules which form HBs with the $-\text{NH}_3^+$ hydrogens have freely dipole-oriented arrangements.

The lability of water molecules surrounding the $-\text{NH}_3^+$ and $-\text{CH}_3$ groups of CH_3NH_3^+ can be interpreted through the self-diffusion coefficient (D), which is calculated from the center-of-mass

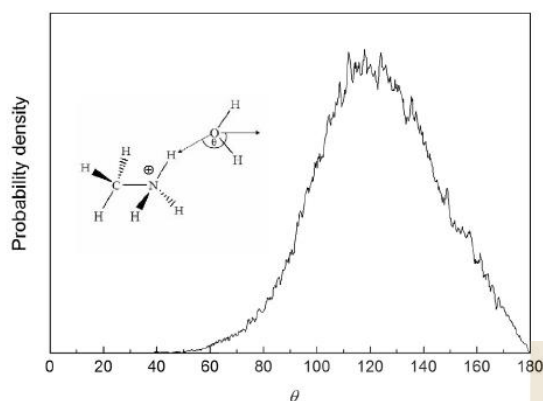


Fig. 8. Probability distributions of θ angle, calculated within the first minimum of the $H_N \cdots O_W$ RDF.

velocity autocorrelation functions (VACFs) of water molecules in the primary regions of the $-NH_3^+$ and $-CH_3$ groups using the Green-Kubo relation [38],

$$D = \frac{1}{3} \lim_{t \rightarrow \infty} \int_0^t C_v(t) dt. \quad (8)$$

By the ONIOM-XS MD simulation, the D values for water molecules in the vicinity of the $-NH_3^+$ and $-CH_3$ groups are estimated to be 2.28×10^{-5} and $1.93 \times 10^{-5} \text{ cm}^2 \cdot \text{s}^{-1}$, respectively, which are close to the value of $2.23 \times 10^{-5} \text{ cm}^2 \cdot \text{s}^{-1}$ of pure water derived by the similar ONIOM-XS MD scheme [18]. This supplies information that water molecules in the primary region of both the $-NH_3^+$ and $-CH_3$ groups are quite labile, *i.e.*, they diffuse in a similar degree of lability of those in the bulk. In particular, it is evident that the “hydrophobic effect” of the $-CH_3$ group results in slightly more attractive water-water interactions in this region, *i.e.*, giving a lower D value when compared to that of bulk water. This corresponds to a scenario in which water molecules adjacent to a nonpolar group are less labile and their water-water HB interactions are (on the average) stronger than those in the bulk.

Water exchange at each hydrogen atom of the $-NH_3^+$ group can be visualized from the plots of time dependence of the $H_N \cdots O_W$ distance, as depicted in Fig. 9. During the ONIOM-XS MD simulation, it is observed that water molecules which formed HBs at each of the $-NH_3^+$ hydrogens are quite labile, *i.e.*, they can easily exchange with other nearest-neighbor waters. Fig. 10 displays the plots of time dependence of the number of water molecules at each hydrogen atom of the $-NH_3^+$ group, calculated within the

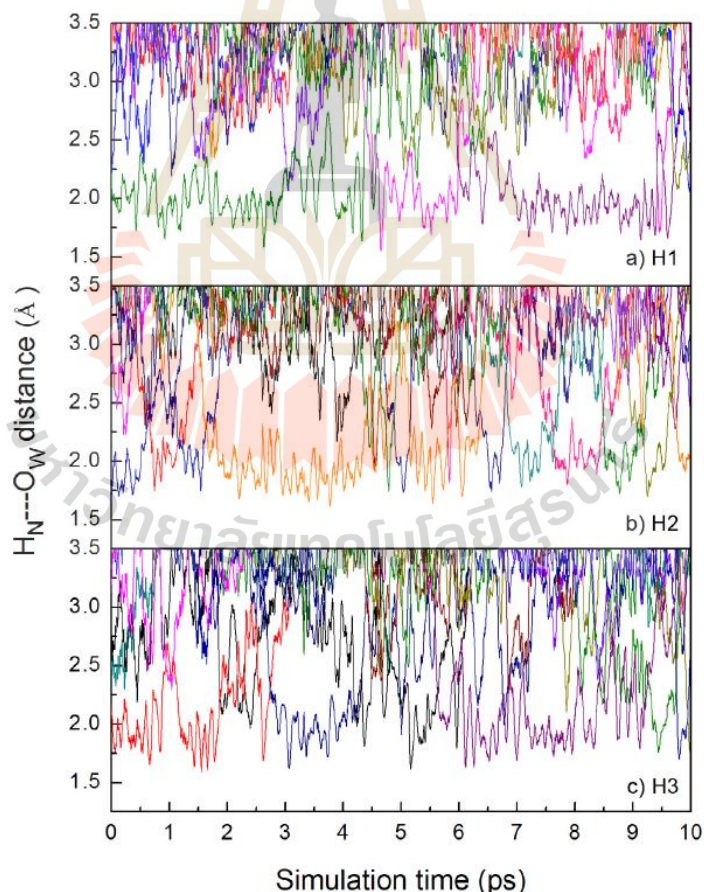


Fig. 9. Water exchange in the first solvation shell of each hydrogen atom of $-NH_3^+$, selected only for the first 10 ps of the ONIOM-XS MD simulation.

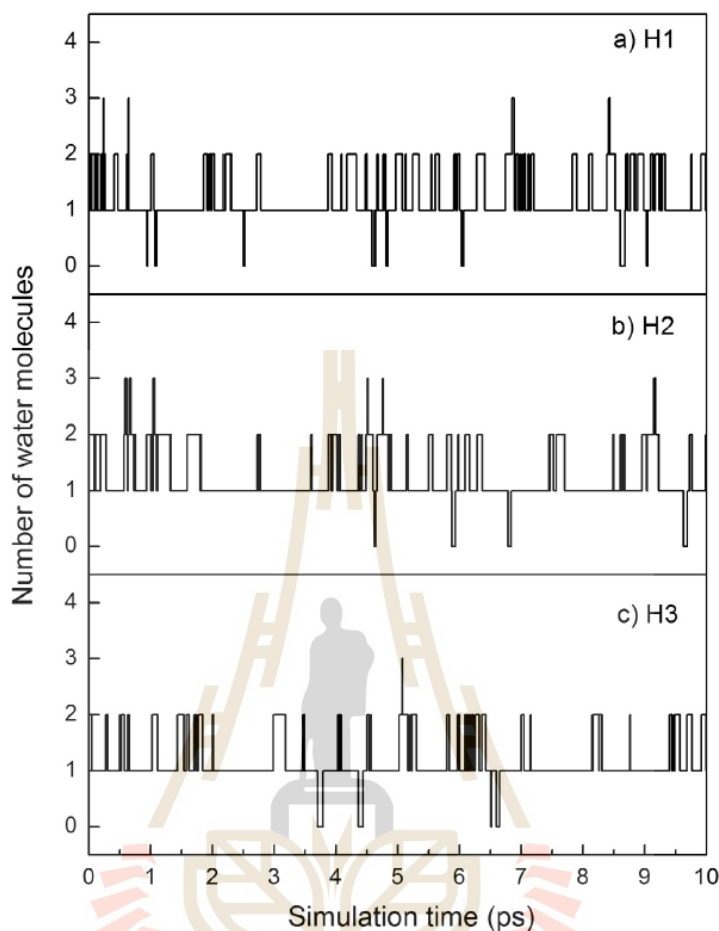


Fig. 10. Time dependence of the number of water molecules in the first solvation shell of each hydrogen atom of $-\text{NH}_3^+$, calculated within the $\text{H}_N \cdots \text{O}_W$ distance of 2.5 Å and selected only for the first 10 ps of the ONIOM-XS MD simulation.

first minimum of the $\text{H}_N\text{-O}_W$ RDF. According to Figs. 9 and 10, it is apparent that each of the $-\text{NH}_3^+$ hydrogens can simultaneously form (either strong or weak) HBs to different numbers of water molecules, leading to various possible species of the CH_3NH_3^+ hydrates formed in aqueous solution. In Fig. 11, some selected conformations of several hydrated CH_3NH_3^+ complexes are shown, which include all nearest-neighbor waters located within the $\text{H}_N\text{-O}_W$ distance of 2.5 Å and some water molecules from the outer region. Interestingly, it is observed that, besides the HB formation between the $-\text{NH}_3^+$ hydrogens and their nearest-neighbor waters, the HB interactions among the shell-shell waters as well as between the first-shell waters and the bulk also exist. These observed phenomena clearly supply information that CH_3NH_3^+ acts as a “structure-breaking” ion in aqueous solution.

The rates of water exchange processes at the $-\text{CH}_3$ and $-\text{NH}_3^+$ species, as well as at each of the $-\text{NH}_3^+$ hydrogens, were evaluated by means of mean residence times (MRTs) of the water molecules. Using the “direct” method [39], the MRT data were obtained from the product of the average number of nearest-neighbor water molecules located within the defined solvation shell with the duration of the ONIOM-XS MD simulation, divided by the observed number of exchange events lasting a given time interval t^* . With

regard to the “direct” method [39], a t^* value of 0.0 ps was proposed as a suitable choice for the estimation of HB lifetimes, while a t^* value of 0.5 ps was used as a good measure for water exchange processes. The calculated MRT data with respect to t^* values of 0.0 and 0.5 ps are summarized in Table 3. To provide a useful discussion with respect to the “structure-breaking” ability of CH_3NH_3^+ , the MRT data for pure water, as derived by the compatible ONIOM-XS MD scheme [18], were also given for comparison. For both $t^* = 0.0$ and 0.5 ps, the MRT values of water molecules in the primary region of the $-\text{NH}_3^+$ group, as well as in the first solvation shell of each of $-\text{NH}_3^+$ hydrogens, are lower than those of bulk water, indicating that the HB interactions between the $-\text{NH}_3^+$ hydrogens and their nearest-neighbor waters are relatively weaker than the water-water HBs in the bulk. For the hydrophobic site, the observed larger MRT data for water molecules in this region correspond to the “hydrophobic effect” of the $-\text{CH}_3$ group, i.e., the influence of the $-\text{CH}_3$ species could be regarded as a small perturbation to slightly strengthen the solvent’s HB structure. Based on the ONIOM-XS MD simulation, the observed flexible hydration structure and the relatively low MRT values of water molecules in the vicinity of the $-\text{NH}_3^+$ group, as well as the observed weak interactions between the $-\text{CH}_3$ group and its surrounding waters, clearly

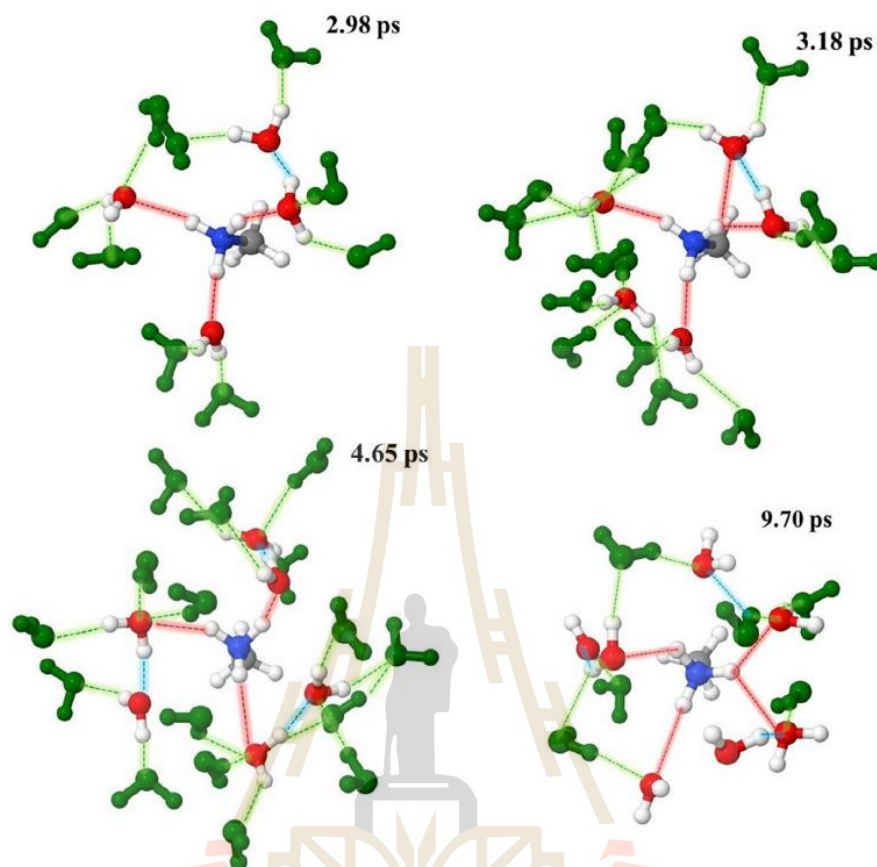


Fig. 11. Selected geometrical arrangements of the CH_3NH_3^+ -water complexes, showing the HB formations between the $-\text{NH}_3^+$ hydrogens and their nearest-neighbor waters (i.e., the dash lines highlighted in "red"), as well as the HB formations among the first-shell waters (i.e., the dash lines highlighted in "blue") and between the first-shell waters and the bulk (i.e., the dash lines highlighted in "green"). Note that water molecules located outside the $\text{H}_N \cdots \text{O}_W$ distance of 2.5 Å are colored in "green". (For interpretation of the references to colour in this figure legend, the reader is referred to the web version of this article.)

Table 3

Mean residence times (MRTs) of water molecules in the bulk and in the primary region of $-\text{CH}_3$ and $-\text{NH}_3^+$. For the $-\text{NH}_3^+$ species, the MRT data of water molecules at each of the $-\text{NH}_3^+$ hydrogens are also given for comparison.

Ion/solute	CN	t_{sim}	$t^* = 0.0$ ps		$t^* = 0.5$ ps		Ref.
			$N_{\text{ex}}^{0.0}$	$\tau_{\text{H}_2\text{O}}^{0.0}$	$N_{\text{ex}}^{0.5}$	$\tau_{\text{H}_2\text{O}}^{0.5}$	
$-\text{CH}_3$	15.1	40.0	1161	0.52	228	2.65	This work
$-\text{NH}_3^+$	4.9	40.0	701	0.28	123	1.59	This work
(H ₁)	1.2	40.0	489	0.10	41	1.17	This work
(H ₂)	1.2	40.0	431	0.11	37	1.30	This work
(H ₃)	1.2	40.0	530	0.09	39	1.23	This work
Pure H ₂ O	4.7	30.0	607	0.23	65	2.17	[18]

confirm the "structure-breaking" ability of CH_3NH_3^+ in aqueous solution. In this context, the ONIOM-XS MD technique can be considered as an elegant simulation approach to obtain more detailed interpretation on the structure and dynamics of such amphiphilic species in aqueous solution.

4. Conclusions

In this work, the sophisticated ONIOM-XS MD technique has been applied for studying the solvation structure and dynamics

of CH_3NH_3^+ in aqueous solution. Based on the ONIOM-XS MD simulation, it is observed that the solvation structure of the CH_3NH_3^+ ion is somewhat flexible, in which various numbers of water molecules, ranging from 3 to 8 and from 12 to 19, are cooperatively involved in the primary region of the $-\text{NH}_3^+$ and $-\text{CH}_3$ groups, respectively. For the hydrophilic side, it is found that the $-\text{NH}_3^+$ group participates in about 3.6 HBs with its nearest-neighbor waters, i.e., consisting of about 1.2 water molecules for each of the $-\text{NH}_3^+$ hydrogens. Interestingly, it is observed that the HB interactions between the $-\text{NH}_3^+$ hydrogens and their nearest-neighbor

waters are not strong, *i.e.*, when compared to the water-water HBs in the bulk. Consequently, this allows several water exchange processes to frequently occur at each of the $-\text{NH}_3^+$ hydrogens. For the hydrophobic side, it is observed that water molecules in this region are labile and they are arranged according to their water-water HB networks, rather than by the influence of the $-\text{CH}_3$ group. In addition, it is evident that the “hydrophobic effect” of the $-\text{CH}_3$ species results in slightly more attractive water-water HB interactions in this region. Overall, the ONIOM-XS MD results clearly reveal the characteristics of CH_3NH_3^+ as a “structure-breaking” ion in aqueous solution.

Acknowledgments

This work was supported by the Thailand Research Fund (TRF), under the Royal Golden Jubilee Ph.D. Program (Contract number PHD/0126/2552), and Suranaree University of Technology (SUT). T.K. acknowledges financial support from Mahidol University. High-performance computer facilities provided by the National e-Science Infrastructure Consortium are gratefully acknowledged.

References

- [1] M. Wolff, *The Basis of Medicinal Chemistry, Burger's Medicinal Chemistry*, 4th Ed., Wiley, New York, 1979.
- [2] M.A. Andrade, S.I. O'Donoghue, B. Rost, *J. Mol. Biol.* 276 (1998) 517.
- [3] T. van Mourik, F.B. van Duijneveldt, *J. Mol. Struct. Theochem.* 341 (1995) 63.
- [4] K.-Y. Kim, U.-I. Cho, D.W. Boo, *Bull. Korean. Chem. Soc.* 22 (2001) 597.
- [5] K.-Y. Kim, W.-H. Han, U.-I. Cho, Y.T. Lee, D.W. Boo, *Bull. Korean. Chem. Soc.* 27 (2006) 2028.
- [6] G.N. Chuev, M. Valiev, M.V. Fedotova, *J. Am. Chem. Soc.* 8 (2012) 1246.
- [7] M.V. Fedotova, S.E. Kruchinin, *Russ. Chem. Bull.* 61 (2012) 240.
- [8] G. Alagona, C. Ghio, P. Kollman, *J. Am. Chem. Soc.* 108 (1986) 185.
- [9] W.L. Jorgensen, J. Gao, *J. Phys. Chem.* 90 (1986) 2174.
- [10] E.C. Meng, P.A. Kollman, *J. Phys. Chem.* 100 (1996) 11460.
- [11] H. Hesske, K. Gloe, *J. Phys. Chem. A* 111 (2007) 9848.
- [12] S. Yoo, X.C. Zeng, S.S. Xantheas, *J. Chem. Phys.* 130 (2009) 221102.
- [13] J.X. Grossman, E. Schwegler, E.W. Draeger, F. Gygi, G. Galli, *J. Chem. Phys.* 120 (2004) 300.
- [14] T. Todorova, A.P. Seitsonen, J. Hutter, F.W. Kuo, C.J. Mundy, *J. Phys. Chem. B* 110 (2006) 3685.
- [15] T. Kerdcharoen, K. Morokuma, *Chem. Phys. Lett.* 355 (2002) 257.
- [16] T. Kerdcharoen, K. Morokuma, *J. Chem. Phys.* 118 (2003) 8856.
- [17] S. Wanprakhon, A. Tongraar, T. Kerdcharoen, *Chem. Phys. Lett.* 517 (2011) 171.
- [18] S. Thaomola, A. Tongraar, T. Kerdcharoen, *J. Mol. Liq.* 174 (2012) 26.
- [19] P. Sripa, A. Tongraar, T. Kerdcharoen, *J. Phys. Chem. A* 117 (2013) 1826.
- [20] P. Sripa, A. Tongraar, T. Kerdcharoen, *J. Mol. Liq.* 208 (2015) 280.
- [21] P. Kabbalee, A. Tongraar, T. Kerdcharoen, *Chem. Phys.* 446 (2015) 70.
- [22] P. Kabbalee, A. Tongraar, T. Kerdcharoen, *Chem. Phys. Lett.* 633 (2015) 152.
- [23] J. Sripradite, A. Tongraar, T. Kerdcharoen, *Chem. Phys.* 463 (2015) 88.
- [24] P. Sripa, A. Tongraar, T. Kerdcharoen, *Chem. Phys.* 479 (2016) 72.
- [25] M. Svensson, S. Humbel, R.D.J. Froese, T. Mutsuvara, S. Sieber, K. Morokuma, *J. Phys. Chem.* 100 (1996) 1935.
- [26] T.H.Jr. Dunning, P.J. Hay, *Modern Theoretical Chemistry; III*, Plenum, New York, 1976.
- [27] M.J. Frisch, G.W. Trucks, H.B. Schlegel, G.E. Scuseria, M.A. Robb, J.R. Cheeseman, J.A. Montgomery, T. Vreven, K.N. Kudin, J.C. Burant, J.M. Millam, S.S. Iyengar, J. Tomasi, V. Barone, B. Mennucci, M. Cossi, G. Scalmani, N. Rega, G.A. Petersson, H. Nakatsuji, M. Hada, M. Ehara, K. Toyota, R. Fukuda, J. Hasegawa, M. Ishida, T. Nakajima, Y. Honda, O. Kitao, H. Nakai, M. Klene, X. Li, J.E. Knox, H.P. Hratchian, J.B. Cross, V. Bakken, C. Adamo, J. Jaramillo, R. Gomperts, R.E. Stratmann, O. Yazyev, A.J. Austin, R. Cammi, C. Pomelli, J.W. Ochterski, P.Y. Ayala, K. Morokuma, G.A. Voth, P. Salvador, J.J. Dannenberg, V.G. Zakrzewski, S. Dapprich, A.D. Daniels, M.C. Strain, O. Farkas, D.K. Malick, A.D. Rabuck, K. Raghavachari, J.B. Foresman, J.V. Ortiz, Q. Cui, A.G. Baboul, S. Clifford, J. Cioslowski, B.B. Stefanov, G. Liu, A. Liashenko, P. Piskorz, I. Komaromi, R.L. Martin, D.J. Fox, T. Keith, M.A. Al-Laham, C.Y. Peng, A. Nanayakkara, M. Challacombe, P.M.W. Gill, B. Johnson, W. Chen, M.W. Wong, C. Gonzalez, J.A. Pople, *GAUSSIAN 03, Revision D.1*; Gaussian, Inc.: Wallingford, CT, 2005.
- [28] F.H. Stillinger, A. Rahman, *J. Chem. Phys.* 68 (1976) 666.
- [29] P. Bopp, G. Jancsó, K. Heinzinger, *Chem. Phys. Lett.* 98 (1983) 129.
- [30] J.E. Carpenter, F. Weinhold, *J. Mol. Struct. (Theochem)* 169 (1988) 41.
- [31] A.E. Reed, R.B. Weinstock, F. Weinhold, *J. Chem. Phys.* 83 (1985) 735.
- [32] A.E. Reed, L.A. Curtiss, F. Weinhold, *Chem. Rev.* 88 (1988) 899.
- [33] H.J.C. Berendsen, J.P.M. Postma, W.F. van Gunsteren, A. DiNola, J.R. Haak, *J. Phys. Chem.* 81 (1984) 3684.
- [34] D.J. Adams, E.H. Adams, G.J. Hills, *Mol. Phys.* 38 (1979) 387.
- [35] P. Intharathep, A. Tongraar, K. Sagarik, *J. Comput. Chem.* 26 (2005) 1329.
- [36] C.L. Perrin, R.K. Gipe, *J. Am. Chem. Soc.* 108 (1986) 1088.
- [37] C.L. Perrin, R.K. Gipe, *Science* 238 (1987) 1393.
- [38] D.A. McQuarrie, in *Statistical Mechanics*, Harper & Row, New York, 1976.
- [39] T.S. Hofer, H.T. Tran, C.F. Schwenk, B.M. Rode, *J. Comput. Chem.* 25 (2004) 211.



CURRICULUM VITAE

MISS PRANGTHONG CHAIYASIT

Education Background:

2006-2009 B.Sc. (Applied Chemistry), Rangsit University, Pathumthani, Thailand

2010-2017 Ph.D. Candidate (Chemistry), Suranaree University of Technology, Nakhon Ratchasima, Thailand

Experiences:

2013-2017 Teaching Assistant, School of Chemistry, Institute of Science, Suranaree University of Technology, Nakhon Ratchasima, Thailand

Grant and Fellowships:

2010-2014 The Royal Golden Jubilee (RGJ) Ph.D. Scholarship from Thailand Research Fund (TRF)